7. REGIONAL CLIMATES—A. Mekonnen, J. A. Renwick, and A. Sanchez-Lugo, Eds.

a. *Overview*

This chapter provides summaries of the 2015 temperature and precipitation conditions across seven broad regions: North America, Central America and the Caribbean, South America, Africa, Europe, Asia, and Oceania. In most cases, summaries of notable weather events are also included. Local scientists provided the annual summary for their respective regions and, unless otherwise noted, the source of the data used is typically the agency affiliated with the authors. Please note that different nations, even within the same section, may use unique periods to define their normals. Section introductions will typically define the prevailing practices for that section, and exceptions will be noted within the text. In a similar way, many contributing authors use languages other than English as their primary professional language. To minimize additional loss of fidelity through reinterpretation after translation, editors have been conservative and careful to preserve the voice of the author. In some cases, this may result in abrupt transitions in style from section to section.

b. *North America*

This section is divided into three subsections: Canada, the United States, and Mexico. Information for each country has been provided by local scientists, and the source of the data is from the agency affiliated with the authors. Where available, anomalies are reported using a 1981–2010 base period; however, due to the different data sources, some anomalies are reported using other base periods. These are noted in the text.

1) Canada—R. Whitewood, L. A. Vincent, and D. Phillips

In Canada, 2015 was characterized by higher-than-average temperatures stretching from the central regions to the Pacific Coast and lower- and drier-than-average temperatures in the northeastern region of the country. Anomalies in this section are reported with respect to the 1961–90 base period.

(i) Temperature

The annual average temperature in 2015 for Canada was 1.3°C above the 1961–90 average, based on preliminary data. This marks the 11th warmest year since nationwide records began in 1948. The warmest year on record for Canada was 2010, at 3.0°C above average, and 4 of the 10 warmest years have occurred during the last decade. The national annual average temperature has increased 1.6°C over the past 68 years (Fig. 7.1). In 2015, annual departures >+2.5°C were recorded in the Yukon and western Northwest Territories, while annual departures <–0.5°C were observed in northern Quebec, Labrador, and Baffin Island (Fig. 7.2a).

Seasonally, winter (December–February) 2014/15 was 1.0°C above average and the 27th warmest since 1948. Warmer-than-average conditions were

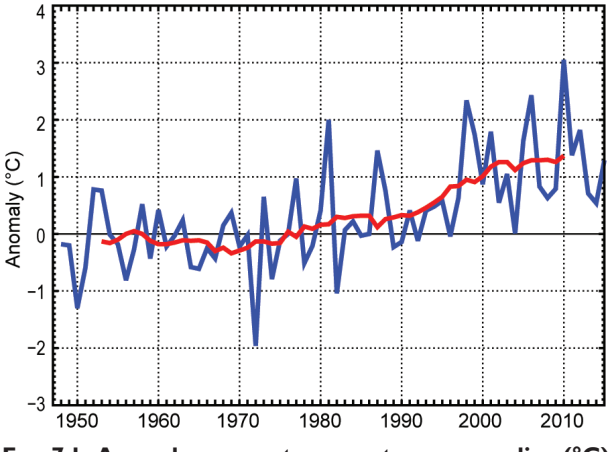

Fig. 7.1. Annual average temperature anomalies (°C) for Canada for 1948–2015 (base period: 1961–90). The red line is the 11-yr running mean. (Source: Environment and Climate Change Canada.)

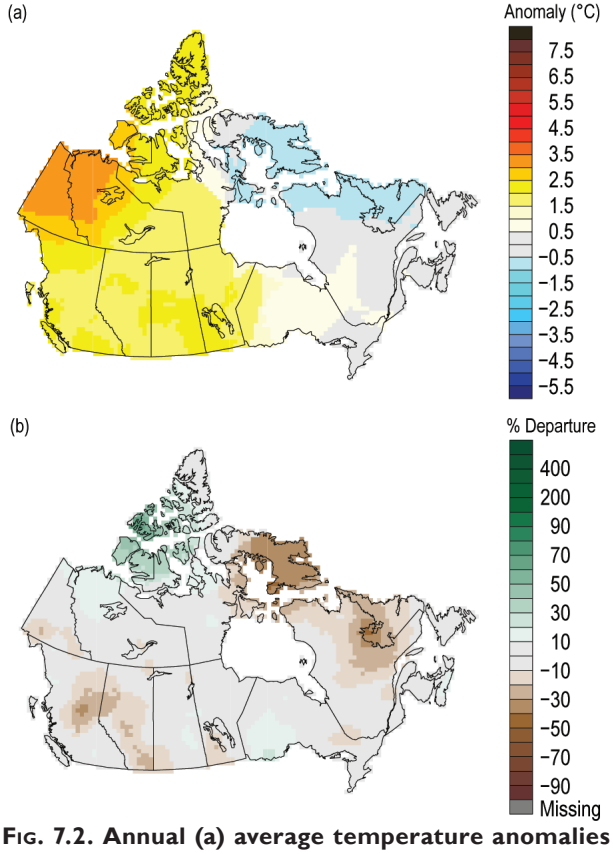

Fig. 7.2. Annual (a) average temperature anomalies (°C) and (b) total precipitation anomalies in Canada (% departure; base period: 1961–90). (Source: Environment and Climate Change Canada.)

observed in Yukon, Northwest Territories, British Columbia, Alberta, and Saskatchewan. Most of Ontario, Quebec, and the Atlantic provinces experienced cooler-than-average conditions. During spring (March–May), the same pattern of warmer-than-average conditions in the western and central regions and cooler-than-average conditions in the eastern regions of the country continued. The nationally averaged temperature for spring 2015 was 1.3°C above the 1961–90 average and the 14th warmest in the 68-year period of record.

Summer (June–August) was 1.0°C above average and the sixth warmest since 1948. British Columbia and northern Nunavut (a territory in the northeast of the country) experienced warmer-than-average conditions. Southern Ontario was the only region with slightly cooler-than-average temperature conditions during summer. Summer temperatures across the remainder of the country were near-average.

During autumn (September–November), the pattern changed with the central regions of the country, from Saskatchewan through the Maritimes, and the northern territories all experiencing warmer-than-average conditions, while British Columbia, Alberta, northern Quebec, and Newfoundland and Labrador experienced near-average conditions. The nationally averaged temperature was 1.7°C above the 1961–90 average; the sixth warmest autumn since 1948.

(ii) Precipitation

Canada as a whole experienced slightly drier-than-average precipitation in 2015. Based on preliminary data, it was the 20th driest year since nationwide records began in 1948, with nationally averaged precipitation 97% of the 1961–90 average. Drier-than-average conditions were observed for eastern Nunavut, northern Quebec and Labrador, in central British Columbia, and Alberta, whereas only the area over the Canadian Arctic Archipelago experienced wetter-than-average conditions (Fig. 7.2b).

Seasonally, winter 2014/15 was the 13th driest since 1948, and nationally averaged precipitation was 90% of the 1961–90 average, with most of the country experiencing drier-than-average conditions. However, wetter-than-average conditions were observed over much of Nunavut and the Atlantic provinces. Spring 2015 was the 10th driest in the 68-year period of record with nationally averaged precipitation 89% of average. Drier-than-average conditions continued across much of the country, with some wetter-than-average conditions in the western Canadian Arctic Archipelago.

Summer 2015 was the 17th wettest since 1948, and national average precipitation was 105% of average. Wetter-than-average conditions were mainly observed in the northwestern regions of the country whereas drier-than-average conditions occurred in British Columbia and Alberta. Autumn 2015 was the 26th wettest since 1948, with nationally averaged precipitation 103% of average. Drier-than-average conditions for the season were experienced in the Yukon, northern British Columbia, most of Quebec, and over Baffin Island in the north. Wetter-than-average conditions were observed in the Prairie Provinces (Alberta, Saskatchewan, and Manitoba) and in the rest of Nunavut for the autumn months.

(iii) Notable events

Winter got off to a slow start for the Maritimes, but conditions changed in January. Snow fell from several storms, often just a few days apart. Atlantic Canada was continually battered through February and March with storm after storm, leaving behind snow amounts not seen in decades. Numerous records were set over the 2014/15 winter in the Maritimes. Halifax International Airport in Nova Scotia recorded total snow accumulation from January to May of 371 cm (normal is 59 cm). The previous snowiest such period at any Halifax station was 330 cm in 1972. Saint John, New Brunswick, received more than double its normal snowfall—495 cm (normal is 240 cm)—its snowiest winter on record. Moncton, New Brunswick, broke the 5-meter level at 507 cm (normal is 325 cm). In Charlottetown, Prince Edward Island, the snowiest city in Canada this winter, an April snowstorm helped set a new record for the most snow in one winter—551 cm—12 cm more than the previous record in 1971/72.

The wildfire season in Canada began early, ended late, and was extremely active, especially in the West. The national wildland fire season was above average for both number of fires and hectares burned, about four times the 15-year average (2001–15) and three times the 25-year average (1991–2015), respectively. Wildfires began in northern Saskatchewan in March. Residents from several communities near La Ronge and La Loche began evacuating to centers in the south. Hot temperatures and dry thunderstorms in May and June contributed to even more volatile fire conditions, with more than 13 000 people evacuated in what was the largest evacuation in Saskatchewan's history. In total, 1.8 million hectares burned in Saskatchewan, six times the provincial average. In Alberta, wildfires burned hot and fast in June when half the province came under a fire advisory. British

Columbia reported more than 1800 wildfires that burned an estimated 300 000 hectares and cost more than 287 million U.S. dollars to fight. The 20-year (1996–2015) average number of fires is about 1050 with an average 43 280 hectares burned. Conditions in British Columbia included extreme heat near 40°C, widespread and persistent dryness, large amounts of dry lightning, and gusty winds, which all contributed to the extreme fire season.

2) United States—J. Crouch, R. R. Heim Jr., and C. Fenimore

The annual average temperature in 2015 for the contiguous United States (CONUS) was 12.4°C, or 0.9°C above the 1981–2010 average—the second warmest year since records began in 1895, behind 2012 (Fig. 7.3). The annual CONUS temperature over the 121-year period of record is increasing at an average rate of 0.1°C per decade. The nationally averaged precipitation total during 2015 was 111% of average, the third wettest year in the 121-year historical record. The annual CONUS precipitation is increasing at an average rate of 4.1 mm per decade. Outside of the CONUS, Alaska had its 2nd warmest and 15th wettest year since records began in 1925. The statewide temperature was 1.6°C above average, while the precipitation total was 108% of average. Complete U.S. temperature and precipitation maps are available at www.ncdc.noaa.gov/cag/.

(i) Temperature

During early 2015, record warmth spanned the western United States with record and near-record cold temperatures in the Midwest and Northeast. The last few months of 2015, particularly December, brought much-above-average temperatures to the East, with near-average temperatures across the West. This pattern resulted in all 48 states in the CONUS observing an above-average annual temperature (Fig. 7.4a). Florida, Montana, Oregon, and Washington (state) each had their warmest year on record. Twenty-three additional states across the West, Great Plains, Gulf Coast, and East Coast each had annual temperatures that ranked in the highest 10th percentile of their historical records.

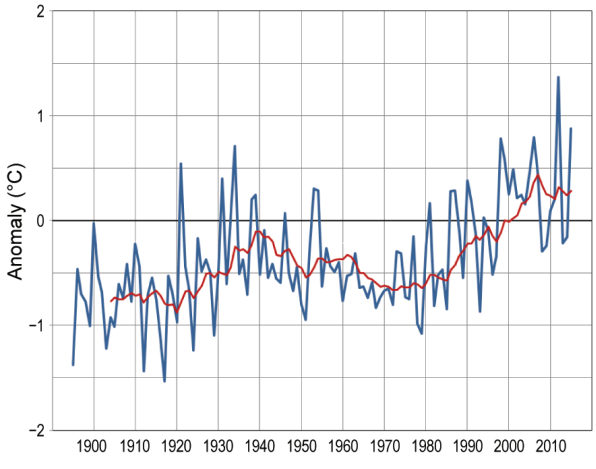

Fig. 7.3. Annual mean temperature anomalies (°C) for the contiguous United States for 1895–2015 based on the 1981–2010 average. The red line is the 10-year running mean. (Source: NOAA/NCEI.)

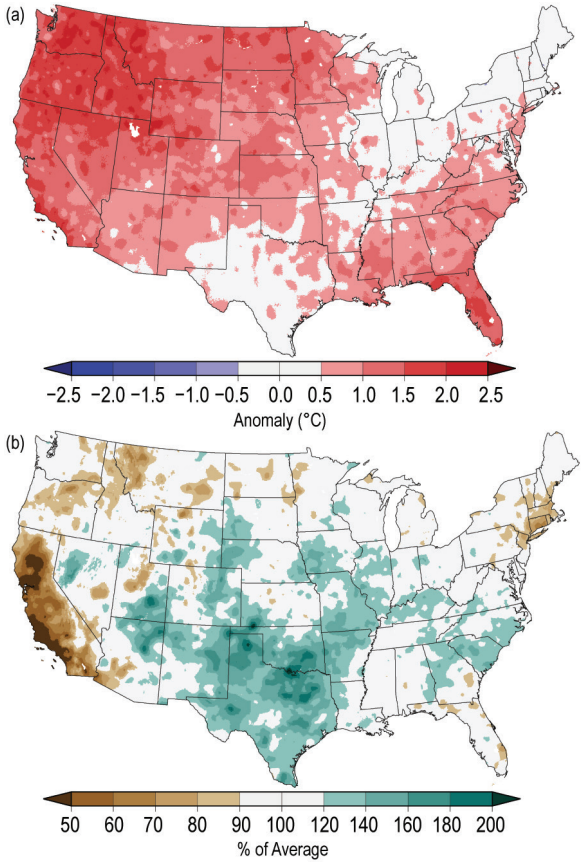

Fig. 7.4. (a) Annual average temperature anomalies (°C) and (b) % of average annual total precipitation in the contiguous United States (base period: 1981–2010). (Source: NOAA/NCEI.)

The winter (December–February) 2014/15 CONUS temperature was 0.4°C above average, ranking in the warmest third of the historical record. Record and near-record warmth were observed in the West, with six states observing record high seasonal temperatures. Below-average temperatures occurred in the East; February was particularly cold, with 24 states observing one of their 10 coldest months on record and numerous cities, including Chicago, Illinois, and Buffalo, New York, being record cold. The CONUS spring (March–May) temperature was 0.7°C above average, the 11th warmest on record. Much-above-average temperatures were observed across the West and Southeast—Florida observed its warmest spring

on record. The summer (June–August) CONUS temperature was 0.5°C above average, the 12th warmest on record. Above-average temperatures continued in the Southeast and West, where California, Oregon, and Washington were record warm, while parts of the Midwest were cooler than average. The autumn (September–November) temperature was 1.5°C above average, the warmest such period on record for the CONUS. Every state had an above-average autumn temperature: 40 states observed one of their 10 warmest on record, with Florida record warm. December ended the year with a record high monthly temperature for the CONUS that was 3.0°C above average. Twenty-nine states across the East were record warm, while near-average temperatures were observed across the West.

(ii) Precipitation

During 2015, much of the central and eastern CONUS were wetter than average, while parts of the West and Northeast were drier than average (Fig. 7.4b). Fourteen states had an annual precipitation total that was within their wettest 10th percentiles. Oklahoma and Texas were both record wet with 145% and 143% of average annual precipitation, respectively. Drought conditions that began in 2010 in both states were eradicated during 2015. California, which was plagued by drought during all of 2015, had its 13th driest year on record; end-of-year precipitation partially erased early year deficits. At the beginning of 2015, the CONUS moderate to exceptional drought footprint was 28.7%; it peaked at 37.8% in May and ended the year at 18.7%. This end-of-year drought footprint was the smallest for the CONUS since December 2010.

The CONUS winter precipitation was 90% of average, ranking in the driest third of the historical record (29th driest). Despite near-average precipitation in the West, record warmth caused much of the high-elevation precipitation to fall as rain and not snow. The below-average mountain snowpack and subsequent below-average spring and summer runoff contributed to near-record low reservoir levels, worsening drought, and a record-breaking wildfire season. Spring was the 10th wettest on record for the CONUS, with 117% of average precipitation. Record and near-record precipitation totals were observed in the southern Great Plains and Central Rockies, with below-average precipitation along both coasts. May was an extraordinarily wet month for the CONUS with 112.8 mm of precipitation, 147% of average, the wettest among all months on record. Much of the precipitation fell across the Southern Plains. The summer precipitation for the CONUS was 108% of average, the 16th wettest on record. Above-average precipitation was observed across the Ohio Valley, where record rain fell during June and July. For autumn, the CONUS precipitation total was 111% of average and the 15th wettest on record. Above-average precipitation was observed across the South and along the East Coast. South Carolina had its wettest autumn on record with 603.5 mm of rainfall, 321% of average. December was record wet for the CONUS, at 160% of average, becoming the only month in the 121-year period of record that was simultaneously wettest and warmest for its respective month.

(iii) Notable events

Tornado activity during 2015 was below average for the fourth consecutive year, with a total of 1177 confirmed tornadoes, compared to the 1991–2010 annual average of 1253. Despite the below-average number of tornadoes, there were 36 tornado-related fatalities, with most occurring during a deadly outbreak in December across the Southern Plains and Lower Mississippi Valley.

Wildfires burned nearly 4.1 million hectares across the United States during 2015, surpassing 2006 for the most acreage burned since record keeping began in 1960. The most costly wildfires occurred in California, where over 2500 structures were destroyed in the Valley and Butte wildfires in September.

Numerous major precipitation events impacted different regions of the CONUS in 2015. Heavy snowfall during late winter and early spring set a new seasonal record for Boston, Massachusetts, with 281 cm of snow. In early October, an upper-level low interacted with moisture from Hurricane Joaquin offshore in the Atlantic to produce rainfall totals exceeding 500 mm in parts of North and South Carolina. In the Southern Plains, late-spring rainfall and summer and autumn rains associated with the remnants of east Pacific tropical cyclones (see section 4e3) caused several significant flooding events. On 30 October, the remnants of Hurricane Patricia dumped 389.7 mm of rain on Austin, Texas, 146.3 mm of which fell in a single hour.

3) Mexico—R. Pascual Ramírez, A. Albanil Encarnación, and J. L. Rodríguez Solís

In Mexico, the annual temperature for 2015 tied with 2014 as the highest since national temperature records began in 1971. The nationally averaged precipitation total was ninth highest since precipitation records began in 1941, with the most notable accumulations during February and March.

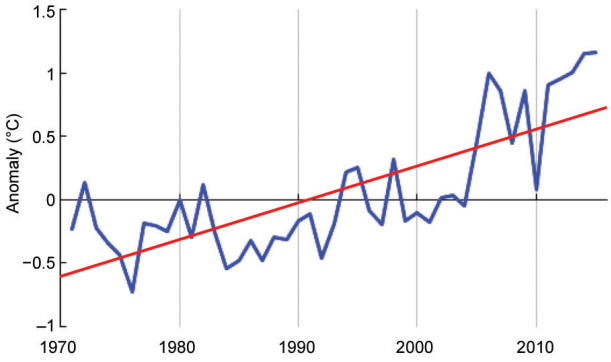

Fig. 7.5. Annual mean temperature anomalies (°C, blue) for Mexico (base period: 1981–2010). A linear trend is depicted by the red line. (Source: National Meteorological Service of Mexico.)

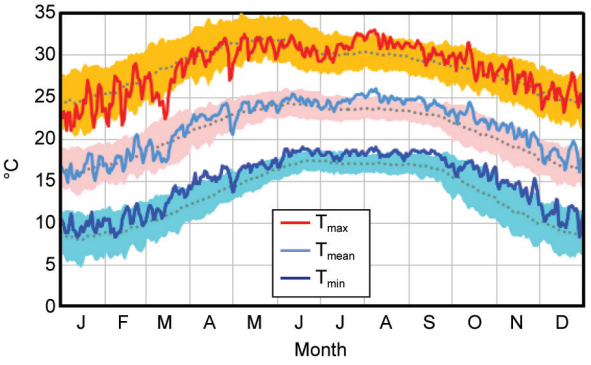

Fig. 7.6. Nationwide daily temperatures (°C) for Mexico. Shaded areas represent the ±2 std. dev. (base period: 1981–2010). Solid lines represent daily values for the three temperature parameters and dotted lines are the climatology. (Source: National Meteorological Service of Mexico.)

(i) Temperature

The 2015 mean temperature for Mexico was 22.1°C, which was 1.1°C above the 1981–2010 average, tying with 2014 as the warmest year since national records began in 1971 and surpassing the previous record of 21.9°C set in 2006 and 2013 (Fig. 7.5). This was also the 12th consecutive year with an above-average annual temperature.

The first three months of the year were near-average; however, the rest of the year was characterized by above-average temperatures and, in some instances, the daily mean, maximum, and minimum temperatures were close to two standard deviations above average (Fig. 7.6). The mean temperature for July–September was 2.3°C above average—the warmest such period on record, surpassing the previous record set in 2013 and 2014 and making the last three years the three warmest for the July–September period on record.

Regionally, the mean temperature in 2015 was below average in northern Baja California, areas of Chihuahua and its borders with Coahuila and Durango, between Colima and Jalisco, the central region (which includes the states of Mexico, Puebla, and Veracruz), and Oaxaca, while the rest of the country observed near-average to above-average temperatures. Eight states had their warmest year since records began in 1971: Campeche, Quintana Roo, and Yucatan in the Yucatan Peninsula; Nayarit, Jalisco, Michoacán, and Guerrero in the west; and Morelos in the central portion of the country. Conversely, the state of Veracruz observed one of its 20 coldest years on record (Fig. 7.7a).

Frost days, defined as daily minimum temperatures ≤0°C, is typical in Mexico during October–March, while hot days—daily maximum temperatures ≥40°C—are typical during April–September. During January–March 2015, only 26.0% of the country, mostly confined to the central region,

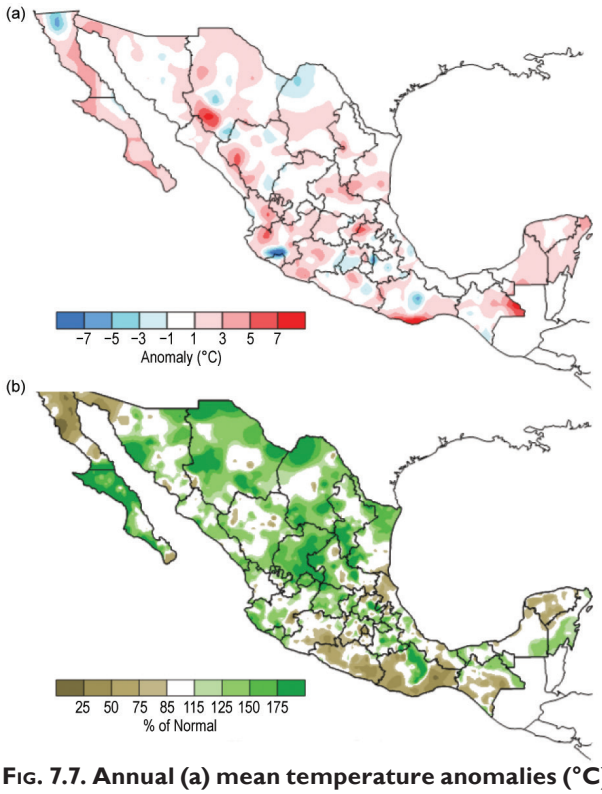

Fig. 7.7. Annual (a) mean temperature anomalies (°C) and (b) precipitation anomalies (% of normal) observed in 2015 over Mexico (base period: 1981–2010). (Source: National Meteorological Service of Mexico.)

experienced frost conditions (compared to the January–March average of 43.3%). Similarly, during October–December 2015, only 28.1% of the country, mainly in the northern areas, observed frost conditions, compared to the October–December average of 38.2%. During April–June, 20.2% of the country, mainly across northwestern and southern Mexico, observed hot days (compared to the average of 41.8%),

while 16.7% of the country, mainly in the northern regions, recorded hot days during July–September (much below the average of 29.6%).

(ii) Precipitation

Above-average rainfall was observed across the north-central region in 2015, while below-average conditions were present across northern Baja California, the South Pacific (coastal areas of Guerrero, Oaxaca, and Chiapas), Veracruz, and the northern Yucatan Peninsula (Fig. 7.7b). The 2015 national rainfall total of 872.0 mm (110.8% of normal) was the ninth highest annual total since national records began in 1941.

March was exceptionally wet. Two winter storms and four frontal passages led to the rainiest March since records began in 1941, with 69.6 mm of rain, providing 8.0% of the annual rainfall for the year compared to a normal contribution (14.7 mm) close to 2.0%. September, which climatologically provides the greatest amount to the annual rainfall total (18.5%), added 132.7 mm in 2015, which represents 15.2% of 2015 annual rainfall.

Nine hurricanes, which all formed in the eastern North Pacific basin (see section 4e3), impacted the nation's western coastal region, leaving, in most cases, significant rainfall. The most activity occurred in September when Tropical Storm Kevin, Hurricane Linda, Hurricane Marty, and Tropical Depression 16-E brought heavy rain to northwestern and southwestern parts of the nation.

Overall, Aguascalientes (central Mexico) and Colima (western Mexico) had their wettest year on record, while Baja California Sur and Chihuahua had their second wettest. Meanwhile, the rainfall deficits were remarkable along the South Pacific coast, with Oaxaca having its second driest year since national records began in 1941.

(iii) Notable events

An EF3 tornado struck Ciudad Acuña, Coahuila, on the morning of 25 May, causing at least 14 deaths and 290 injuries and destroying 750 homes. This was only the second tornado to reach EF3 intensity over the past 15 years, following the tornado in Piedras Negras on 24 April 2007, also in the state of Coahuila.

Hurricane Patricia was the strongest hurricane on record in the eastern North Pacific basin and one of the most intense to strike Mexico. It developed on 20 October and reached Category 5 hurricane strength on the Saffir–Simpson scale, with maximum sustained winds of 174 kt (88 m s^{-1}) and a minimum pressure of 879 mb (see section 3e4). Patricia was only the second tropical cyclone to make landfall in Mexico on the Pacific shores as a Category 5 storm since records began in the Pacific basin in 1949. The previous Category 5 landfall was in October 1959, when Hurricane No. 12 made landfall in the Tenacatita Bay, Jalisco, similar to Patricia's trajectory.

c. Central America and the Caribbean

1) Central America—J. A. Amador, H. G. Hidalgo, E. J. Alfaro, A. M. Durán-Quesada, and B. Calderón

For this region, nine stations from five countries were analyzed (Fig. 7.8). Stations on the Caribbean slope are: Philip Goldson International Airport, Belize; Puerto Barrios, Guatemala; Puerto Lempira, Honduras; and Puerto Limón, Costa Rica. Stations located on the Pacific slope are: Tocumen International Airport and David, Panama; Liberia, Costa Rica; Choluteca, Honduras; and Puerto San Jose, Guatemala. For 2015, the NOAA/NCEI GHCN daily precipitation dataset showed a considerable amount of missing data. For some stations, the daily rainfall amount was incomplete, whereas in other cases the value was flagged because it did not pass a quality control test. Precipitation historical records for the above-mentioned stations were recovered from Central American national weather services (NWS). The station climatology (1981–2010) and anomalies for 2015 were recalculated using NWS data by filling the gaps in the daily data records of the NOAA/NCEI database (especially those considered initially as zero based on the flags listed in the metadata of this database). In some stations (e.g., David and Choluteca), differences in precipitation totals between NWS data and the NOAA/NCEI dataset were as high as 420 and 560 mm, respectively, for 2015. In the station climatology, the largest differences were found in David and Liberia (490 and 820 mm, respectively). Previous years' station climatology from the NOAA/NCEI database and procedures used for all variables can be found in Amador et al. (2011).

(i) Temperature

Mean temperature (Tm) frequency distributions for the nine stations are shown in Fig. 7.8. Most stations, with the exception of Limon and Liberia, experienced a higher frequency of above-average daily mean temperatures in 2015. There was a near-normal negative skewness in Tm at Philip Goldson (Tm1) and Puerto Barrios (Tm2) on the Caribbean slope and a near-average number of cold surges during the winter months. Stations in Panama (Tm5 and Tm6) and Honduras (Tm8) show a shift to the right of the Tm distribution with a higher frequency of warm Tm values during 2015.

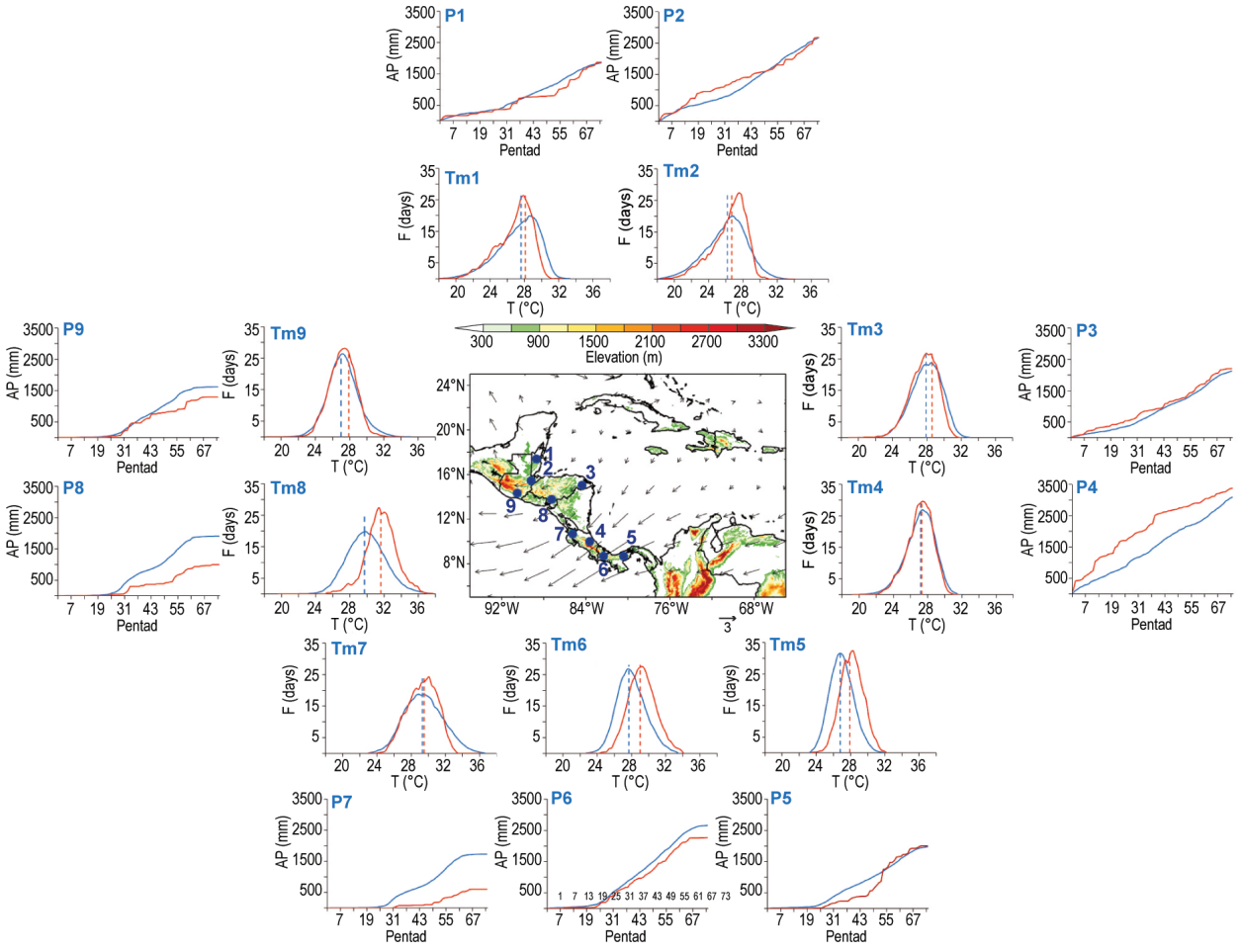

Fig. 7.8. Mean surface temperature (Tm) frequency (F; days) and accumulated pentad precipitation (P; mm) time series are shown for nine stations (blue dots) in Central America: (1) Philip Goldson International Airport, Belize; (2) Puerto Barrios, Guatemala; (3) Puerto Lempira, Honduras; (4) Puerto Limón, Costa Rica; (5) Tocumen International Airport, Panamá; (6) David, Panamá; (7) Liberia, Costa Rica; (8) Choluteca, Honduras; and (9) Puerto San José, Guatemala. The blue solid line represents the 1981–2010 average values and the red solid line shows 2015 values. Vertical dashed lines depict the mean temperature for 2015 (red) and the 1981–2010 period (blue). Vectors indicate July wind anomalies at 925 hPa (1981–2010 base period). Shading depicts regional elevation (m). (Source: NOAA/NCEI and Central American NWS.)

(ii) Precipitation

Annual precipitation totals were below normal at all stations on the Pacific slope (Fig. 7.8). At Liberia and Choluteca, the values were extremely low (in the tail of the distribution at the $p = 0.05$ level), and these areas experienced a long dry spell that extended past pentad 50 (beginning of September). Subsequent rains helped increase the accumulations later in the year, but they were not sufficient to move out of the "extremely dry" classification. A similar type of variation also occurred in Tocumen, where lack of precipitation caused an extremely dry condition until around pentad 47 (third week of August), but subsequent rains led to a close-to-normal annual total. The other stations in the Pacific slope (David and Puerto San Jose) showed no or little indication of this "late-rains" effect. Stations on the Caribbean slope observed relatively normal accumulations at the end of the year. Puerto Limon was extremely wet most of the time from the beginning of the year to pentad 40 (third week of July). A subsequent reduction of rainfall at this station resulted in moderately wetter-than-normal conditions for the year as a whole.

Low-level moisture appeared sensitive to ENSO conditions. Regional rainfall resembled conditions associated with the development of the El Niño event in 2015. Near-surface moisture flux convergence anomalies were computed based on ERA Interim reanalysis data. Results (not shown) reveal that wetter-than-normal conditions in late 2014 evolved into drier-than-normal after spring 2015.

Table 7.1. Summary of events and impacts, including number of fatalities (f), missing people (m), and affected people (a) by country and specific region. [(Sources for the Guatemala landslide in October 2015: www.redhum.org/documento_detail/17300 and the Pacific slope of Cenral America: OCHA-ROLAC (in Spanish: Oficina de Coordinación de Asuntos Humanitarios-Oficina Regional para América Latina y el Caribe, reliefweb.int/sites/reliefweb.int/files/resources/Crisis%20por%20sequia%20en%20America%20Central%20en%202015.pdf)]

Country(ies)	Dates (2015)	Hydrometeorogical Conditions	Fatalities (f) Missing People (m) Affected People (a)	Specific Region
Panamá	22 Sep	Extreme below-average rains	Unknown number of affected farmers, 2500 cattle died	Azuero Peninsula
Costa Rica	27–28 Oct	Floods	4f	Central Valley
	19 Nov	Floods	1f	Alajuela and Corredores
Nicaragua	2–14 Jun	Heavy rainfall and floods associated with low pressure systems	6f, 35 000a	Managua
El Salvador	15–20 Oct	Floods and landslides	4f, more than 210a	San Cayetano, Zaragoza, San Miguel, Luis de Moscoso
Honduras	07–15 Jun	Heavy rainfall, landslides and floods	2f, 2m, 300a	Tegucigalpa
	16–18 Oct	Floods	8f	Central Honduras
	7–8 Dec	Floods and landslides	3f	Northern Honduras
	15 Dec	Landslides	1f	Cuculmeca
Guatemala	7 Jun	Floods and landslides	8000a	Departments of Guatemala, Sacatepéquez, Santa Inés, and San Miguel Petapa
	8 Aug	Floods associated with a tropical wave	5f	Caribbean slope
	13 Oct	Landslides	274f, 353m	El Cambray II Community, and Santa Catalina Pinula
Pacific Slope of Central America	Up to 6 Oct	Extreme below-average rains	An estimated 3.5 million people affected, with more than 2 million in need of food, medical, and sanitary assistance	Azuero Peninsula, Panama; Guanacaste, Costa Rica; Pacific slopes of Nicaragua, El Salvador, Honduras, and Guatemala

(iii) Notable events

Tropical storm activity during 2015 was below average for the Caribbean basin (6°–24°N, 60°–92°W). There were three named storms: Danny, Erika, and Joaquin. Joaquin became a hurricane and reached major hurricane status in early October. No significant impacts were reported for Central America associated with any of these tropical systems. Stronger-than-average Caribbean low-level jet (CLLJ; Amador 1998), 925-hPa winds during July (vectors in Fig. 7.8) were consistent with El Niño (Amador et al. 2006). Central America experienced contrasting hydrometeorological conditions between the Pacific and Caribbean slopes from January to May. The impacts were severe, but different, across the region (Table 7.1).

2) Caribbean—T. S. Stephenson, M. A. Taylor, A. R. Trotman, S. Etienne–LeBlanc, A. O. Porter, M. Hernández, D. Boudet, C. Fonseca, J. M. Spence, A. Shaw, A. P. Aaron-Morrison, K. Kerr, G. Tamar, D. Destin, C. Van Meerbeeck, V. Marcellin, A. C. Joseph, S. Willie, R. Stennett-Brown, and J. D. Campbell

Prevailing El Niño conditions were associated with below-normal annual rainfall and above-normal annual mean temperatures over much of the region (Fig. 7.9). Abundant dry and dusty air from the Sahara Desert in Africa also contributed to the dry weather for the year, particularly during the first six months. The base period for comparisons is 1981–2010.

(i) Temperature

Some Caribbean countries, including Anguilla, Barbados, Cayman Islands, Cuba, Dominican Republic, St. Kitts and Nevis, St. Maarten, and St. Lucia, experienced above-normal to record temperatures during 2015. The average annual temperatures were the highest on record since 1951 for Cuba (26.6°C) and second highest since 1946 for Piarco, Trinidad (27.4°C). Other temperature extremes for Piarco include the highest mean maximum temperature since 1946 for October (33.6°C) and November (32.7°C) and the second highest for August (33.6°C). V. C. Bird International Airport, Antigua, recorded its second-highest maximum temperature of 34.6°C (on 30 September) since records began in 1971 and observed a high mean minimum temperature of 24.5°C for the year, tying the record set in 2001 and 2002. Sangster International Airport, Jamaica, recorded its highest mean maximum temperature for May (33.0°C) since 1973, and Crown Point, Tobago, set records for August (33.2°C), September (33.9°C), and November (33.0°C) since records began in 1969. During October–December, record high mean maximum temperatures were observed in Freeport, Bahamas (25.3°C), and Grand Cayman (31.3°C) since 1990 and 1971, respectively, and the highest absolute maximum temperature was observed for Dominica (35.5°C) in the 45-year record.

(ii) Precipitation

While annual rainfall for 2015 was below normal for most of the Caribbean, contrasting rainfall anomalies were observed in some territories during the first quarter of the year. The January–March rainfall was above normal for Dominican Republic, Grenada, Aruba, Barbados, and eastern Jamaica, and below normal for Anguilla, Antigua and Barbuda, and St. Maarten. St. Thomas, U.S. Virgin Islands, recorded its wettest February (339.1 mm) since 1953. The transition to drier conditions commenced in the second quarter for Aruba, Dominican Republic, and Jamaica, with Dominica, Guadeloupe, St. Kitts, and St. Lucia also recording very dry conditions.

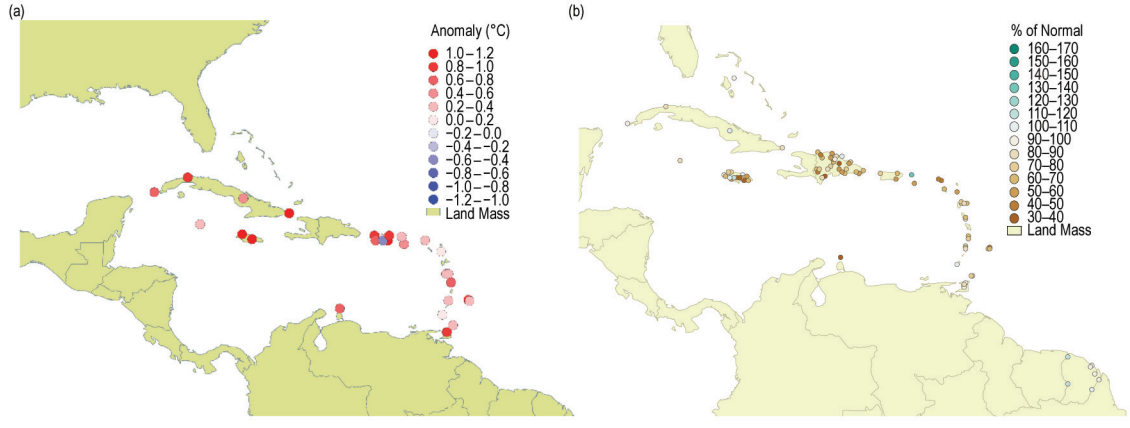

Fig. 7.9. Annual (a) temperature anomalies (°C) and (b) percent of normal (%) rainfall for 2015 across the Caribbean basin with respect to the 1981–2010 annual mean. (Source: Caribbean Institute for Meteorology and Hydrology and the Instituto de Meteorología de la República de Cuba.)

Dry weather persisted from July to September across much of the Caribbean, including Aruba, Barbados, central Cuba, Grand Cayman, Dominica, southern and eastern Dominican Republic, Grenada, western Jamaica, the Leewards, and St. Lucia, though in August, wet conditions were recorded for Dominica and below-normal to near-normal rainfall for Puerto Rico. This is consistent with a below-normal Atlantic hurricane season (see section 4e2) in relation to El Niño that produced strong vertical wind shear, increased atmospheric stability, and subsidence over the Atlantic. July was the driest on record for St. Maarten (8.4 mm) since 1953 and second driest for St. Thomas (5.6 mm). Tobago had its fifth driest August (83.3 mm) since 1969.

For the last quarter, very dry conditions were recorded in Antigua, Aruba, Dominica, and northwestern Dominican Republic, with very wet conditions in northern Dominican Republic and western Puerto Rico. Antigua's all island-averaged rainfall for December was 49.0 mm, its 10th driest on record, and rainfall for the three-month period of October–December was the ninth lowest on record (246.1 mm) since 1928. Record-low October–December rainfall was also observed at a number of stations, including Bowmanston, Barbados, (245.1 mm) since records began in 1981, and Rio San Juan and Villa Vasquez in Dominican Republic (230.7 and 31 mm, respectively) since 1971.

A number of territories and stations recorded their driest year (Table 7.2). The second driest year was observed at Hewanorra, St. Lucia, (1336.6 mm) since 1973 and the third driest for Jamaica (1308.0 mm) since 1881 and St. Croix (586.0 mm) since 1951. Conversely, St. Thomas (1276.4 mm) observed its sixth wettest year on record since 1953.

Table 7.2. List of Caribbean territories and stations that had their driest year in 2015.

Station/Country	Annual rainfall recorded (mm)	Year records began
Antigua	574.5	1928
Aruba	134.2	1971
St. Barths	465.6	1971
St. Maarten	495.4	1953
Tobago	1064.6	1969
Grantley Adams, Barbados	789.5	1979
Santo Domingo, Dominican Republic	813.8	1971
Potsdam, Jamaica	762.0	1971
George F. L. Charles Airport, St. Lucia	1148.6	1967

(iii) Notable events

Several significant events impacted the Caribbean in 2015:

- Prevailing droughts were observed in Anguilla, Antigua, Barbados, Cuba, Dominica, Dominican Republic, Jamaica, Puerto Rico, St. Kitts and Nevis, and St. Lucia, with widespread agricultural losses and/or very low water production and rationed distribution. St. Lucia declared a water emergency for the period May to August amid continuing drought.
- Water shortage was experienced in the eastern half of Puerto Rico, with San Juan (capital of Puerto Rico) having strict water rationing for much of 2015.
- Low rainfall totals in 2015 in Antigua led to Potworks Dam, with a capacity of 1 billion gallons, being completely dry. There were more bushfires than usual, and 65% of farmers were forced out of business. The drought continued throughout 2015 and was deemed the worst on record. The duration of the drought conditions in Antigua was the second longest of any drought on record and, by far, the greatest deficit of rainfall (records date to 1928). The longest drought occurred in 1964–67, lasting 32 months. The return period for 2015 rainfall is 1 in 500 years.
- On 27 August, flash floods from Tropical Storm Erika caused catastrophic damage across Dominica, dumping over 320.5 mm of rain in 12 hours, with 225.0 mm in less than six hours.

d. South America

Positive SST anomalies were present along the tropical equatorial Pacific since the beginning of 2015. With the onset of El Niño, SST anomalies increased and expanded along the southeastern Pacific Ocean during the second half of the year. As is typical, El Niño influenced regional weather conditions in South America during most of 2015 (Fig. 7.10).

The annual temperature and precipitation anomalies were computed using data from 1190 stations provided by national meteorological services from South America and processed by El Centro Internacional para la Investigación del Fenómeno de El Niño (CIIFEN). Air temperature was above normal across most of the continent, with anomalies 0.5°–2.0°C (Fig. 7.11a) above average. El Niño impacts across

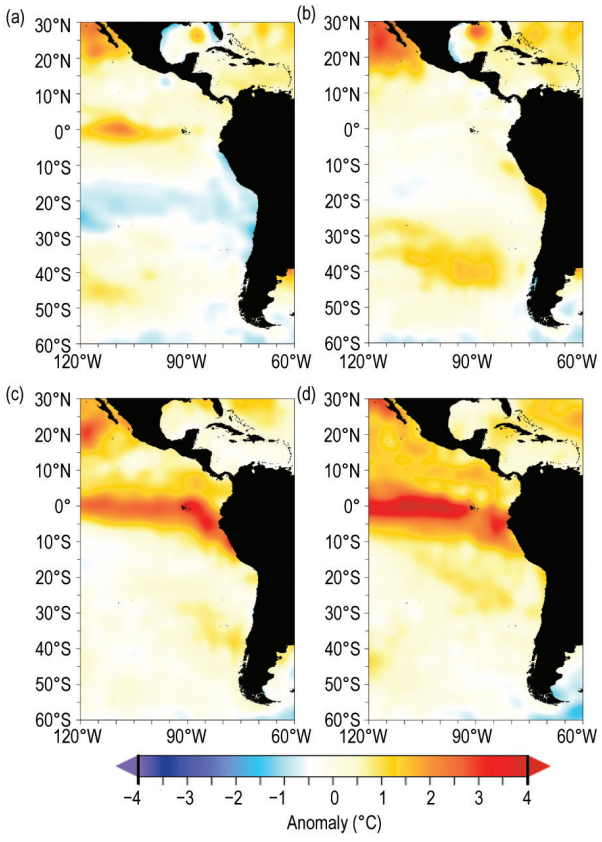

Fig. 7.10. Seasonal mean sea surface temperature anomalies (°C) for 30°N–60°S, 120°–60°W (base period: 1971–2000). Data source: NOAA–NCEP (Processed by CIIFEN, 2016).

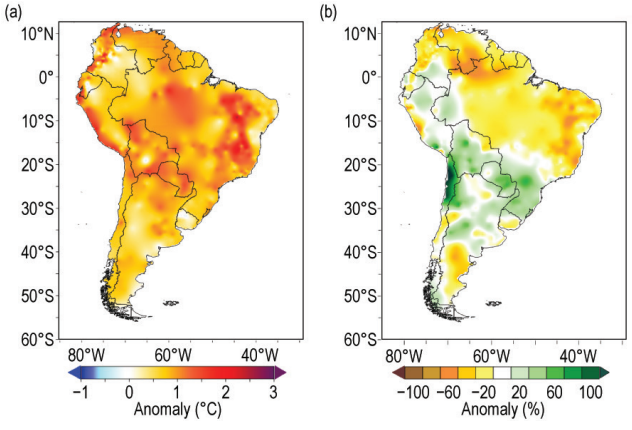

Fig. 7.11. 2015 South American annual (a) temperature anomalies (°C) and (b) precipitation anomalies (%; base period: 1981–2010). (Sources: Data from 1190 stations provided by National Meteorological Services of Argentina, Brazil, Bolivia, Chile, Colombia, Guyanas, Ecuador, Paraguay, Peru, Suriname, Uruguay, and Venezuela. The data were compiled and processed by CIIFEN 2016).

South America generally include, but are not limited to, drier-than-average conditions across northern South America, with wetter-than-average conditions across the southeast. Dry conditions, observed since 2014, persisted and, in some instances, deteriorated during 2015, especially in northern South America. Above-normal precipitation with severe impacts was observed in southeastern South America (Fig. 7.11b). Along the west coast of South America, the El Niño effects during the last quarter of the year were modulated by regional factors such as the persistent positive sea level pressure anomalies in the southeastern Pacific Ocean and strong winds, which reduced convection near Ecuador and northern Peru.

All anomalies in this section are with respect to the 1981–2010 average unless otherwise noted.

1) Northern South America and the tropical Andes—R. Martínez, A. Malheiros, J. Arévalo, G. Carrasco, L. López Álvarez, J. Bazo, J. Nieto, and E. Zambrano

This subsection covers Bolivia, Colombia, Ecuador, Peru, and Venezuela.

(i) Temperature

Above-normal temperatures were predominant across Venezuela throughout the year. In the highlands (Tolima) and Caribbean coast (Cesar) of Colombia, record maximum temperatures were observed in September and December, respectively, with anomalies as high as +5°C. In Ecuador, above-average temperatures were present most of the year, with anomalies of +1.5°C to +2.0°C. Temperatures across Peru were above normal during March–May and June–August. During July and August, above-average temperatures (between +1°C and +4°C) were observed along the coastal zone, in some instances surpassing record high temperatures set in 1998. In Bolivia, temperatures were near- to above normal most of the year. From August to November, at least 12 maximum temperature records were reported at stations in central and eastern Bolivia.

(ii) Precipitation

Venezuela and Colombia experienced drier-than-normal conditions during 2015. During the first half of the year, anomalous subsidence was the main driver for the lack of precipitation in northern and southeastern Venezuela, which was just 40%–60% of normal. On the Caribbean coast of Colombia a slight precipitation deficit was also observed in this period. During the second half of the year, as a consequence of the El Niño onset, precipitation anomalies were 50%–70% of normal across most of Venezuela

and as little as 20% of normal in the Andean region (Departments of Tolima, Huila, Cauca, Valle) and Caribbean (central and northern) regions in Colombia. In Ecuador, precipitation was above normal during the first half of the year, with anomalies up to 200% of normal on the central coast. During the second half of the year, precipitation over the Amazon region was 50%–80% of normal; meanwhile, precipitation was 120%–150% of normal in the northern and central coastal regions during September–November. In Peru, extreme below-normal precipitation was observed in the northwest of the country and in the southern Andes. Above-normal precipitation prevailed during the second half of 2015 in the southern and central Amazon region.

In northern Bolivia, precipitation was above normal from January to August, with anomalies up to 159% of normal during March–May. During September–November, 88% of normal precipitation was observed. Over the Altiplano region (western Bolivia), precipitation was predominately above normal with anomalies ranging from 117% to 149% of normal throughout the year. In central Bolivia, precipitation was near normal. Above-normal precipitation (up to 150% of normal) was recorded in southeastern Bolivia during June–August. Below-normal precipitation (63% of normal) was observed during September–November.

(iii) Notable events

On 24 March, unusually heavy rainfall caused landslides in the District of Lurigancho-Chosica (Lima region), Peru, leading to eight fatalities and destroying over 150 houses.

During April, northwestern Venezuela experienced a week-long heat wave, with some stations registering daily maximum temperatures as high as 40°C (April average maximum temperature is 34.9°C).

Northern Ecuador was affected by flooding during December that caused crop and cattle losses.

Colombia and Venezuela were impacted by a severe drought during most of the year, causing restrictions in water supply for human consumption, agriculture, and hydropower generation.

2) Tropical South America east of the Andes—J. A. Marengo, J. C. Espinoza, J. Ronchail, and L. M. Alves

This region includes Brazil, Paraguay, southern Venezuela, and the Amazon lowland sectors of Peru, Colombia and Bolivia.

(i) Temperature

Monthly mean temperatures across most of the region were about 1°–3°C higher than average most of the year. In São Paulo, Brazil, the January mean temperature was 3.5°C above normal—the second warmest January since 1943. In October, temperatures were about 4°–5°C above normal in southeastern and west central Brazil, with the most notable warmth in Rio de Janeiro, which recorded a maximum temperature of 40°C, compared to the average October maximum temperature of 25°C. Maximum temperatures were slightly above average for autumn (March–May) and winter (June–August), with a mean temperature anomaly of +1.0°C. Notable temperatures of 2.0°–3.0°C above average were observed across Paraguay in June.

Various cold fronts during May–September brought well-below-freezing temperatures, hail, and the highest snowfall in 10 years in the Andean region, located more than 3500 meters a.s.l.

(ii) Precipitation

Below-average rainfall (20%–75% of normal) was observed over southeastern Brazil, eastern Bolivia, and Paraguay during January–March. An atmospheric blocking pattern and a high pressure system over large parts of tropical Brazil and the South Atlantic, together with the absence of the South Atlantic convergence zone during January, were responsible for the lack of precipitation over most of subtropical South America east of the Andes, which lasted through mid-February. Between April and December, rainfall totals of 20%–50% of normal were recorded in northeastern Brazil, north-central Amazonia, eastern Peru, and the Amazon lowland sectors of Colombia and Venezuela. A weak and/or anomalously northward displaced intertropical convergence zone contributed to the below-average precipitation.

(iii) Notable events

Drought conditions in southeastern Brazil that began in January 2014 (Nobre et al. 2016) continued through April 2015, particularly over the Cantareira reservoir system, which supplies water to nearly half of São Paulo's population (about 18 million residents). Summer (December–February 2014/15) rainfall was marginally less than average. However, during November and December 2015, above-average rain (100–150 mm month^{-1} above normal) fell over the region, allowing the Cantareira Reservoir system to recover its volume.

The drought conditions that started in 2012 in northeast Brazil continued to persist in 2015, however, with less severity (Fig. 7.12a). Figure 7.12b shows that very dry conditions were present across the northern

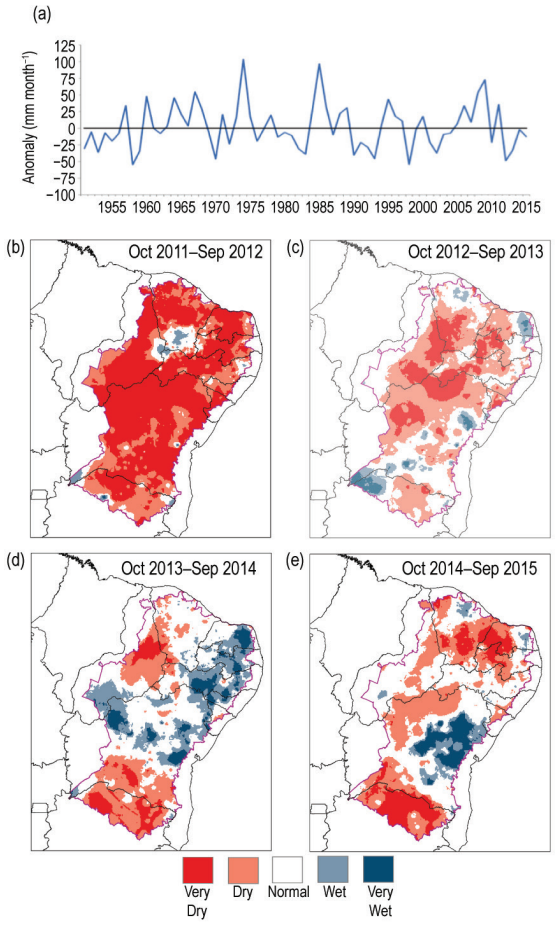

Fig. 7.12. (a) Average rainfall anomalies (mm month^{-1}) during the peak rainy season (Feb–May) in northeast Brazil for 1951–2015. (Source: Global Precipitation Climatology Centre; updates from Marengo et al. 2013.) (b) Categories of observed precipitation based on percentiles for northeast Brazil during the hydrological year Oct–September (b) 2011/12, (c) 2012/13, (d) 2013/14, and (e) 2014/15. (Source: CEMADEN.)

part of the state of Bahia, and particularly in the semiarid region of northern northeast Brazil and the region between southern Bahia and the northern parts of the state of Minas Gerais. The extreme dry conditions observed in this region contributed to an increase in wildfires and damages to crops, with local residents depending on water to be trucked in.

Between January and April, 32 000 families were affected by heavy rains in the lowlands of Bolivia, with the worst impacts occurring on 20 February when the Acre River flooded the city of Cobija, capital of Pando in western Amazonia.

As a result of heavy rains in the northwesternmost Amazonian regions (north of the Peruvian Amazon and western state of Amazonas in Brazil), the Peruvian government declared a state of emergency on 9 April. During March and April, more than 115 000 people were affected by floods. Also, in April, flooding and landslides affected more than 20 000 people in Colombia. On 29 June, heavy rainfall in southern and southwestern Venezuela caused flooding, with more than 40 000 people affected. On 4 April, a severe storm hit several towns in the department of Concepción in northern Paraguay, affecting houses, crops, and farm animals. Authorities estimate that 5000 people were affected. Precipitation patterns shifted in October, as is typical during the presence of El Niño in the tropical Pacific Ocean (see section 4b), resulting in above-average rainfall across the same region. Abundant rainfall over southern Brazil and most of the La Plata basin caused significant floods.

During 8–10 July, minimum temperatures between –18°C and –22°C were measured in high areas of the Arequipa, Moquegua, Tacna, and Puno regions of the Peruvian southern Andes. According to the Empresa de Pesquisa Agropecuaria e de Extensao Rural of the state of Santa Catarina (EPAGRI) in southern Brazil, the same cold spell affected the southern region of Brazil, with minimum temperatures ranging between –3.0°C and 2.0°C in the highland city of São Joaquim on 5 July, compared with the average July minimum temperature of 6.1°C.

The above-normal rainy season in southeastern South America, which typically starts in October and ends in May, was 100–300 mm above normal in December 2015, leading to floods in Paraguay, Bolivia, and southern Brazil due to the overflow of the main rivers. The highest levels in 110 years were recorded along the Paraguay River, which produced slow-onset flooding that forced the evacuation of 18 545 families in the city of Asunción. Four people died and 130 000 were evacuated by the end of the year.

3) Southern South America—M. Bidegain, J. L. Stella, M. L. Bettolli, and J. Quintana

Argentina, Chile, Uruguay, and adjacent areas of southern Brazil are considered here.

(i) Temperature

Above-normal temperatures were observed over most of southern South America (SSA) during 2015, with mean temperature anomalies between +0.5°C and +1.5°C (Fig. 7.11a). According to preliminary analysis of the official data for 2015, the mean temperature anomaly for Argentina and Uruguay was estimated to be +0.71°C and +0.51°C, respectively. Argentina had its second warmest year in the country's 55-year period of record, behind 2012, with the past four years (2012–15) the four warmest on record. The cities of Buenos Aires, Iguazú, Santa Fé, Rosario, and Pehuajó were each record warm in 2015. Chile observed warmer-than-

average monthly temperatures most of the year. The largest positive annual anomalies were observed in the northern (+1.1°C) and central (+1.0°C) regions; however, September and October were cooler than average in the central and southern regions. Above-normal maximum temperatures were observed in Chile, particularly in the central region, with anomalies between +1.0° and +1.5°C.

Summer (December–February) 2014/15 had near-average temperatures, with no significant heat waves observed across Argentina and Uruguay. In Chile, anomalies of −0.8°C were observed across the north coast.

Autumn (March–May) was extremely warm. The most notable warmth was observed during April and May, with mean temperature anomalies as high as +2.0°C and +2.5°C in central Argentina and Uruguay, respectively. Argentina observed its warmest autumn since national records began in 1961, with a mean temperature 1.51°C above average. Chile had above-average temperatures during March–May, with much of the central to northwest regions 1.5°–3.0°C above average.

Above-average temperatures were observed across much of SSA during winter (June–August), with the most notable warmth across northeastern Argentina, Uruguay, southern Brazil, and Chile, where mean temperatures anomalies were as high as +3.0°C. Argentina also had its warmest winter on record. Much warmer-than-average conditions dominated the country during August, with many locations experiencing record high temperatures.

Below-average temperatures were present across Argentina, Uruguay, and Chile during spring (September–November). In Chile and central and southern Argentina, an increase in frequency of frontal systems and abundant cloudiness resulted in the region's coldest October on record. In Argentina, anomalies were 6°–7°C below average in some areas and more than 35% of stations set new daily low temperature records. Extremely cold conditions, including rare snowfalls and late frosts, affected Buenos Aires province during September and the Cuyo region during October.

(ii) Precipitation

Drier-than-average conditions were observed during January–July, especially from March to July, in eastern Argentina (Corrientes, Entre Ríos, and Buenos Aires provinces), northeastern Argentina (Misiones province), Uruguay, and central Chile. During August–December, above-average precipitation fell across central and northeastern Argentina, northern Uruguay, southern Brazil, and central Chile, as is typical during El Niño. The 2015 annual rainfall for Argentina and Uruguay was 109% and 103% of normal, respectively, and marked the second consecutive year since 2013 in which precipitation was above average in Argentina. However, some regions south of 34°S in Uruguay and Buenos Aires province recorded below-normal precipitation in 2015. As a result of severe water deficit, the Minister of Agriculture in Uruguay declared an "agricultural emergency" in May to assist farmers. Santiago, the capital of Chile, had its driest June on record, with no precipitation recorded for the first time since records began in 1866. During the second half of 2015, especially during October–December, some locations in northeastern Argentina and northern Uruguay were severely affected by floods, especially cities located near the Paraná and Uruguay Rivers.

(iii) Notable events

Some areas of southern Chile experienced their driest January in at least 65 years. In northern Chile, unusually heavy rainfall during 24–26 March impacted the extremely dry regions of Atacama and Antofagasta. Some areas received well over their annual rainfall during this event. Antofagasta received 24.4 mm of rainfall in a 24-h period during 25–26 March (normal annual average rainfall for this location is 1.7 mm). Three people were killed by the impacts of the floods in Antofagasta and 23 people perished in Atacama.

Heavy precipitation fell across parts of northeastern Argentina in August. The downpours overflowed rivers and produced floods. The highest rainfall totals during August were in eastern Argentina, mainly in the south of the province of Corrientes, Entre Ríos, and northeast of Santa Fé, where values reached 300 mm. There was also significant precipitation in the province of Buenos Aires, with 200–250 mm recorded in August. Many other locations set new August precipitation total records (Table 7.3).

During December, abundant precipitation fell over northeastern Argentina and Uruguay, with several locations setting new records for the month (Table 7.4). Heavy rainfall mainly affected Corrientes and Misiones provinces in Argentina, with thousands of people forced to evacuate.

Above-normal temperatures and below-normal rainfall at the beginning of 2015 in Patagonia (southern Argentina) favored the development of one of the largest wildfires in the history of Argentina. The fire lasted nearly two months and burned 41 000 hectares of native forests.

Table 7.3. Locations in Argentina that set new August precipitation totals (mm) in 2015.

Locations	2015 Record (mm)	Previous Record (mm)
Reconquista	330.2	138.8 (1956)
Mercedes Aero	170.0	134.3 (1975)
Paso de los Libres Aero	188.0	182.9 (1971)
Monte Caseros Aero	262.6	218.0 (1972)
Concordia Aero	358.8	198.0 (2012)
Junin Aero	201.0	151.4 (1976)
San Fernando	252.1	237.1 (2012)

Table 7.4. Locations in Argentina that set new December precipitation totals (mm) in 2015.

Locations	2015 Record (mm)	Previous Record (mm)
Formosa	425.3	357.5 set in 1979
Posadas Aero	466.9	416.1 set in 2012
Oberá	477.0	447.5 set in 2012
Mercedes Aero	458.1	337.0 set in 1968
El Calafate	42.2	30.5 set in 2012

e. *Africa*

In 2015, most of Africa experienced above-average temperatures and below-average precipitation. Extreme weather caused loss of life and property damage in many parts of the continent. This extreme weather included torrential rains across western Africa and heavy rainfall related to a tropical storm over western Indian Ocean island countries. In contrast, eastern African countries, including Ethiopia, Somalia, and parts of Kenya, were impacted by drought. The drought in Ethiopia, the worst in several decades, was associated with the El Niño that developed early in the year. Extreme high temperatures were observed over northern, southern, and southwestern parts of Africa.

The 2015 climate assessment for Africa is based on the 1981–2010 reference period. Both observed and reanalysis datasets are presented for analysis.

1) Northern Africa—K. Kabidi, A. Sayouri, M. ElKharrim, A. Ebrahim, and A. Mekonnen

Countries considered in this region are Morocco, Algeria, and Egypt. Overall, below-normal precipitation and above-normal temperature conditions dominated during 2015. The annual temperature was the warmest since 1960 over Morocco, and successive heat waves were observed both during winter and summer in Egypt. Heavy downpours were reported in May and August 2015 in Morocco.

(i) Temperature

The annual mean maximum temperature over northwestern Morocco was about 1°C higher than normal. However, temperatures during January and February were markedly below average in association with a cold air surge from the Black Sea to the Maghreb (northwestern African countries). In January, temperatures were 2.4°C below normal in northeastern Morocco. In February they were 2.7°C below normal in southern Morocco. Generally, the winter (December–February 2014/15) mean surface seasonal temperatures over Algeria and Morocco were about 1°C below normal (Fig. 7.13), while winter surface temperatures over Egypt were mainly above normal. However, minimum temperatures as low as 1°C were observed in January in northeastern Egypt.

Temperatures during spring, summer, and autumn were all above normal in Morocco and Algeria. The average mean monthly temperature in Morocco and Algeria was 3°C above normal in May (Fig. 7.14). Overall, summer temperatures in Egypt were above normal, while isolated locations recorded below-average temperatures.

(ii) Precipitation

Annual precipitation was marked by deficits over southern Egypt and surpluses over the northern regions. Winter precipitation was about 50% of normal over western Egypt, while heavy rainfall events

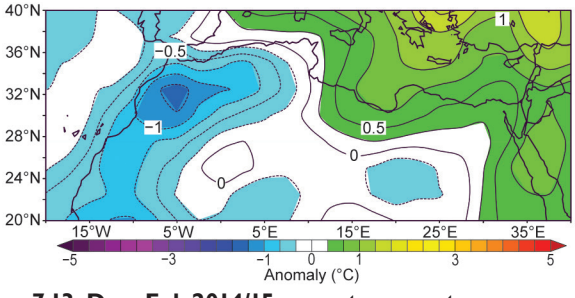

Fig. 7.13. Dec–Feb 2014/15 mean temperature anomaly (°C; base period 1981–2010). (Source: NCEP–NCAR reanalysis.)

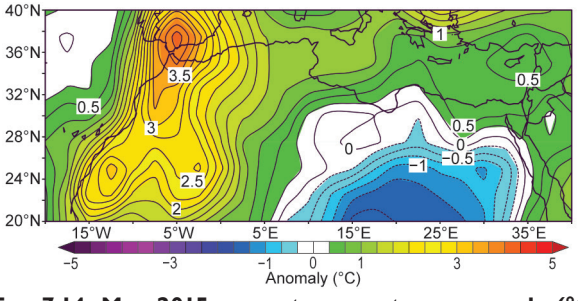

Fig. 7.14. May 2015 mean temperature anomaly (°C; base period 1981–2010). (Source: NCEP–NCAR reanalysis.)

were observed in January. Winter precipitation over Morocco was also highly variable. The average deficit in Morocco was about 89% of normal in January and 71% of normal in February (Fig. 7.15). Lack of rainfall was associated with dominant atmospheric high pressure conditions on the Moroccan Atlantic coast and in western Europe.

Monthly precipitation in spring was generally below normal in Morocco. However, above-normal rainfall ranging between 145% and 230% of normal was observed in March across central Morocco. New 24-h rainfall records ranging between 20 and 55 mm were observed during 23–25 May at various places in Morocco.

Convective precipitation brought extreme weather conditions in summer, especially during July and August, leading to excess rainfall, with an average amount of around 158% of normal over Morocco. Total precipitation received during August was well above normal (e.g., 45 mm at Marrakech compared to the normal of 2.7 mm; 23.2 mm at Sidi Ifni compared to the normal of 2.1 mm).

Unlike the recent autumns of 2013 and 2014, which were marked by a series of above-normal rainy conditions, autumn precipitation in 2015 was generally below normal over most of Morocco. Monthly rainfall ranged from 7% of normal at Casablanca to about 86% of normal at Midelt.

(iii) Notable events

During January and February, a series of cold spells affected the region, resulting in heavy snow. Three meters of snow fell over northeastern Morocco during February, the highest total for February in the past 30 years. In Egypt, Alexandria received much-above-normal rainfall in October (238% of normal). A record rainfall of 127 mm was observed on 6 October 2015 at Alexandria.

Conversely, May, July, and August were marked by several heat waves (defined as daily maximum temperatures much higher than the daily mean), resulting in high maximum temperatures. These heat waves were associated with continental dry air intrusions from the intense heat source in the Sahara. The heat waves, associated with an east wind, caused several forest fires, which devastated hundreds of hectares of forest, especially in northern Morocco. In Luxor, Egypt, a record temperature of 48°C was observed on 28 May.

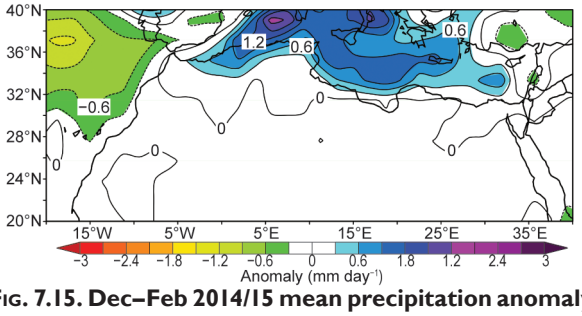

Fig. 7.15. Dec–Feb 2014/15 mean precipitation anomaly (mm day^{-1}; base period 1981–2010). (Source: NCEP–NCAR reanalysis.)

2) West Africa—S. Hagos, I. A. Ijampy, F. Sima, S. D. Francis, and Z. Feng

West Africa refers to the region between 17.5°W (eastern Atlantic coast) and approximately 15°E (along the western border of Chad) and north of the equator (near Guinea coast) to about 20°N. Countries included are Senegal, the Gambia, Guinea-Bissau, Guinea, Sierra Leonne, Liberia, southern regions of Mali and Niger, Burkina-Faso, Côte d'Ivoire, Ghana, Togo, Benin, Cameroon, and Nigeria. It is often divided into two climatically distinct sub regions: the semiarid Sahel region (north of about 12°N) and the relatively wet coast of Guinea region to the south.

(i) Temperature

The annual mean temperature over West Africa was slightly above the 1981–2010 average with much of the northwestern Sahel region about 0.5°C above average. In May, much warmer-than-average conditions were reported over the region, with record warmth observed in Togo, Benin, and Burkina Faso. The majority of northern cities in Nigeria experienced above-average mean temperatures. Minna, Yelwa, Zaria, Katsina, and Kano experienced the highest annual mean temperature departures for 2015, as did Benin, Ikom, Ondo, and Warri in the South. Similarly, record high temperatures were observed across eastern Senegal in June, while Sierra Leone, central Mauritania, and eastern Nigeria recorded temperatures up to 3°C above normal in July (Fig. 7.16). The maximum temperature over the western part of The Gambia was higher than normal (by 3%–6%), while the minimum temperature increased by 5%–8% compared with normal in the central and eastern part of the country. Warmer-than-average conditions persisted over most of West Africa during August and September.

(ii) Precipitation

Wetter-than-average conditions persisted over most of the Sahel region. Rainfall totals for June–September, during which time the West African monsoon provides much of the annual precipitation, are shown in Fig. 7.17a. Relatively dry conditions prevailed over most of the coast of the Gulf of Guinea

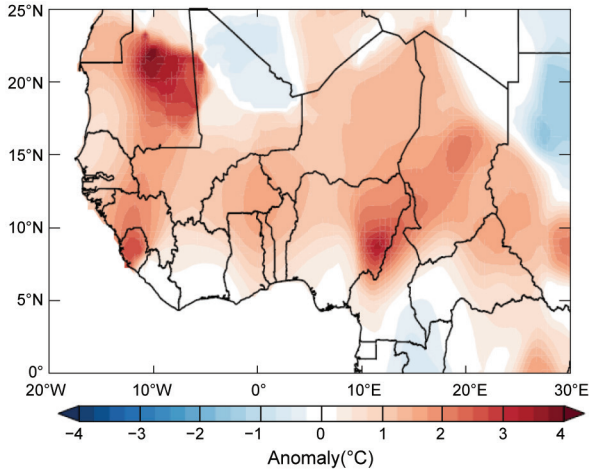

Fig. 7.16. Temperature anomalies (°C) for West Africa in Jul 2015 (base period: 1981–2010). (Source: NOAA–NCEP reanalysis.)

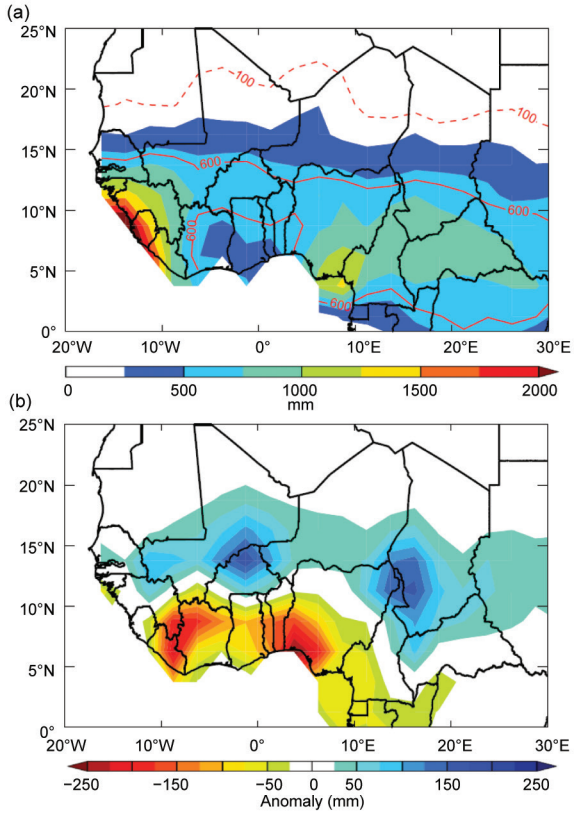

Fig. 7.17. (a) Jun–Sep 2015 precipitation (mm) for West Africa as total accumulated precipitation. The red dashed and solid lines mark 100 mm and 600 mm isohyets. (b) Jun–Sep 2015 precipitation anomaly, departure from 1981–2010 normal. (Source: NOAA–NCEP Reanalysis.)

region from Liberia to Cameroon. Specifically, much drier-than-normal conditions over the Niger Delta and wetter-than-normal conditions in the Lake Chad region were observed during summer. Rainfall over most parts of Nigeria was near normal. However, wetter-than-normal conditions were experienced over parts of central and northern Nigeria and drier conditions over pockets in the southwestern and eastern parts. The Gambia experienced a late onset of rains with late withdrawal and, overall, received above-normal rainfall for the season. Significant rainfall amounts prevailed during July–September, with the highest amounts, between 275 and 475 mm, recorded in August. The greater part of The Gambia experienced significant annual rainfall, ranging from 750 mm to more than 1000 mm. The country average seasonal rainfall during 2015 stood at 960.5 mm, 136% of the 1981–2010 mean (705.1 mm). The above-average rainfall over much of West Africa resulted in an above-average harvest according to the Famine Early Warning Systems Network. The dipole-like precipitation with a dry Guinean coast and wet Sahel region (Fig. 7.17b) often occurs as the intertropical convergence zone (ITCZ) precipitation is shifted farther north due to warmer SSTs over northeastern subtropical Atlantic and cooler-than-average SST conditions over the southeastern subtropical Atlantic (e.g., Hagos and Cook 2008). This condition persisted throughout the summer, especially notable during August and then into September. El Niño, typically associated with dry conditions over the Sahel (Janicot et al. 1998), had relatively little impact this year.

(iii) Notable events

In northern Nigeria, torrential rain led to the failure of a dam in August. According to the UN Office for the Coordination of Humanitarian Affairs, 300 000 people were affected by the associated floods associated. Flash floods were also reported in some states. The floods led to 53 fatalities and destruction of property in about 11 states, and displaced about 100 000 people from their homes.

In early June, Togo, Benin, and Ghana experienced significant flooding; on 3 June, 84 mm of rain fell in Cotonou, Benin, in a 24-h period. Local media reported that flooding damaged several homes and blocked streets in the largest city and economic center of Benin.

The 2015 wet season (July–September) for The Gambia was characterized by several extreme events, including floods, lightning, and windstorms, resulting in loss of life and significant disruption in livelihood.

3) Eastern Africa—G. Mengistu Tsidu

Eastern Africa refers to countries located within 20°–50°E and 15°S–20°N. The region is comprised of the Sudan, South Sudan, Ethiopia, Eritrea, Dji-

bouti, and north and central Somalia, which are located north of 5°N, with the main rainfall season in June–September; southern Somalia, Kenya, northern Tanzania, Uganda, Rwanda, and Burundi, located between 5°N and 5°S, with the main rainfall season in March–May; and central and southern Tanzania, located south of 5°S, with the main rainfall season in December–February. Note also that Somalia, Kenya, northern Tanzania, Uganda, Rwanda, Burundi, and southern and southeastern Ethiopia receive a significant portion of their annual rainfall in autumn, with a peak rainfall shifting from October over Ethiopia and Somalia to November over the rest of the countries following the annual migration of the ITCZ. Therefore, rainfall analysis is also included for the extended September–December rainfall season.

The assessment for this region is based on rainfall from the latest version-2 Climate Hazards Group Infrared Precipitation with Stations (CHIRPS) data and European Centre for Medium-Range Weather Forecasts (ECMWF) Interim reanalysis (ERA-Interim) daily mean temperatures at a horizontal resolution of 0.25°.

(i) Temperature

The December–February 2014/15 mean temperature was above normal over Sudan, Eritrea, western Ethiopia, Djibouti, Uganda, Rwanda, Burundi, most parts of Kenya, and northwestern Tanzania (Fig. 7.18a). Near-normal temperatures over the eastern half of Ethiopia and cold anomalies of up to –2°C were observed over part of northern Tanzania. The warm anomalies observed in December–February expanded eastward to cover most parts of Ethiopia while cold anomalies over Tanzania during the same season expanded northeastward to cover Kenya, southeastern Ethiopia, and Somalia during March–May (Fig. 7.18b). During June–August, the whole region experienced warm anomalies exceeding +2°C, with the exception of some pockets over northern Tanzania, western Kenya, and southwestern Ethiopia, which reported normal to below-normal temperatures (Fig. 7.18c). The mean temperature remained above normal during September–November over most parts of the region, with the exception of below-normal temperatures at places in northern Tanzania and along the Ethiopia–Somalia border (Fig. 7.18d).

(ii) Precipitation

During December–February 2014/15, southern Uganda, Rwanda, Burundi, northern Tanzania, and southern Kenya received substantially below-normal rainfall. However, some places in Tanzania and southern Kenya along the coast received 110%–150% of their normal precipitation (Fig. 7.19a). Rainfall during March–May was normal to above normal

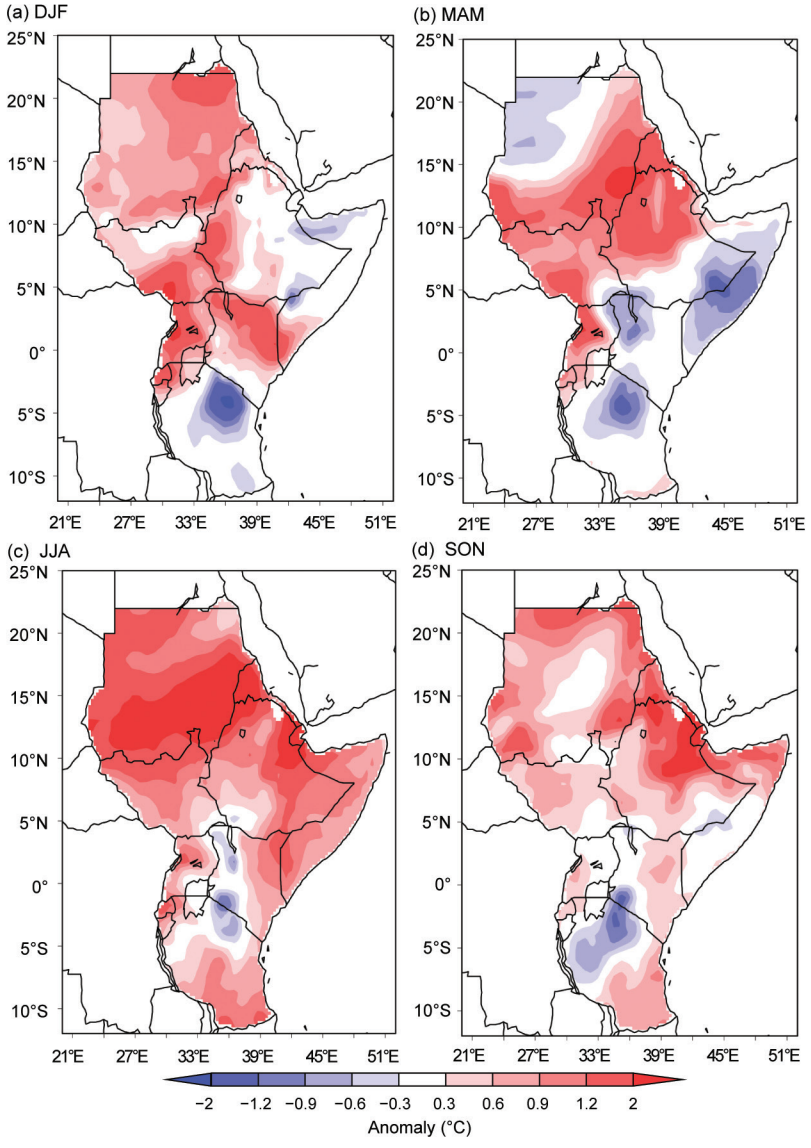

Fig. 7.18. Eastern Africa seasonally averaged mean temperature anomalies (°C) for (a) DJF 2014/15 and (b) MAM, (c) JJA, and (d) SON 2015, with respect to the 1981–2010 base period.

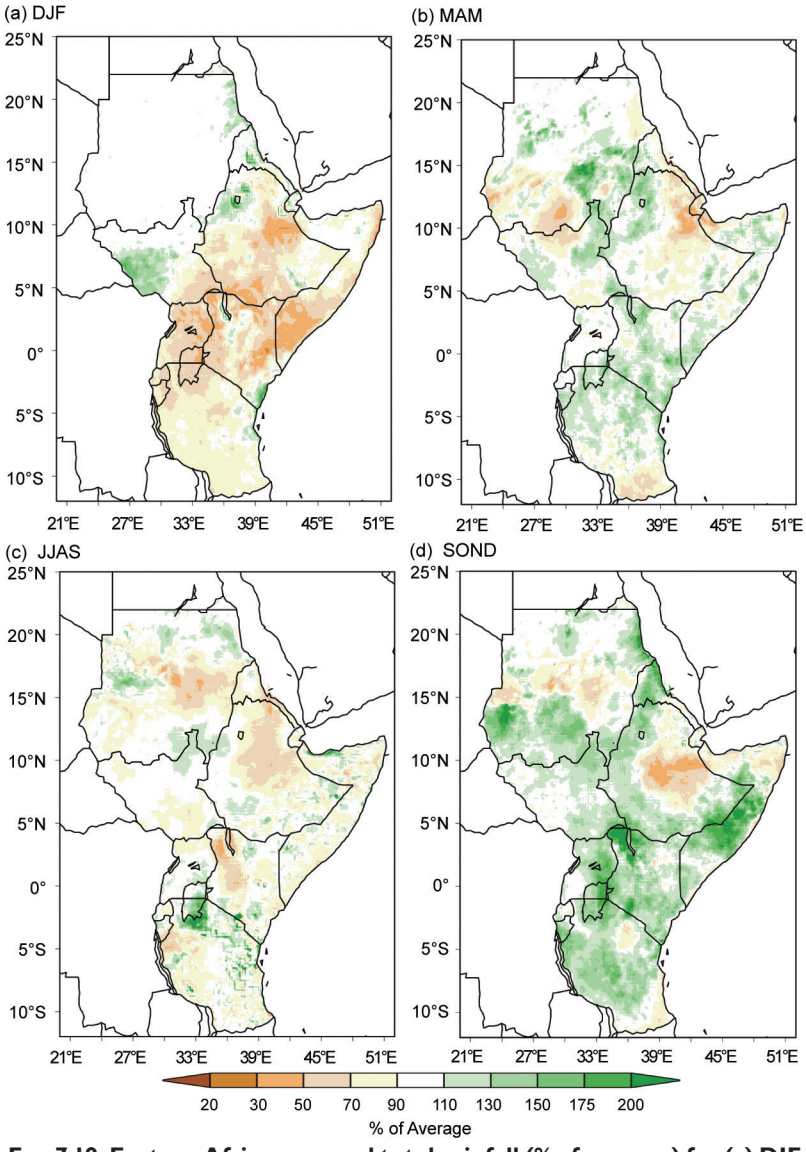

Fig. 7.19. Eastern Africa seasonal total rainfall (% of average) for (a) DJF 2014/15 and (b) MAM, (c) JJAS, and (d) SOND 2015, with respect to the 1981–2010 base period.

over southwestern and southeastern lowlands of Ethiopia, adjoining areas over South Sudan, most parts of Somalia, Kenya, and Tanzania except for small pockets over the southern tip of Tanzania, the southeastern highlands of Ethiopia and southeastern Ethiopia, and Somalia border areas, which received 50%–90% of normal rainfall (Fig. 7.19b). Most parts of Ethiopia, with the exception of southeastern lowlands, South Sudan, and southern parts of the Sudan, receive their main rainfall during June–September. However, below-average rainfall, associated with the strong El Niño event (see section 4b), dominated the region in 2015. As a result, northern, central, and southeastern Ethiopian highlands received 50%–90% of their normal rainfall. The most affected northeastern highlands of Ethiopia received as little as 30% of normal rainfall (Fig. 7.19c). The dry conditions persisted during the usual September–December rainfall season over central and southeastern highlands of Ethiopia (Fig. 7.19d).

(iii) Notable events

The failure of rainfall in Ethiopia in the summer of 2015, attributed to El Niño, led to the worst drought in decades, as reported by media outlets and later confirmed by the government of Ethiopia. According to the UN Office for the Coordination of Humanitarian Affairs, about 8.2 million people were in need of emergency food aid in Ethiopia.

The 2015 drought event can be illustrated using the standardized precipitation index (SPI) which provides a better representation of abnormal wetness and dryness than many other indices (Guttman 1998; McKee et al. 1993, 1995; Hayes et al. 1999). To account for the accumulation of drought effects over time, the SPI on 3-, 6-, 9-, and 12-month time scales during October 2014–September 2015 are considered based on the climatology of 1981–2015 for the region. Figure 7.20a shows 3-month SPIs from July to September 2015, which reveal moderate (SPI values between –1.0 and –1.49) to extreme (SPI values less than –2.0) drought over central, northern, and southeastern Ethiopian highlands as well as central Rift Valley of Ethiopia. Southern South Sudan and adjoining northern Uganda experienced moderate to severe (SPI values between –1.5 and –1.99) drought. However, the moderate to severe drought disappeared in the 6-month-SPI (April–September 2015) over these areas while the moderate to extreme drought over Ethiopia persisted (Fig. 7.20b). The moderate to extreme drought over Ethiopia continued to prevail in the 9-month (January–September 2015) and 12-month (October 2014–September 2015) SPIs (Figs. 7.20c,d) consistent with the prolonged observed rainfall anomalies in 2015 over Ethiopia. Thus, both the observed rainfall anomalies during the different seasons and the SPI confirm the failure of rains over a longer period of time.

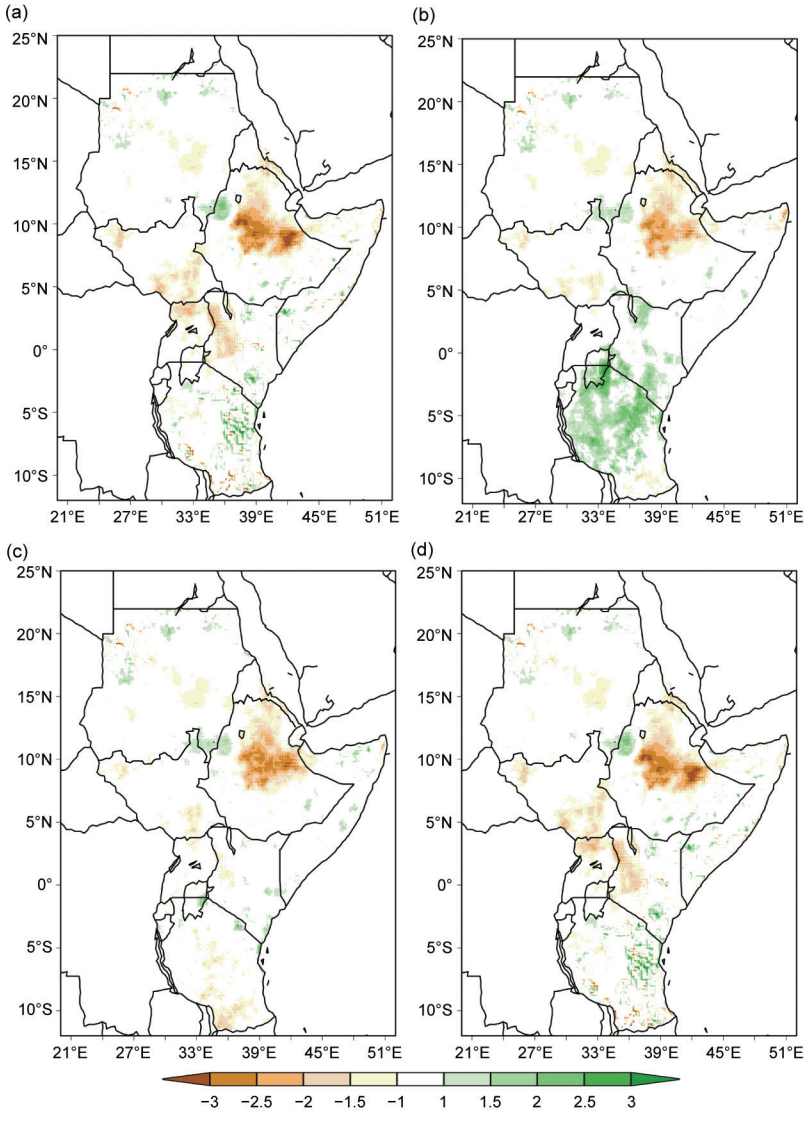

Fig. 7.20. SPI indices for eastern Africa for Oct 2014–September 2015 at (a) 3-month, (b) 6-month, (c) 9-month, and (d) 12-month times scales, based on 1981–2015 rainfall climatology.

4) Southern Africa between 5° and 30°S—G. Mengistu Tsidu

This region comprises countries bordering the Kalahari Desert within 5°–30°S and 10°–40°E, including Angola, Zambia, Botswana, Zimbabwe, and Namibia. The climate ranges from semiarid and subhumid in the east to arid in the west. Also included are Malawi and Mozambique, located in the east, with climate conditions ranging from dry to moist subtropical to midlatitude types. This region is located between two semipermanent high pressure systems over the South Atlantic and south Indian Oceans. The region is prone to frequent droughts and uneven rainfall distribution with two distinct seasons: a wet season from roughly November to April and a dry season roughly from May to October. The east coast is influenced by the southward-flowing Mozambique Current, which brings warm water and humid air from the equator and creates a humid, warm climate while the west coast is influenced by the cold Benguela Current from the Atlantic Ocean, which produces a drier climate. Total seasonal rainfall exhibits a strong spatial gradient along an axis oriented southwestward from above 700 mm over Zambia, Malawi, and Mozambique to below 25 mm over southern and eastern Namibia, southeastern Botswana, and eastern Angola during the peak rainy period of December–February (not shown).

Analyses are based on the same data sources as for section 7e3.

(i) Temperature

During December–February 2014/15, temperatures were well above normal over southern Angola, much of Namibia, and Botswana, and moderately above normal along the border between Malawi and Zambia (Fig. 7.21a). In contrast, the rest of the region had normal to below-normal temperatures. Warm anomalies exceeding +2°C were observed over the region bordering Namibia, Botswana, and Angola. The warm anomalies in the southwestern part of the region expanded eastward in March–May (Fig. 7.21b) and covered nearly the whole region in June–August (Fig. 7.21c) and September–November (Fig. 7.21d). The only exceptions were near-normal temperatures over areas that extended from the Mozambique–Zimbabwe border to close to the Mozambique–Malawi border during June–August and northern Angola and Zambia during September–November. Extreme warm anomalies exceeding +2°C during this period covered wider areas including the western half of Botswana, eastern half of Namibia, and southern part of Angola and Zambia (Fig. 7.21d).

(ii) Precipitation

In December–February, southern Africa received substantially lower-than-normal rainfall with the

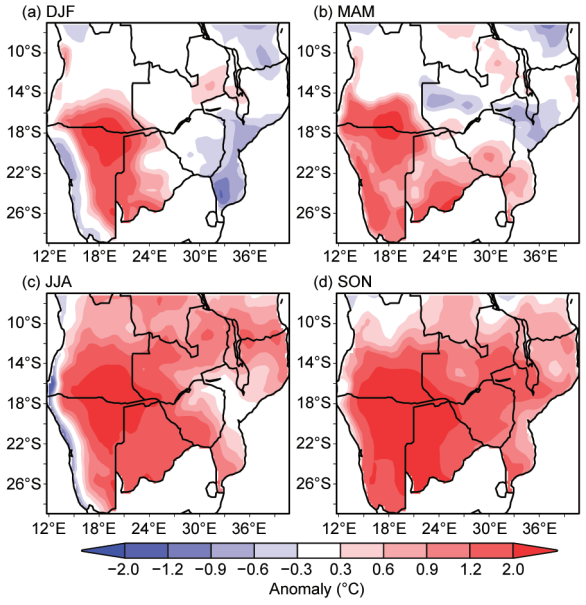

Fig. 7.21. Southern Africa seasonally-averaged mean temperature anomalies (°C) for (a) DJF 2014/15 and (b) MAM, (c) JJA, and (d) SON 2015, with respect to the 1981–2010 average.

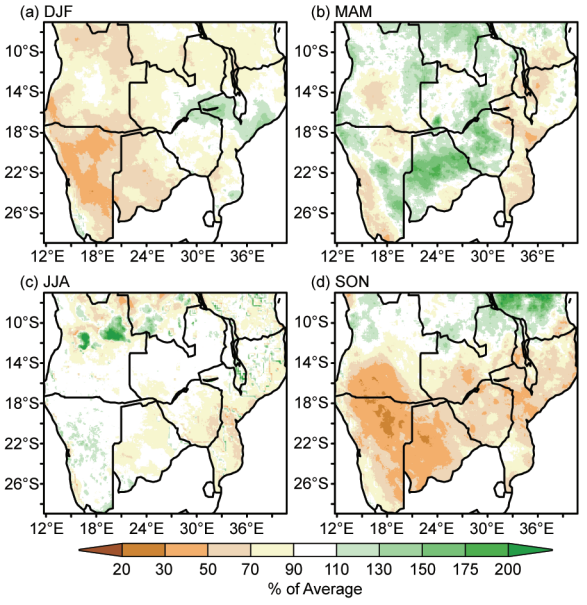

Fig. 7.22. Southern Africa seasonal total rainfall (% of normal) for (a) DJF 2014/15 and (b) MAM, (c) JJA, and (d) SON 2015, with respect to the 1981–2010 average.

exception of an isolated zonal band of normal to wet anomalies over northern Zimbabwe bordering Zambia and Mozambique, extending across Malawi to eastern Mozambique (Fig. 7.22a). Scattered normal-to-wet anomalies were observed in March–May (Fig. 7.22b) and June–August (Fig. 7.22c). The whole region received below-normal rainfall again during September–November (Fig. 7.22d). The deficit during this period is significant, as October and November constitute part of the extended climatological rainy period. Thus, overall rainfall over southern Africa was below normal in 2015.

(iii) Notable events

The below-normal rainfall was also investigated using the standardized precipitation index (SPI) on the 3-, 6-, 9-, and 12-month time scales from May 2014 to April 2015 which encompasses the peak rainy months over the region based on the climatology of 1981–2015 (not shown). The analyses revealed the presence of moderate to severe drought over the northern half of the region. On 10 November, the BBC reported that, as a result of the drought, significant portions of the population in Malawi and Zimbabwe needed food aid, citing a UNICEF assessment.

Southern Hemisphere heat waves were observed during SON over much of the region. The 90th percentile of heat wave duration (TXHW90, the maximum number of consecutive days with maximum temperatures higher than the 90th percentile calculated for each calendar day based on the 1981–2010 normal using running 5-day windows) is used (de Lima et al. 2013; Zhou and Ren 2011). In 2015, the longest period of consecutive days warmer than the 90th percentile of the normal maximum was, on average, more than 20 days over northern Namibia during September–November (Fig. 7.23d). Large parts of Botswana, Namibia, and southern Angola experienced 9- to 15-day periods warmer than the 90th percentile of normal maximum. There were warm anomalies of longer duration during other seasons over approximately the same areas (Figs. 7.23a–c).

5) South Africa—A. C. Kruger and C. McBride

The year 2015 was dominated by dry and abnormally hot conditions over most of the country.

(i) Temperature

In some parts of interior South Africa, mean maximum temperature deviations for January were more than 3°C above normal. Many areas in Western Cape, Free State, Limpopo Province, and Northern Cape had maximum temperature deviations in excess of +2° to +3°C during the first three months of the year.

The annual mean temperature anomaly for 2015 (based on data from 26 climate stations) was 0.86°C above the reference period (1981–2010), making it the warmest year for South Africa since records began in 1951 (Fig. 7.24). A warming trend of 0.14°C decade^{-1} is indicated by the data of these particular climate stations, statistically significant at the 5% level.

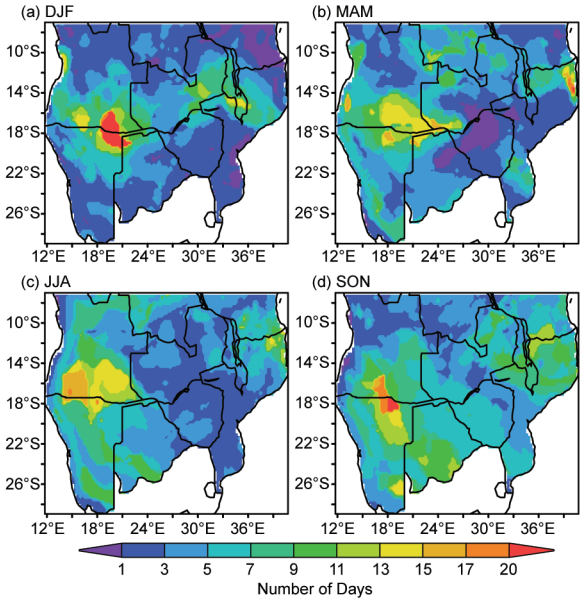

Fig. 7.23. The 90th percentile TXHW90 anomalies (in days) for Southern Africa during (a) DJF 2014/15 and (b) MAM, (c) JJA, and (d) SON 2015, with respect the 1981–2010 climatology.

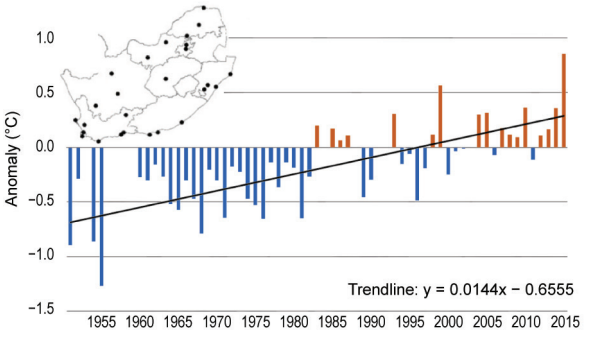

Fig. 7.24. Annual mean temperature anomalies (°C; base period 1981–2010) of 26 climate stations in South Africa, as indicated in the map, for the period 1951–2015. The linear trend is indicated. (Source: South African Weather Service.)

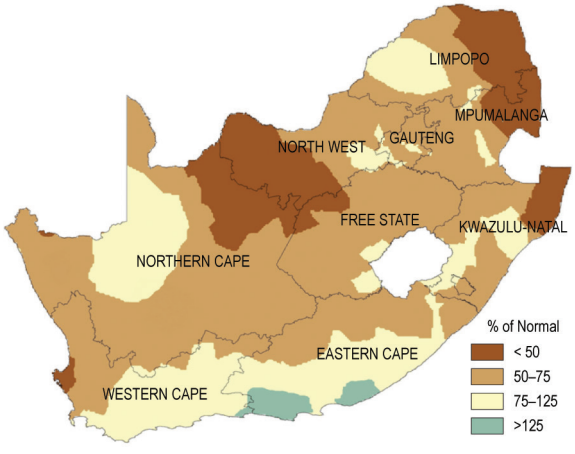

Fig. 7.25. Rainfall anomalies (% of normal; base period 1981–2010) for South Africa during 2015 (Source: South African Weather Service.)

(ii) Precipitation

Figure 7.25 presents the annual rainfall anomalies for 2015 compared to the 1981–2010 reference period. The most significant feature was below-normal rainfall across most of the country, with particularly dry conditions in northern KwaZulu-Natal province, the far northeast and western North West, and northeastern Northern Cape provinces.

The beginning of the year was characterized by dry conditions in the western and northwestern interior and, due to below-normal rainfall conditions during the 2014/15 austral summer rainfall season, the northern and northeastern parts were already classified as very dry.

In June and July, the western half of the country, as well as some parts in the east, got temporary relief from the dry conditions, with most places receiving more than double their average rainfall for the month. In September the rainy season in the summer-rainfall areas commenced well, with comparatively high rainfall totals reported in the northern interior. However, (austral) spring and beginning of summer of 2015 had dry conditions accompanied by recurring heat waves in many places.

The July–June 2014/15 period was on average the driest season for South Africa since 1991/92 and the third driest since 1932/33.

(iii) Notable events

With drought conditions firmly in place, by February some agricultural organizations requested that provinces, such as North West, be declared drought-stricken. In KwaZulu-Natal, a substantial loss in the sugarcane yield was expected, while water restrictions were in place over much of the province. By March, other provinces also considered applying to be declared drought-stricken areas, including the Western Cape, Free State, and Limpopo Province. The provinces of Northern Cape, North West, KwaZulu-Natal, Mpumalanga, and Limpopo, and the Free State were all declared drought disaster areas in November. By the end of (austral) summer, the prolonged drought conditions severely affected maize, sugar cane, and sorghum harvests.

In the spring, record high temperatures were broken on a regular basis, with Vredendal recording a temperature of 48.4°C on 27 October 2015, setting a new global record for the highest temperature ever observed for this month. The previous highest maximum temperature for this station was 42.5°C,

recorded on 30 October 1999. Extremely high maximum temperatures also occurred in Gauteng from 4 October, and resulted in prolonged heat wave conditions for 9 consecutive days in Pretoria and 8 consecutive days in Johannesburg. Lephalale in Limpopo Province also experienced heat wave conditions for 6 consecutive days. Heat wave conditions also occurred in November, beginning on the 7th and prevailing over four provinces: Gauteng Mpumalanga, the Limpopo Province, and North West.

An extensive dust storm occurred about 60 km north of Bloemfontein between Winburg and Verkeerdevlei on 11 November. According to reports, the wall of dust was estimated between 20 and 25 km wide and at least 3 km high. The dust storm was accompanied by strong winds blowing at 60–70 km hour^{-1}.

6) Western and central Indian Ocean island countries—G. Jumaux, L. Randriamarolaza, M. Belmont, and H. Zahid

This region consists of several island countries, namely Madagascar, La Réunion (France), Mayotte (France), Seychelles, and Maldives.

Overall, the 2015 mean temperature for the region was well above normal. Precipitation was also generally above normal, especially during the second half of the year in the Maldives and Réunion, but was below normal in Mayotte for the same period (Fig. 7.26).

(i) Temperature

In Madagascar, 2015 was the fourth warmest year since records began in 1971 (the warmest year was 2011). The overall annual mean temperature was 24.2°C, corresponding to an anomaly of about +0.5°C. All stations had positive anomalies, with the highest departure observed at Ambohitsilaozana (northeastern Madagascar; 1.8°C above average), except Antsiranana (northern Madagascar) station (0.1°C below; Fig. 7.27). During austral summer (January–March), the seasonal mean temperature was below the reference period. The mean temperature for July–August was above normal.

For Réunion Island, 2015 was the third warmest year since records began there in 1969, with an annual mean temperature anomaly (based on six stations) of +0.7°C. Only February and March were below or near-normal. Minimum and maximum annual temperatures were 0.5°C and 0.9°C above the 1981–2010 mean, respectively.

For Mayotte Island (Pamandzi Airport), 2015 was the warmest year since records began in 1961, with an annual mean temperature anomaly of +0.7°C (+0.6°C for maximum temperature and +0.8°C for minimum

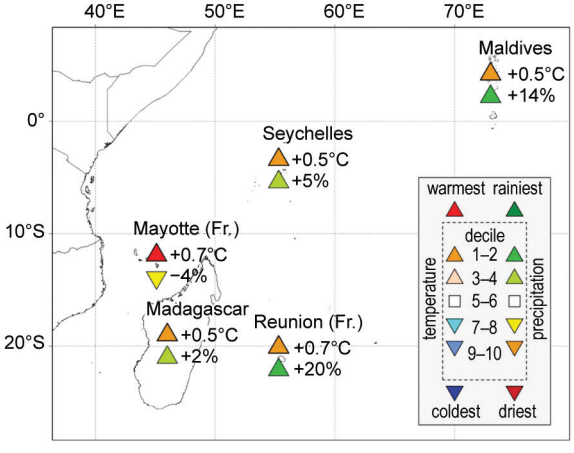

Fig. 7.26. Mean annual temperature anomalies (°C), annual rainfall anomalies (%), and their respective deciles for the Indian Ocean islands (Sources: Météo France; and Meteorological Services of Madagascar, Seychelles, and Maldives.)

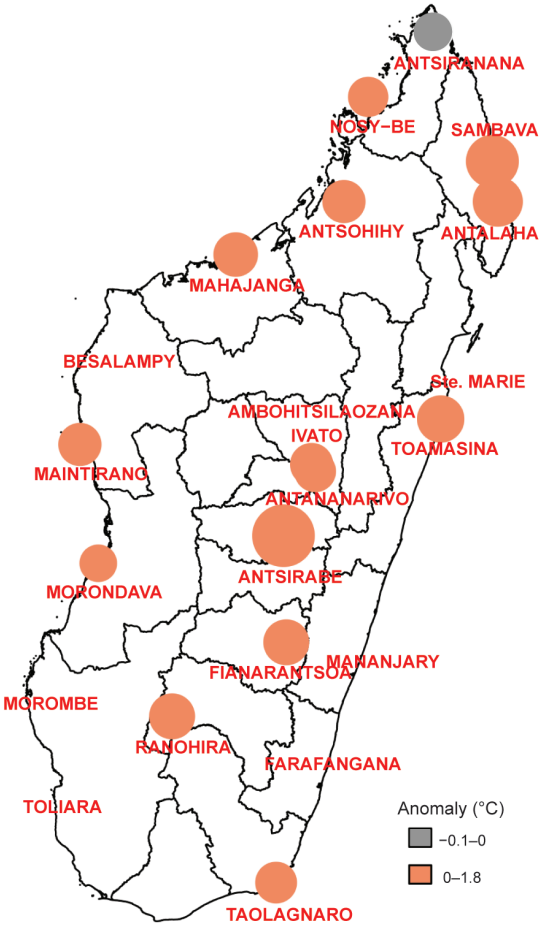

Fig. 7.27. Annual mean temperature anomalies (°C) based on 1981–2010 average. The circle dimension is related to the anomaly absolute values. (Source: Climate Change and Climatology Service, Meteorology of Madagascar.)

temperature, both highest on record). December was the warmest month of the year, with an average daily maximum temperature of 32°C.

For Seychelles, all months had above-normal mean maximum temperatures (at Seychelles International Airport) except January and February. The warmest month was April with a maximum temperature average of 32.3°C and a minimum temperature average of 26.2°C (respective anomalies of +0.7°C and +0.8°C). The annual mean temperature in 2015 was 0.5°C above average, marking the second warmest year since 2009.

For the Maldives, the annual mean temperature (based on two stations: Gan and Hulhule) in 2015 was 28.8°C, +0.5°C compared to normal. Mean temperatures were above average for all months, with the highest anomaly of +1.2°C observed in December (Fig. 7.28). These elevated temperatures are associated with the 2015 El Niño event. Overall, 2015 was the third warmest year since records began in 1981.

(ii) Precipitation

In Madagascar, annual accumulated precipitation was slightly above the 1981–2010 average. However, 10 of 22 stations indicated below-average annual total precipitation. The highest positive anomaly was recorded in Morombe (200% of normal) in southwestern Madagascar, while the lowest negative anomaly was observed in Sainte Marie (47% of normal) in northeastern Madagascar. In addition, more stations were drier than average in northern Madagascar than in the south (Fig. 7.29). During austral summer (January–March), rainfall was above average, but was below average from April to December. In addition, the number of dry days (rainfall < 0.1mm) were 12 on average during summer, compared with 22 days on average for April–December.

For Réunion Island, the annual rainfall was about 120% of average, marking the ninth rainiest year since records began in 1969. March was the wettest month of the year due to heavy rainfall in the wake of tropical storm Haliba's passage near Réunion on 9 March. The number of substantial rainy days (56 days compared with an average of 37) was the highest on record (followed by 1982, 1972, and 2008).

For Mayotte Island, the annual rainfall amount (based on two stations) was slightly below average. January was the wettest month of the year, especially on the eastern part of the island. Pamandzi airport recorded 510 mm, which is the rainiest January for this station since records began in 1961 (followed by 1971, 1986, and 2008).

In Seychelles, annual rainfall total in 2015 was 105% of normal. Below-normal rainfall and fewer-than-normal rain days were reported from January to April and in July. May–October is the dry season in Seychelles but, with the presence of an active

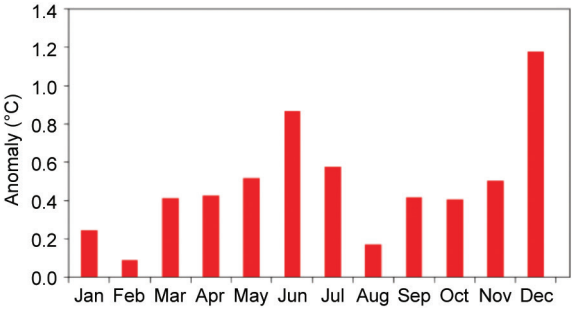

Fig. 7.28. Monthly mean temperature anomalies (°C) in 2015 in Maldives (average of two stations) with respect to the 1981–2010 base period. (Source: Maldives Meteorological Service.)

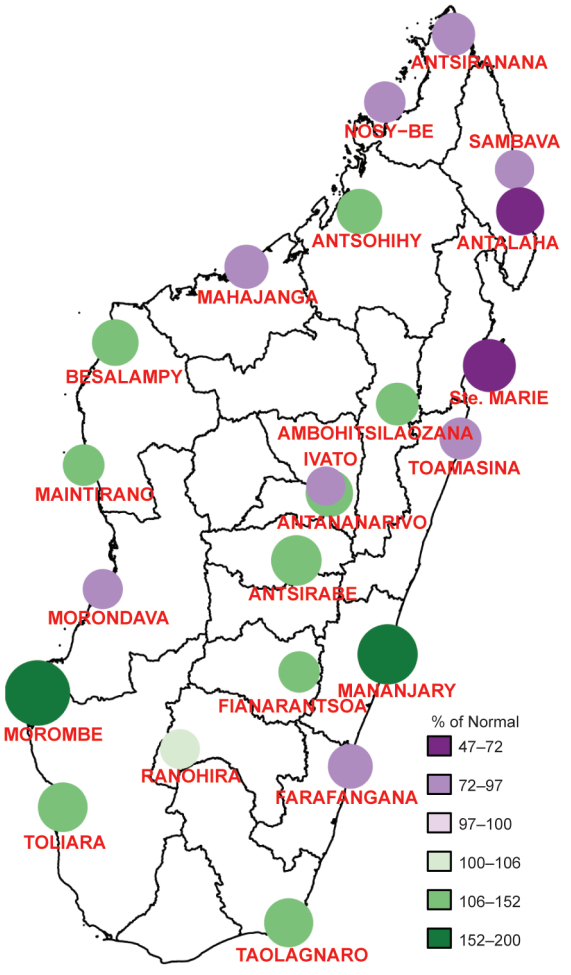

Fig. 7.29. Annual total precipitation (% of normal) with respect to the 1981–2010 period. The circle dimension is related to the anomaly absolute values. (Source: Climate Change and Climatology Service, Meteorology of Madagascar.)

El Niño, several months received abnormally high rainfall (Fig. 7.30). August received 298.3 mm (normal is 122.5 mm); October recorded 337.6 mm (normal is 177.7 mm); and November recorded 353.9 mm (normal is 192.5 mm). Many days with daily rainfall above 50 mm were recorded during the last five months of 2015. The highest daily value (122.6 mm) was recorded on 9 November at Seychelles Airport.

For the Maldives, the annual rainfall amount in 2015 was 2408 mm, 114% of average, making 2015 was the fourth wettest year since records began in 1981. August was the wettest month of the year, with an average rainfall of 370 mm over the Maldives (Fig. 7.31). As is typical, February was the driest month of the year, with average rainfall of 24 mm. On average, the Maldives experienced about 140 rainy days in 2015, 5 more than average. In 2015, the highest number of rainy days was recorded in August, September, and October (19 days each). On the other hand, the lowest number of rainy days (3) was experienced in January.

(iii) Notable events

The absolute maximum temperature was recorded at Antsohihy (northwestern Madagascar) on 13 October and 11 November (+38.7°C) and the absolute minimum temperature was recorded at Antsirabe (central Madagascar) on 21 July (–1.2°C).

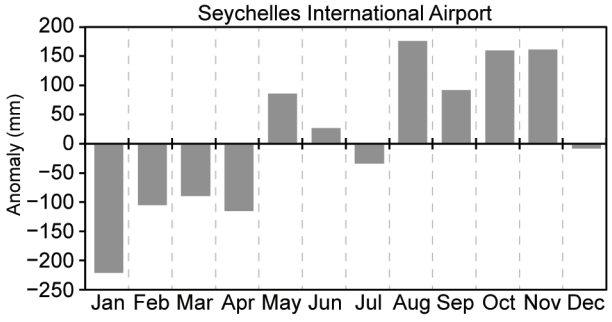

Fig. 7.30. 2015 monthly rainfall anomalies (mm) at Seychelles International Airport. (Source: Seychelles Meteorological Services.)

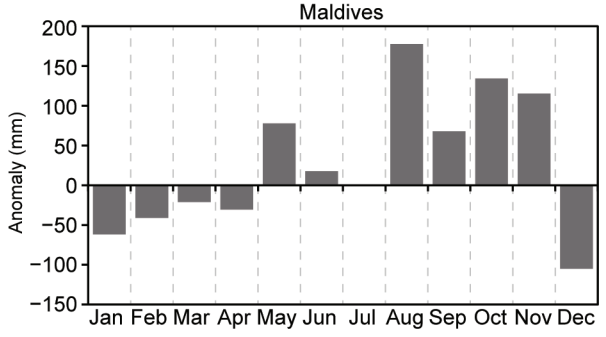

Fig. 7.31. 2015 monthly rainfall anomalies (mm) in Maldives (Source: Maldives Meteorological Services.)

The highest 24-h accumulated precipitation was 318 mm recorded in Maintirano (western Madagascar) on 2 February, which is a 12-year return period event. Grand-Ilet station (Salazie, in the highlands) recorded 1277 mm in 4 days (5-year return period).

Associated with cyclones and other systems in the region, the Maldives experienced rough sea conditions and flooding. Average winds of 24 km hour^{-1} prevailed in the central atolls from 10 January until the end of the month. Due to strong, sustained winds, moderate to rough seas prevailed in the area, which caused a passenger boat to run aground on a reef near Kaafu Maniyafushi. All 24 passengers were rescued, but the boat sank in the reef as the Coast Guard was unable to continue rescue efforts in the area due to the strong winds and rough seas. No cyclones directly impacted the Maldives in 2015.

On the other hand, Madagascar was affected by three tropical systems that formed in the Mozambican Channel on 13 January (Tropical Storm Chaedza), 5 February (Tropical Storm Fundi), and 3 March (a tropical depression). The persistence of the ITCZ amplified the conditions, leading to an event that had never occurred in February since records began in 1961. On 26 February, in Antananarivo, significant rainfall of 129.2 mm caused the destruction of a dam, which led to a major flooding event. Madagascar's disaster management agency, the Bureau National de Gestion des Risques et des Catastrophes (BNGRC), reported that 19 lives were lost, 36 956 residents displaced, and more than 60 000 people affected by the disaster. An estimated 517 houses were destroyed and 1698 were damaged in the floods. BNGRC also reported that the floods damaged 6339 hectares of rice fields.

Associated with a cloud cluster that formed south of the Maldives on 24 November, 228 mm of rain fell in the southernmost region in Addu City, the highest recorded 24-h rainfall for the Maldives, breaking the previous record of 188 mm. Three hours of torrential rain and more than 12 hours of incessant rainfall left most parts of Addu City under water, and flood water damaged household appliances and furniture in hundreds of households. It is estimated that more than 200 houses experienced flooding, and damage was estimated to be in excess of 200 000 U.S. dollars.

f. Europe and the Middle East

This section covers western Europe, from Scandinavia to the Mediterranean, and extends from Ireland and the United Kingdom to eastern Europe, European

Russia, and parts of the Middle East. While the entire region is covered in the Overview, not all countries provided input to this report, so some individual national details are not included.

Throughout this section, normal is defined as the 1961–90 average for both temperature and precipitation, unless otherwise specified. European countries conform to different standard base periods applied by their national weather services. All seasons mentioned in this section refer to the Northern Hemisphere. Significance implies an exceedance of 5th or 95th percentiles.

More detailed information, including monthly statistics, can be found in the Monthly and Annual Bulletin on the Climate in RA VI – European and the Middle East, provided by WMO RA VI Regional Climate Centre Node on Climate Monitoring (RCC Node-CM; www.dwd.de/rcc-cm). All statistics reported here are for three-month seasons.

1) Overview

Europe was, on average, much warmer than normal in 2015. The mean land surface air temperature for the European region (35°–75°N, 10°W–30°E) from the CRUTEM4 dataset (Jones et al. 2012) was +1.51°C above the 1961–90 normal, only 0.2°C short of the previous record set in 2014 (Fig. 7.32). According to the E-OBS dataset (van der Schrier et al. 2013b; Chrysanthou et al. 2014), which uses different meteorological stations over an area extending farther west and east (25°W–45°E), the European annual mean land surface temperature was the highest on record (+0.93°C above the 1981–2010 average; Fig. 7.33). However, differences between both datasets are within the level of uncertainty (allowing for the different base periods).

Across Europe and the Middle East, temperature anomalies ranged between +1°C in northwestern areas and +3°C in northeastern and Alpine regions (Fig. 7.34).

Precipitation totals in 2015 (Fig. 7.35) were below average across most of continental Europe and Iceland (60%–80% of normal). Parts of the British Isles, northern Europe, and the central and eastern Mediterranean recorded significantly above-average totals of 125% of normal and locally up to 170% of normal.

Winter 2014/15 (December–February) was exceptionally mild over Scandinavia and the eastern European region, with surface and 850-hPa temperature anomalies up to +4°C (Fig. 7.36a). The Icelandic low (negative anomalies of –12 hPa) and the Azores high (positive anomalies of +12 hPa) were well established as reflected by the North Atlantic Oscillation index

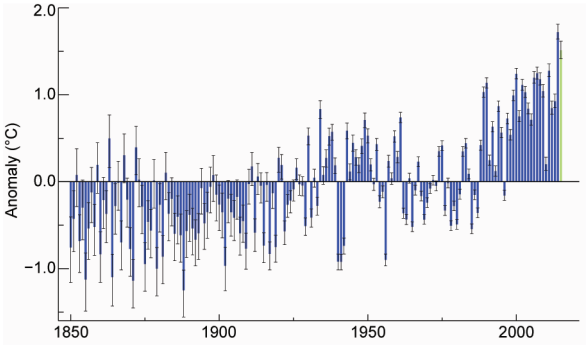

Fig. 7.32. Annual average land surface air temperature anomaly (°C) for the European region (35°–75°N, 10°W–30°E) relative to the 1961–90 base period. The blue bars show the annual average values and the black error bars indicate the 95% confidence range of the uncertainties. The green bar is the annual value for 2015. Data are from the CRUTEM4 dataset (Jones et al. 2012.)

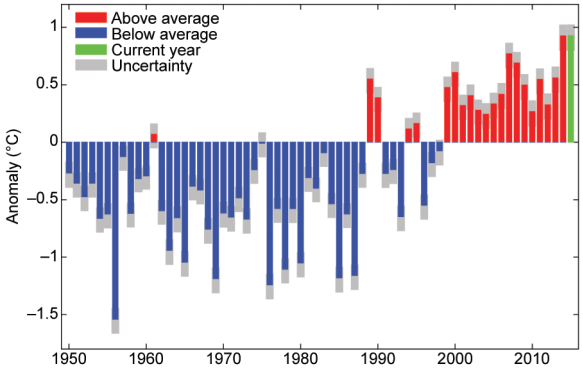

Fig. 7.33. Annual land surface air temperature anomaly (°C) for Europe, similar to Fig. 7.32, but based on the E-OBS dataset (van der Schrier et al. 2013b and Chrysanthou et al. 2014) from 1950 to 2015. [Source: KNMI (Royal National Meteorological Institute) Netherlands.]

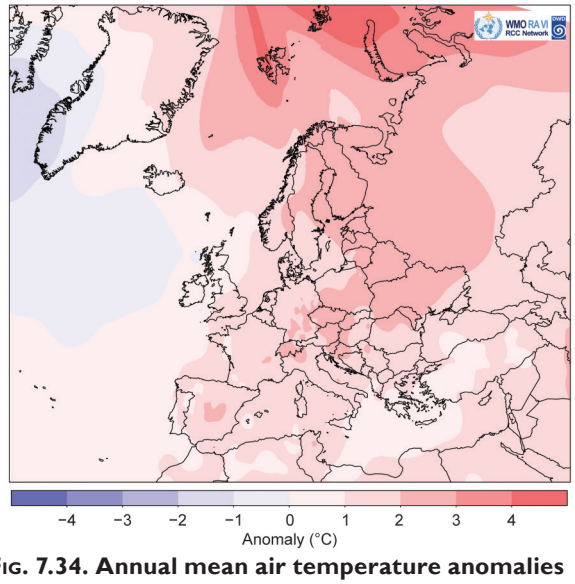

Fig. 7.34. Annual mean air temperature anomalies (°C; 1961–90 base period) in 2015. (Source: DWD.)

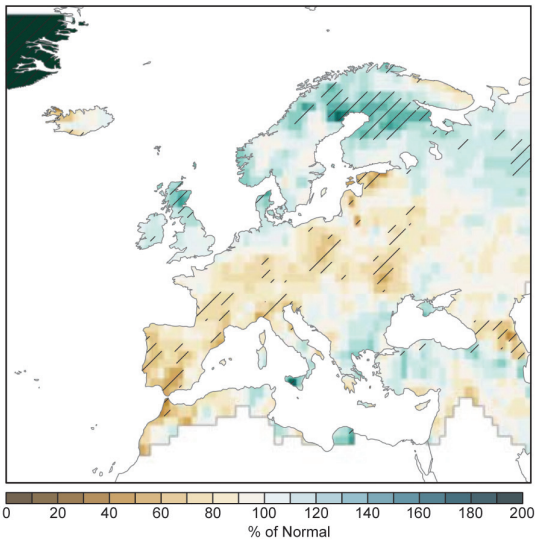

Fig. 7.35. European precipitation totals (% of 1951–2000 average) for 2015. Hatched areas indicate regions where precipitation is higher than the 95th percentile of the 1961–90 distribution. Only grid points with mean annual precipitation >15 mm month^{-1} are represented. [Source: Global Precipitation Climatology Centre (Schneider et al. 2015).]

[NAO +1.65, normalized pressure difference between the Azores High (Ponta Delgada, Azores) and the Icelandic Low (Reykjavík, Iceland)]. This synoptic pattern allowed for a frequent westerly flow of mild Atlantic air masses that brought precipitation totals of up to 170% of normal, particularly in northern parts of Europe and in the southeast (Fig. 7.37a, hatched). In contrast, the Iberian Peninsula and southwestern France had below-average surface temperature anomalies of up to –1°C due to the influence of high pressure and precipitation less than 40% of normal in places.

During spring (March–May) significant above-average 500-hPa heights centered over Iberia led to well-above-normal temperatures in southwestern Europe (Fig. 7.36c, dotted). March in particular contributed to the anomalous warmth. It was the third straight month of extensive westerlies and southwesterlies advancing over northeastern Europe where temperature anomalies exceeded +4°C.

Northern Europe was affected by frequent Atlantic cyclones throughout the season that caused a significant precipitation surplus of locally more than 180% of normal (Fig. 7.37b, hatched), whereas the western half of Europe, including most of the British Isles, had below-average totals.

The summer season (June–August) was characterized by a hot spell across western, central, and eastern Europe (see Sidebar 7.1) as a result of significant above-average 500-hPa heights (Fig. 7.36e, dotted). In

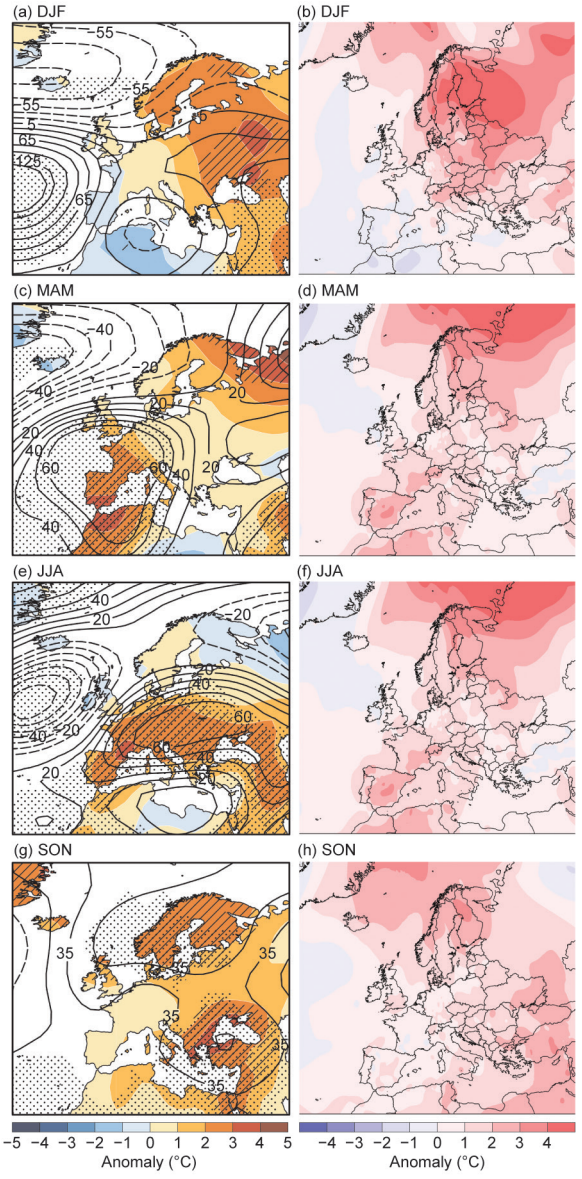

Fig. 7.36. Seasonal anomalies of (left) 500-hPa geopotential height (contour, gpm) and 850-hPa temperature (shading, °C) and (right) near-surface air temperature, using data from the NCEP–NCAR reanalysis for (a), (b) DJF (winter), (c), (d) MAM (spring), (e), (f) JJA (summer), and (g), (h) SON (autumn). In left column, dotted areas indicate regions where 500-hPa geopotential is above (below) the 95th percentile (5th percentile) of the 1961–90 distribution, while hatched areas represent the corresponding thresholds but for 850-hPa temperature. Base period used for both analyses is 1961–90. (Source: Deutscher Wetterdienst.)

contrast, the British Isles, Scandinavia, and northern European Russia were influenced by frequent low pressure systems. These regions recorded surface temperature anomalies of 0° to –1°C accompanied by above-average rain amounts of up to 170% of normal (Fig. 7.37c).

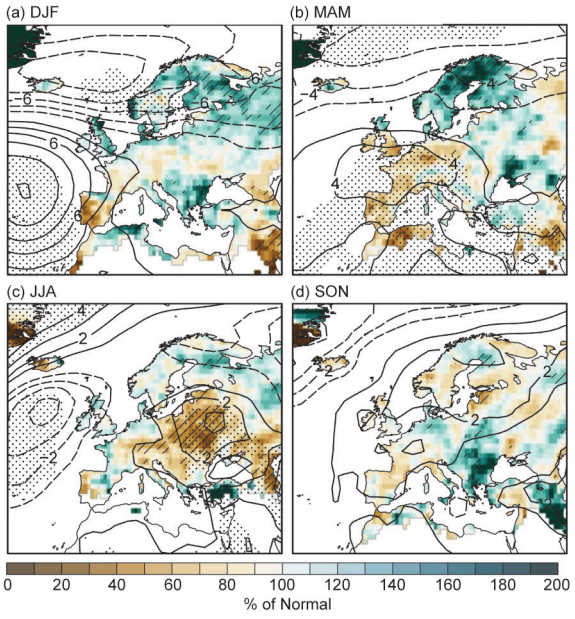

Fig. 7.37. Seasonal anomalies for 2015 (1961–90 base period) of sea level pressure (hPa) from NCAR–NCEP reanalysis (contours) for (a) DJF (winter); (b) MAM (spring); (c) JJA (summer); and (d) SON (autumn). Colored shading represents the percentage of seasonal mean precipitation for 2015 compared with the 1961–90 mean from the monthly Global Precipitation Climatology Centre (Schneider et al. 2015) dataset (only grid points with climatological mean seasonal precipitation above 15 mm month^{-1} are represented). Dotted areas indicate regions where SLP is higher (lower) than the 95th percentile (5th percentile) of the 1961–90 distribution, while hatched areas represent the corresponding thresholds but for precipitation.

In autumn the atmospheric circulation featured above-average 500-hPa heights (Fig. 7.36g), and temperatures were warmer than normal in nearly all regions. Scandinavia and the eastern Mediterranean, including the Black Sea region, were especially affected by high pressure conditions and recorded significantly positive surface and 850-hPa temperature anomalies of more than +3°C in places. According to the E-OBS dataset, it was the third warmest autumn since 1950 for the European region. Eastern Turkey and the Balkan States received localized precipitation totals of more than 200% of normal (Fig. 7.37d).

The year ended exceptionally warm, with a strong positive NAO (+2.24) phase in December. The synoptic pattern was associated with exceptionally widespread positive temperature anomalies that exceeded +4°C. Large parts of Europe recorded their warmest December since 1950. Only the eastern Mediterranean experienced below-average temperatures, with anomalies reaching –2°C.

2) Central and western Europe

This region includes Ireland, the United Kingdom, the Netherlands, Belgium, Luxembourg, France, Germany, Switzerland, Austria, Poland, Czech Republic, Slovakia, and Hungary.

(i) Temperature

Annual temperatures in central Europe were warmer than normal and nearly all areas of the region were around 2°C above their long-term means. Switzerland had its warmest year since national records began in 1864 (+2.1°C). Austria, Germany, Slovakia, and Hungary each experienced their second warmest year since 1767, 1881, 1961, and 1901, respectively, with anomalies ranging between +1.7°C and +2.2°C.

The winter season 2014/15 was exceptionally mild, particularly for the eastern part of the region, which was more often than normal under the influence of subtropical air masses. Spring was characterized by above-average temperatures except for most of Ireland, where deviations of –1°C were recorded. May in particular contributed to the cooler-than-normal conditions in Ireland, where deviations down to –1.7°C were recorded.

During summer, the atmospheric circulation featured significantly widespread anomalous high temperatures across continental Europe. Near the Alps, the blocking ridge led to positive temperature anomalies up to +4°C. In contrast, the British Isles were affected by frequent westerly flow of Atlantic air masses that led to a summer with mostly near-normal temperatures, although a brief heat wave occurred in early July, particularly affecting southern parts of the United Kingdom.

Temperature anomalies in autumn ranged between –1°C in parts of France to +2°C in the southern United Kingdom and eastern areas of the region. November was especially warm (2°–4°C above average), when many daily high temperature records were broken. Germany reported its warmest November on record (3.5°C above average). The United Kingdom and Switzerland reported deviations of +2.6°C and +2.7°C, respectively, with each having their third warmest November since 1910 and 1864, respectively.

The year ended with exceptionally warm December temperatures that were more than +4°C from the reference period across nearly the entire region. An exceptionally strong southwesterly flow associated with a strong positive phase of the NAO contributed to these spring-like temperatures.

(ii) Precipitation

Annual precipitation totals were mostly below the long-term mean. Only Ireland, Scotland, Benelux, and northern Germany had slightly above-normal precipitation.

Winter 2014/15 was characterized by below-average precipitation in central Europe, with locally less than 60% of normal. The United Kingdom was affected by frequent cyclonic conditions that gave rise to a surplus of up to 140% of normal precipitation.

Spring was drier than normal across the entire region, except in Scotland. France, central Germany, and western Poland each received 60%–80% of normal precipitation and locally even less, associated with areas of significantly above-average sea level pressure (SLP, dotted areas in Fig. 7.37b). Over the British Isles, below-average totals of 70% of normal in southern England contrasted with values in western Scotland of more than 150% of normal.

During summer, below-average precipitation totals continued, especially in eastern and central Europe and the Alpine region where totals as low as 40% of normal were registered. Hungary reported its sixth driest June since 1901.

Autumn precipitation was above normal in the eastern part of the region, while western areas, including the British Isles, experienced a rain deficit. High pressure over northern Europe during September and October brought dry conditions to the United Kingdom, with 54% and 65% of normal rain, respectively. The season ended with very wet conditions when the Icelandic low was well established. This synoptic pattern was associated with 250% of normal totals in most regions, except France and the Alpine region. Repeated low pressure systems continued to the end of the year, and precipitation remained well above normal.

(iii) Notable events

Two storms crossed the North Sea during 9–11 January. At the central German mountain station Brocken, wind gusts of more than 43 m s^{-1} were measured.

During July and August, Hungary reported a record 27 days of heat wave conditions, and Budapest experienced a record-breaking 34 tropical nights, the most since records began in 1901.

Two intense rainstorms crossed southeastern France during 12–13 September, bringing 200–242 mm rain within 6 hours. The latter amount is a new record at station Grospierres.

In November, many record high temperatures were measured. On 7 November, a station in Freiburg, southwest Germany, recorded 23.2°C, its highest daily maximum temperature for November.

Ireland reported its sixth wettest November since records began in 1866. Newport, on the west coast of Ireland, observed a record daily rainfall of 66.2 mm (190% of normal) on 14 November.

Several storms traversed central Europe in November. During the 17th and 18th, a core pressure below 985 hPa brought wind gusts of more than 48 m s^{-1}, causing traffic disturbance and damage to trees and buildings.

3) The Nordic and the Baltic countries

This region includes Iceland, Norway, Denmark, Sweden, Finland, Estonia, Latvia, and Lithuania.

(i) Temperature

Annual temperatures in 2015 were well above normal in the Nordic and Baltic countries. Finland and the Baltic States experienced anomalous temperatures of +2° to +3°C. Lithuania and Finland experienced their warmest year on record, with anomalies of +2.1°C and +2.6°C, respectively. Norway observed its third warmest year since records began in 1900, with an anomaly of +1.8°C. Iceland, however, recorded only slightly-above-average temperatures (0° to +1°C) and had its coldest year since 2000.

Winter 2014/15 was exceptionally mild in Scandinavia and the Baltic States, with the largest deviations of more than +4°C in Estonia, Finland, and central Sweden. The anomalous temperatures were caused by persistent southwesterly flow, which brought subtropical air far into Scandinavia. February in particular contributed to the anomalous warmth. Finland, on average, had temperatures 7°C above normal, marking its third warmest February, behind 1990 and 2014. Norway's average anomaly was +4.2°C, with anomalies at stations in southern and central regions up to +6°C and +9°C, respectively.

In spring, temperatures remained above the long-term mean, with anomalies between +3° and +4°C in northern Scandinavia (hatched areas in Fig. 7.36b). March was especially warm when mild subtropical air advanced far into the north. Lithuania reported positive anomalies of +4.9°C. Norway also experienced a mild March, at 3.8°C above average. Locally, in Finnmark and Troms (far northern Norway), deviations of +5° to +7°C were reported.

During summer, temperatures were near-normal on balance. Above-average temperatures of +1°C over the Baltic States contrasted with below-average conditions (–1°C) over Iceland and most of Scandinavia. June and July were cooler than normal, with anomalies as much as –2°C over the Scandinavian countries where below-average 500-hPa heights prevailed.

Temperatures in autumn were significantly warmer than normal throughout all regions due to dominant high pressure (dotted areas in Fig. 7.36g). The strongest deviations occurred in northern Scandinavia, at +2° to +3°C. In November, a strong positive NAO phase (+1.7) led to many locations in Scandinavia observing temperatures above their 90th percentile.

In December, a combination of prolonged high pressure over the central Mediterranean and warm air advection caused exceptionally mild conditions in the Nordic region. Widespread positive anomalies of more than +4°C were recorded across most regions, except for Iceland, where below-average temperatures in western areas contrasted with warmer conditions in the east.

(ii) Precipitation

With the exception of Iceland and the Baltic States, annual precipitation totals were above normal. Denmark reported its second wettest year since 1874, and Norway observed 125% of normal precipitation on average, which is third wettest in its 116-year record.

Winter 2014/15 was wetter than normal across nearly all of the Nordic countries due to a strong positive NAO phase (+1.65). Below-average 500-hPa heights were associated with frequent cyclonic conditions that brought up to 170% of normal precipitation to the region (hatched areas in Fig. 7.37a).

In spring, wetter-than-normal conditions remained, especially across Scandinavia where 125%–170% of normal totals were widely observed. Norway experienced its second wettest May on record (after 1949), with 175% of normal rainfall.

Precipitation in summer was close to normal except for the Baltic States. A persistent blocking ridge centered over continental Europe resulted in dry conditions, with only 60% of normal rainfall recorded (dotted in Fig. 7.37c). August was especially dry, with nearly all regions recording below-average totals. Exceptionally low rainfall of less than 20% of normal was recorded across the Baltic States. Lithuania reported just 16% of its normal rainfall.

During autumn, precipitation totals were mostly below the long-term mean, except for parts of north-central Finland and Denmark (>125% of normal totals). The Baltic States recorded a deficit between 40% and 60% of normal totals. Exceptionally strong southwesterlies in December brought well-above-normal precipitation totals to the Nordic countries. Denmark received up to 250% of normal precipitation. Only parts of central and northern Scandinavia registered a rain deficit, 60%–80% of normal.

(iii) Notable events

In January, Norway and Sweden experienced extreme precipitation totals. Some stations in Norway received up to 400% of normal; at Eikemo (coastal western Norway) 782.3 mm was measured, corresponding to 280% of normal. Station Piteå in northeast Sweden reported a monthly rain accumulation of 1346 mm, which is the most since the record began in 1890.

During 9–11 January, the Danish coast was hit by two successive storms. On the morning of 11 January, water in Lemvig (northwest Denmark) rose to 1.95 m above normal, breaking the previous record of 1.81 m.

During a period of strong westerlies in February, Norway reported record-breaking wind gusts of more than 46 m s^{-1} in southern mountainous areas; 70 000 people lost power. Givær, an island in Bodø (northern Norway), was evacuated during a spring high tide.

In September, Norway was hit by thunderstorms and accompanying extreme precipitation. In the south, station Gjerstad received monthly totals of 478 mm (330% of normal), and station Postmyr i Drangedal received 449.5 mm (350% of normal). On 2 September, the latter recorded its highest daily total of 117.8 mm.

On 2 October, a storm caused forest damage in central Finland and left over 200 000 households without power.

In November, two storms hit Denmark with record-breaking wind gusts. During 7–8 November, the first storm produced Hanstholm's (on the northwest coast) highest wind gust of 34.6 m s^{-1} and a record-breaking 10-minute mean wind of 27.3 m s^{-1}. On 29 November, the second storm passed with wind gusts up to 45.9 m s^{-1}.

4) Iberian Peninsula

This region includes Spain and Portugal. In this subsection, anomalies refer to a reference period of 1981–2010, with the exception of precipitation for Portugal, which the country reports with respect to a 1971–2000 reference period.

(i) Temperature

The Iberian Peninsula experienced a warmer-than-normal year in 2015. Spain recorded an annual anomaly of +0.9°C and tied with 2011 for its warmest year on record, which dates to 1961. Portugal reported positive anomalies compared to the 1981–2010 reference period between +0.6°C in southern regions and +1.7°C in east-central parts of the country.

Winter 2014/15 was colder than normal throughout Iberia due to cold air advection from the north. Spain and Portugal were 0.6°C and 1°C below average, re-

spectively. A colder-than-normal winter was followed by a very warm spring, and the entire Iberian Peninsula registered positive temperature anomalies and significantly above-average 500-hPa heights (dotted in Fig. 7.36a,c). Spain reported a mean anomaly of +1.5°C, with an extremely warm May (+2.4°C), which was the second warmest in its 55-year record.

Significantly anomalous above-normal temperatures remained in summer due to a blocking high pressure ridge over Europe, and anomalies exceeded +2.5°C in most areas. During July, Spain experienced its highest monthly average temperature on record. This month also featured unusually persistent heat wave conditions. In central and southeastern parts of the country, positive anomalies of +3°C were recorded; it was the second warmest summer season on record, behind 2003.

Autumn, overall, was also warmer than normal but with only slightly-above-average values. Very warm conditions in November remained in December, with monthly anomalies of +2°C as a result of an eastward extending Azores high (positive SLP anomalies of up to +10 hPa over the Iberian Peninsula).

(ii) Precipitation

Annual precipitation totals over Iberia were mostly below average (60%–80% of normal). For Portugal the year was extremely dry and only 68% of the normal rain was measured (25% of normal totals based on the 1971–2000 reference period used for precipitation in Portugal). Spain received 77% of its normal precipitation, mainly due to extremely dry conditions in April, May, November, and December.

Winter 2014/15 was characterized by a strong positive NAO, which was reflected in the precipitation distribution over the Iberian Peninsula. While the northernmost part was influenced by northerly flow bringing 125% of normal precipitation, the remaining region experienced a very dry season. Widespread below-average totals of less than 60% of normal were recorded.

During spring, the Azores high extended far into the European continent and led to well-below-normal precipitation totals. May brought an extreme rain deficit. Spain reported mean monthly precipitation totals just 25% of normal, its driest May on record. Portugal also observed extreme rain deficits, but mostly in the southern half of the country.

In summer, wetter-than-normal conditions in northeastern Spain contrasted with below-average totals in the remainder of the country. Southern Portugal received only 20%–40% of normal totals and locally even less.

Precipitation in autumn was below average throughout the Iberian Peninsula, with 60%–80% of normal rainfall over central to northeastern Spain. Only southeastern areas recorded a surplus, up to 125% of normal.

The year ended with very dry conditions, caused by a strengthening of the positive NAO phase (+2.2 in December). Spain reported December rainfall just 20% of normal, the driest December at many eastern stations (several reported no rain at all), and Portugal saw less than 50% of its normal precipitation in some regions.

(iii) Notable events

During the first 10 days of February, Spain recorded a significant cold spell due to an intrusion of continental cold air masses from central Europe. A minimum temperature of –11.9°C was measured at the station Molina de Aragon in central Spain.

In northern Spain along the coast of the Bay of Biscay, heavy rainfall in February set new record high totals, with precipitation 300% of the wintertime normal.

Although spring was overall drier than normal in Spain, heavy precipitation events occurred in March. Starting on 5 March, a week of heavy rain, combined with meltwater, led to flooding in the northeast. On 22 March, Castellón de la Plana-Almazora on the eastern coast recorded 133.8 mm within 24 hours.

In May, Spain and Portugal were affected by a heat wave with record-breaking high temperatures. Valencia Airport registered 42.6°C on 13 May, 6.6°C higher than the previous record. By 14 May, the southern station of Beja had already reported 19 days in 2015 with maximum temperatures above 30°C, which was 14 days more than normal.

In summer, Spain suffered from an extraordinarily long, intense heat wave (nearly continuous from 27 June to 22 July), particularly affecting the central and southern regions, where temperatures above 45°C were reported on 6 and 7 July.

On 4 September, Palma de Mallorca (island south of Barcelona) received 124.3 mm rain from thunderstorm activity within 24 hours, the highest for any time of year since the record began in 1973.

On 15–16 September, a low pressure system with a core pressure of 990 hPa delivered more than 100 mm precipitation to several stations in Portugal. Rainfall totals were 150%–200% of normal for September in northern Portugal. The highest accumulated rain was recorded at northern station Cabril (160.4 mm).

Intense rainfall occurred on 1 November at the Algarve in Portugal. Daily accumulated precipitation

SIDEBAR 7.1: UNUSUALLY STRONG AND LONG-LASTING HEAT WAVE IN EUROPE

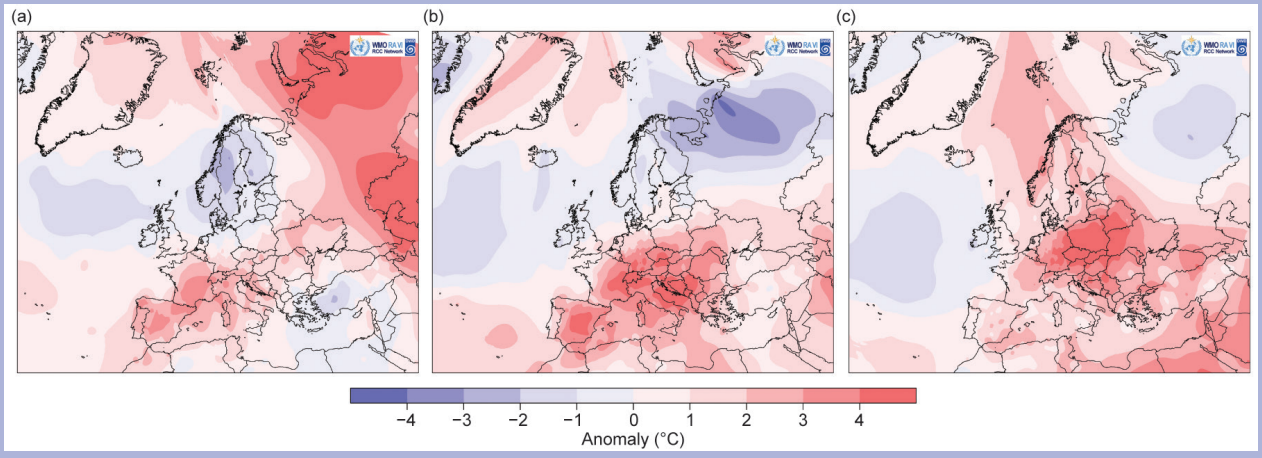

Fig. SB7.1. Monthly air temperature anomalies (°C, 1961–90 reference period) for Europe in (a) Jun, (b) Jul, and (c) Aug 2015. (Source: Deutscher Wetterdienst.)

From late June to early September 2015, much of Europe was under the influence of an unusually strong and long-lasting heat wave. Spain and Portugal also had well-above-normal temperatures in May. The heat was associated with an exceptional rain deficit that led to drought conditions in several regions from southwestern Iberia to eastern Europe, while at the same time heavy thunderstorms were recorded in the central and eastern Mediterranean.

The heat wave affected much of Europe during June, July, and August (Fig. SB7.1). At the end of June, a blocking high pressure system developed over southwest-to-central Europe, with a meandering upper level jet stream, allowing hot air to flow from Africa to Europe, where it became trapped. In mid-July, the Azores high extended farther into central Europe, and by the end of the month, it shifted eastward. The anticyclone caused large-scale subsidence, and western Europe recorded maximum temperatures up to around 40°C. By the end of August, two anticyclones developed over eastern Europe. The resulting southerly flow of hot air masses brought high temperatures to eastern and central Europe.

On an areal average, the European region experienced its third warmest summer season since 1910, behind 2003 and 2010, with temperatures +1.7°C above the 1961–90 mean. August contributed most to the anomalous warmth, with a record high anomaly of +2.3°C, while July was sixth warmest (+1.5°C); June was 15th warmest, with slightly-above-normal temperatures (+0.9°C).

For much of June, Iberia, France, and the western Alpine region observed high temperatures, with anomalies of +3° to +4°C. Portugal registered a monthly mean temperature of 21.8°C, its fifth highest on record, at +2.4°C above the 1961–90 mean. The absolute maximum of 43.2°C was measured on 29 June at Beja, in the south of the country. In France, many

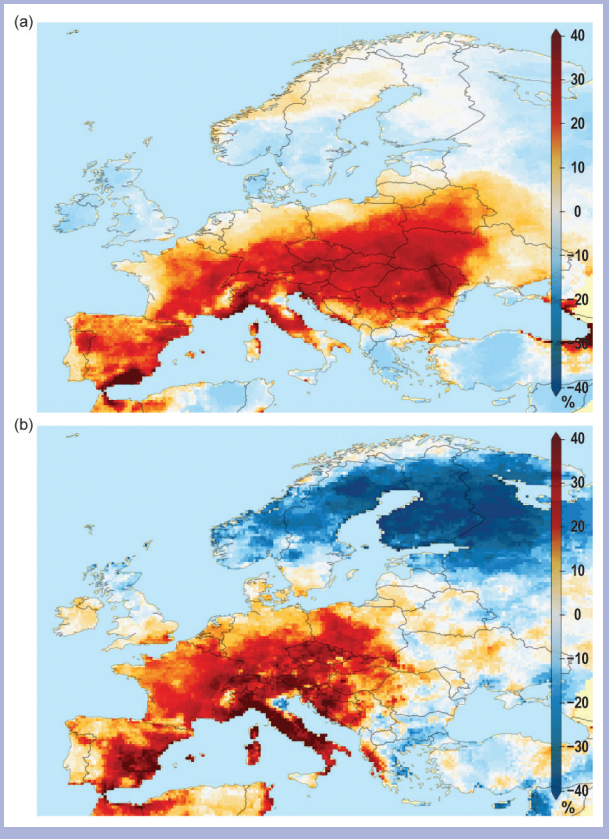

Fig. SB7.2. Percentages of (a) warm days and (b) warm nights for 2015. A warm day or night is defined as a day where the maximum or minimum temperature exceeds the 90th percentile of the values from the 1981–2010 average. (Source: E-OBS dataset, EURO4M.)

maximum temperature records were broken at the end of June. On the 30th, temperatures were as much as 12°C above the seasonal mean in western areas.

In July, the core region of the heat wave moved to central Europe, the Mediterranean, and the Balkan region. However, Spain still experienced its warmest July in its 55-year record, with anomalies of +2.5°C above the 1981–2010 mean. Germany observed a record-breaking maximum temperature of 40.3°C at Kitzingen (central region) on 5 July, and France had a new record maximum temperature, 41.1°C, at Brive-la-Gaillarde (central southern France). Austria recorded temperatures 3.1°C above normal, its warmest July since records began in 1767. In Vienna, a new record daily minimum temperature of 26.9°C was measured. August brought extremely high temperatures to eastern and central Europe, with anomalies exceeding +4°C. In Belarus (Brest) and Lithuania (Kaunas), record daily maximum temperatures of 36.7°C and 35.3°C, respectively, were observed.

The unusual and long-lasting high temperatures were reflected in the fact that warm days and nights (see section 2b5) were more than 40% more frequent than in a normal summer (Fig. SB7.2). High nighttime temperatures in particular can affect human health, and in Belgium and the Netherlands, strongly increased mortality was registered during this period. During July and August, Hungary reported a record 27 days of extremely warm conditions, and Budapest experienced a record-breaking 34 tropical nights, the most since records began in 1901.

The heat wave was also associated with sub-regional severe rain deficits. Southern Spain and Portugal each received only 10 mm rain per month during June, July, and August, which corresponds to less than 40% of their normal totals. After several weeks of persistent heat and continuous rain deficit, southern Portugal and northeastern continental Europe suffered from extreme drought conditions (Fig. SB7. 3) in August. On 31 August, 74% of Portugal was categorized as severely or extremely dry. As a result, wildfires occurred in the Mediterranean from Iberia to Turkey and in the Balkan States. The rain deficit also caused low water of the rivers Elbe, Rhine, and Danube, which affected shipping. The river Dnjepr in Belarus had record low levels.

In contrast, several regions experienced well-above-normal precipitation during summer, especially in Greece, western Turkey, and Sicily. The rain surplus was generated by heavy thunderstorms induced by anomalous warm sea surface temperatures (anomalies up to +4°C) in the Tyrrhenian Sea.

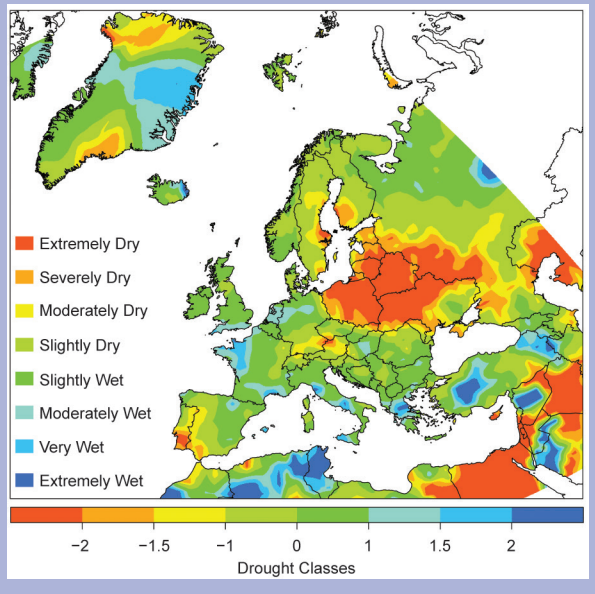

FIG. SB7.3. DWD standardized precipitation index (1961–90 average) for Augv 2015. (Source: Deutscher Wetterdienst.)

exceeded 100 mm. The highest amount of 144.8 mm was observed in Algoz, near the southern coast.

5) MEDITERRANEAN AND BALKAN STATES

This region includes Italy, Malta, Slovenia, Croatia, Serbia, Montenegro, Bosnia and Herzegovina, Albania, Macedonia, Greece, Bulgaria, and Turkey.

(i) Temperature

Averaged over the year, temperature anomalies in 2015 were between +1°C in the central and western Mediterranean and +2°C over the Balkans. Temperatures up to 3°C above normal occurred near the Alps. Much of Montenegro experienced its warmest year on record. Slovenia observed its third warmest year.

Winter 2014/15 was warmer than normal (+2° to +3°C) especially in northern parts of the region. Only some parts of southern Greece and southern Italy/Sicily had below-average temperatures, with anomalies up to −1°C. Croatia saw a mild season and registered positive anomalies up to +2.7°C in northeastern areas.

Above-average temperatures dominated almost the entire region in spring when the Azores high extended far into the European continent. Serbia recorded temperature anomalies of +2°C in northern areas. Croatia had positive anomalies of +1.8°C in its northern areas. During April, colder-than-normal conditions occurred over southeastern areas. In central Turkey, temperature anomalies ranged from −2° to −3°C.

Most of the region experienced a very warm summer, induced by prolonged anticyclonic conditions

centered over continental Europe. The northern Balkan States recorded large anomalies that ranged between +3°C and +4°C; Serbia and Croatia reported anomalies of +2.1°C to +3.8°C. In contrast, Greece's Peloponnese had only slightly-above-normal conditions.

During autumn, temperatures remained above the long-term mean. With the exception of northern Italy, which had only slightly-above-average temperatures, anomalies ranged between +1°C and +2°C. Southern Croatia reported temperature departures up to +2.8°C. The highest anomalies (+3°C to +4°C) occurred at the Bosporus, due to prevailing high pressure.

The year ended with contrasting conditions. While the northernmost areas of the region were under the influence of extremely strong westerlies and associated mild temperatures (3°–4°C above normal) during December, the southern Balkans experienced cool anomalies of –1°C.

(ii) Precipitation

With the exception of northern Italy, annual precipitation totals were above normal. The largest rainfall departures occurred in Sicily, eastern Greece, Bulgaria, and western Turkey, where 125%–170% of normal totals were observed. In the southern Alpine region, drier-than-normal conditions of 60%–80% of normal were recorded. Croatia reported just 63% of its normal precipitation in the northwest.

Winter 2014/15 was very wet for most regions (hatched in Fig. 7.37a). Over the Balkans, precipitation totals of 125%–170% of normal were measured. Southern Serbia had 175% of normal rainfall, and localized areas in Croatia observed 225% of normal.

Precipitation totals in spring mainly ranged between 60% and 125% of normal. While drier-than-normal conditions occurred near the Southern Alps and in Albania, central and southern Italy, as well as easternmost parts of the region, experienced a surplus of precipitation. In Serbia, totals ranged from 67% of normal in eastern areas to 180% of normal in localized spots. Croatia experienced dry conditions in northwestern parts of the country, with 45% of normal precipitation. In April, above-average 500-hPa heights over Europe led to well-below-average precipitation over southern regions. Sicily and southern Peloponnese had very dry conditions with rainfall less than 20% of normal.

During summer, below-average rain in the north of the region contrasted with wet conditions in the south. Greece and parts of Turkey recorded totals greater than 170% of normal, whereas most of the Balkans received below-average precipitation. Eastern Serbia and Croatia reported 25%–30% of normal rainfall. In June, heavy rains fell over northern and central Turkey, bringing totals up to 250% of normal, while July was exceptionally dry across the entire region. Most areas observed less than 40% of normal rainfall, except parts of Italy that received 125% of normal.

Autumn remained wet over the Balkans, whereas the Alpine region recorded below-normal precipitation. Serbia reported very wet conditions, with up to 230% of normal precipitation, and above-normal precipitation prevailed in Bulgaria and northern Greece. October contributed to the overall surplus of rain, when the dipole pattern associated with a split flow brought storms and above-average precipitation across southern Europe. Nearly all areas of the region received more than 170% of their normal precipitation. Croatia rainfall was 140%–410% of normal. In contrast, November was very dry in the Alpine region, with less than 20% of normal rain in northern Italy.

Dry conditions were also evident in December 2015, associated with an exceptionally strong southwesterly flow. Nearly all of Turkey, Italy, and the northern Balkans received less than 40% of their normal rainfall, with some areas observing less than 20% of normal.

(iii) Notable events

Southern Italy was hit by heavy thunderstorms on 5 September. The area surrounding Naples observed hail, the largest with a diameter of 11.5 cm and a weight of 350 g. The hail injured several people and animals, and caused damage to vehicles, houses, trees, and crops.

During 13–14 September, extremely intense precipitation over the Emilia Romania in central-north Italy caused a flood that destroyed roads and bridges. Record-breaking rainfall of 123.6 mm within 1 hour (189.0 mm within 3 hours) at Cabanne and 107.6 mm within 1 hour (201.8 mm within 3 hours) in Salsominore caused floods in the basin of the Aveto, Trebbia, and Nure Rivers. At Nure River, the water levels reached 7 m; the water entered the ground floors of nearby houses.

Bosnia and Herzegovina reported a nationwide heat wave that lasted six days, starting on 15 September. Many new September maximum temperature records were observed, for example, 38.0°C in Sarajevo and 40.9°C in Zenica, both on 18 September.

6) Eastern Europe

This region includes the European part of Russia, Belarus, Ukraine, Moldova, and Romania.

(i) Temperature

Averaged over the year, temperatures across eastern Europe were well above normal, with departures mostly in the +2° to +3°C range. Belarus had its warmest year on record, 2.6°C above normal, surpassing the previous record years of 1989 and 2008. Moldova had its second warmest year, after 2007, and recorded departures from +2.1° to +2.7°C across the country.

Temperatures in winter 2014/15 were extremely mild, especially in northwestern and eastern European Russia, where anomalies exceeded +4°C (hatched in Fig. 7.36a). Belarus reported a national temperature 3.8°C above average, its fifth warmest such period since records began in 1945. In February, above-average 500-hPa heights over central Siberia caused widespread anomalous mild conditions across eastern Europe (more than +4°C). At the end of February, Moldova observed daily temperatures 5°–6.5°C above the long-term mean, which, on average, occurs once every 10 years.

Spring remained warmer than normal, with a meridional gradient in the temperature anomalies due to prolonged high pressure over central Siberia. While northern European Russia experienced anomalies that exceeded +4°C, the Caucasus region had near-normal conditions.

Summer was characterized by high pressure over continental Europe, whereas northern areas were affected by frequent cyclones. In northeastern areas of the region, below-normal temperature anomalies as low as −1°C were registered, while positive anomalies up to +4°C were recorded in westernmost and southernmost places. July was very cool in northern European Russia (down to −4°C) as a result of SLP anomalies of −12 hPa over western Siberia.

During autumn, temperature departures of −1°C in eastern European Russia contrasted with positive anomalies between +1° and +2°C in the remaining regions. Southeastern Ukraine and southern European Russia observed temperatures up to +3°C due to advection of subtropical air masses.

The year ended with significant mild conditions. Moldova reported positive deviations of +2.7°C to +4.5°C in December. On the 27th, areas across Moldova set new records in maximum temperature that ranged from 14° to 18°C.

(ii) Precipitation

Annual precipitation totals in 2015 were above average (>125%) over northeastern areas of the region, while southwestern areas had near-normal conditions. Only the Caucasus region, western Ukraine, and northern Moldova recorded rainfall less than 80% of normal.

Winter 2014/15 was characterized by a strong Icelandic low associated with stronger-than-normal westerly winds that brought a precipitation surplus of more than 125% to most of European Russia (hatched in Fig. 7.37a). Along Romania's Black Sea coast, 170% of normal precipitation fell. Only southwestern Russia and Ukraine received below-average totals, less than 80% of normal.

In spring, precipitation was near normal for the westernmost areas but above average in the Black Sea region. The eastern half of Ukraine recorded totals more than 170% of normal. In contrast, parts of northern European Russia experienced drier-than-normal conditions.

During summer, prevailing high pressure conditions featured a strong rain deficit in western and southern areas of eastern Europe, where less than 60% of normal totals were observed (dotted in Fig. 7.37c). Northern and eastern European Russia were influenced by frequent low pressure systems that brought 125%–170% of normal totals to the region. August was dominated by exceptionally dry conditions in western and southern areas, with less than 20% of normal rainfall. Belarus reported just 16% of normal totals, experiencing its driest August on record since 1945.

Precipitation totals in autumn were unevenly distributed. While the majority of areas had near-normal precipitation, the western Black Sea region received more than 170% of normal, and Romania observed up to 250% of normal precipitation in places. In contrast, western European Russia recorded below-average totals, with some localized observations just 60% of normal.

In December, exceptionally strong westerlies brought well-above-average precipitation to most of the region, with more than 250% of normal totals measured in southern places.

(iii) Notable events

Belarus reported a thunderstorm on 14 June with hailstones measuring 3 cm in diameter. On 27 July, 34.5 mm of rain fell within 30 minutes at station Zhitkovichi in the south.

Moldova experienced high temperatures during 1–2 September. Record-breaking maximum air temperatures of 35.3°C and 38.6°C were measured.

7) Middle East

This region includes Israel, Cyprus, Jordan, Lebanon, Syria, West Kazakhstan, Armenia, Georgia, and Azerbaijan.

(i) Temperature

Annual temperatures were higher than normal, at +1° to +2°C above the long-term mean throughout the Middle East, except for Cyprus, where near-normal conditions prevailed. Armenia observed its third warmest year since records began in 1961 (+1.8°C) and Israel also had its third warmest year in its 65-year record.

Winter 2014/15 was characterized by anomalous temperatures between +2° and +3°C, associated with above-average 500-hPa heights and advection of subtropical air (Fig. 7.37a). Armenia reported significantly warmer conditions with positive anomalies of +2.6°C; locally, in January and February, temperatures were 4°–5°C above average.

In spring, temperatures were near to slightly below normal in the Caucasus region and western Kazakhstan, while the eastern Mediterranean countries experienced warmer-than-normal conditions (+1°C to +2°C). March contributed to the positive seasonal anomalies, due to a combination of high pressure over western Russia and warm air advection from subtropical regions. Armenia observed a national temperature 1.4°C above normal.

During summer, prevailing anticyclonic conditions induced positive temperature anomalies across the entire region (hatched and dotted areas in Fig. 7.36e). Western Kazakhstan and the Caucasus region had anomalies up to +3°C, and the eastern Mediterranean countries also experienced higher-than-normal temperatures of 1°–2°C above average. Armenia observed its second warmest summer, behind 2006, in its 55-year record, with anomalies of +2.4°C. The highest values were recorded in June, where most stations measured temperatures more than 3°C above the long-term mean. In Israel, colder-than-normal anomalies in June (–1°C) contrasted with well-above-average temperatures in August (+2°C).

Temperatures in autumn remained anomalously high in the Middle East. The eastern Mediterranean region experienced areawide anomalies of +3°C, whereas the Caucasus and western Kazakhstan were 1°–2°C above normal. Some places in northwestern Kazakhstan saw temperature anomalies down to –1°C. September was very warm, as a high pressure system associated with large subsidence developed over western Kazakhstan. Israel observed temperatures 2.5°–3°C above normal, marking its warmest September on record, while Cyprus reported its second warmest, with anomalies of +2°C. Armenia also had its second warmest September (2010 was warmer), exceeding the long-term mean by 3°C.

In December, colder-than-normal temperatures in the southern part of the region contrasted with exceptional positive anomalies in northern areas. Areawide anomalies exceeded +4°C in western Kazakhstan.

(ii) Precipitation

Averaged over the year, much of the region saw near-normal precipitation totals. Only western Kazakhstan and the Caucasus region experienced drier-than-normal conditions (< 80%), while much of Jordan received totals up to 125% of normal.

Winter 2014/15 was mostly drier than normal, with as little as 60% of normal precipitation. Only areas in the southern Caucasus region and parts of western Kazakhstan received above-average totals (more than 125% of normal). During February, westernmost Kazakhstan experienced very dry conditions, less than 20% of normal precipitation, whereas northern Israel saw 120%–170% of normal rainfall.

In spring, above-average precipitation in northern areas of the region contrasted with a rain deficit in the eastern Mediterranean countries due to significant above-average SLP. Locally, less than 40% of normal total precipitation was received in some places.

During summer, conditions changed when the region was under the influence of significantly above-average SLP (dotted in Fig. 7.37c). Azerbaijan reported a very dry summer, with less than 40% of normal precipitation. In contrast, the eastern Mediterranean countries mostly received an extreme surplus of rain, locally exceeding 500% of normal in some areas, despite its being the dry season.

In autumn, western Kazakhstan and much of the eastern Mediterranean recorded 60%–80% of normal precipitation, whereas the Caucasus region received 125% of normal. September was dry, whereas October was wet. Israel reported 130% of normal rainfall in the central and southern coastal plain.

In December, low pressure over central European Russia brought precipitation to western Kazakhstan that totaled more than 167% of normal. The Mediterranean region was affected by a high pressure ridge that caused a rain deficit, as little as 20% of normal, in the eastern half and parts of the Caucasus.

(iii) Notable events

Cyprus experienced heavy rainfall accompanied by floods during 5–6 January. Station Kelokedara received 276.6 mm of rain within 24 hours, the highest 1-day precipitation total during January since 1916.

On 7 January, Azerbaijan reported a daily maximum temperature of 15°C, the highest for January since records began in 1900.

During 6–8 January and 18–19 February, Cyprus received heavy snowfall, with 15 cm accumulation in the first event. In both events, schools in mountainous areas were closed.

On 13–14 June, Tbilisi, the capital of Georgia, was hit by heavy rain and thunderstorms. Flooding and an associated landslide led to 12 fatalities and damaged the local zoo, where many animals also perished.

From 25 to 30 October, Israel was hit by a major storm with strong winds of 13–20 m s^{-1} and maximum wind gusts of 36.6 m s^{-1}. Hailstones with diameters of 4–5 cm damaged agriculture crops. On 28 October, 80–85 mm rain fell within 2–3 hours and caused floods in central and eastern parts of the country. A station near Tel Aviv received a monthly accumulation of 246 mm, which is a national record.

g. Asia

This section covers Russia, East Asia, South Asia, and Southwest Asia. There is no information for Southeast Asia as no corresponding author was identified for the region. Throughout this section the normal periods used vary by region. The current standard is the 1981–2010 average for both temperature and precipitation, but earlier normal periods are still in use in several countries in the region. All seasons mentioned in this section refer to the Northern Hemisphere.

1) Overview

Based on data from WMO CLIMAT reports, annual mean surface air temperatures during 2015 were above normal across most of Asia and Siberia (Fig. 7.38). Annual precipitation amounts were above normal in eastern China, from southern Mongolia to northwestern China, and from western Siberia to northern India, and they were below normal in Southeast Asia (Fig. 7.39).

Figure 7.40 shows seasonal temperature and precipitation departures from the 1981–2010 average during the year. Seasonal mean temperatures were above normal across Siberia in all seasons, except for the east in spring and the south in autumn. Temperatures were also above normal in northern China in winter, in parts of central and Southeast Asia in spring, in Southeast Asia in summer, and across Southeast Asia and India in autumn. Temperatures were below normal from central China to India in winter, from the western part of central Asia to India in spring, from eastern China to central Pakistan and in European Russia in summer, and across central Asia in autumn.

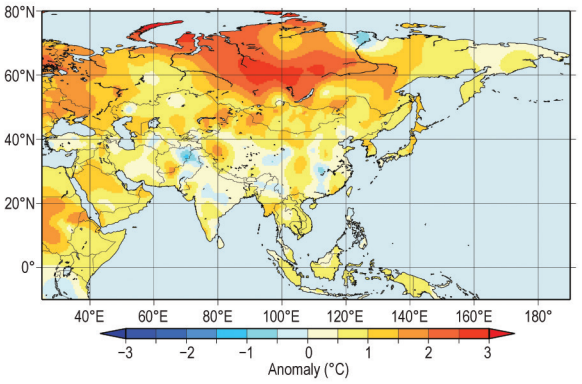

Fig. 7.38. Annual mean temperature anomalies (°C; 1981–2010 base period) over Asia in 2015. (Source: Japan Meteorological Agency.)

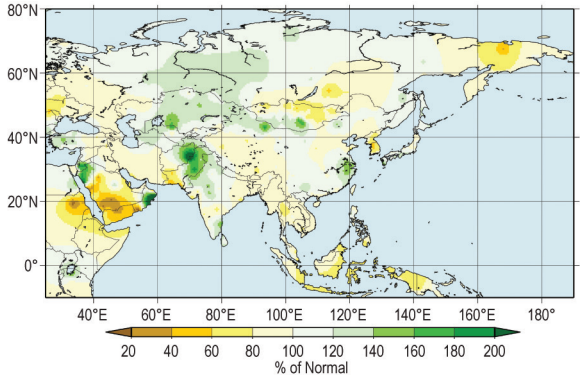

Fig. 7.39. Annual precipitation (% of normal; 1981–2010 base period) over Asia in 2015. (Source: Japan Meteorological Agency.)

Seasonal precipitation amounts were above normal in large areas from western to central Siberia in all seasons, especially in winter and summer. In contrast, they were below normal in Southeast Asia, especially in summer and autumn. They showed greater spatial variability across East, central, and South Asia.

Surface climate anomalies were associated with several distinct circulation features. Convective activity was suppressed over Southeast Asia except in winter (see Fig. 7.41), in association with El Niño conditions. In summer, the monsoon circulation over the Indian Ocean was weaker than normal (see Fig. 7.41c), and overall activity of the Asian summer monsoon was below normal. The northwestward seasonal extension of the northwest Pacific subtropical high was weaker than normal (see Fig. 7.42c), contributing to cool wet summer conditions from southeastern China to western Japan.

2) Russia—O. N. Bulygina, N. N. Korshunova, M. U. Bardin, and N. M. Arzhanova

Analyses are based on hydrometeorological observations conducted at Roshydromet Observa-

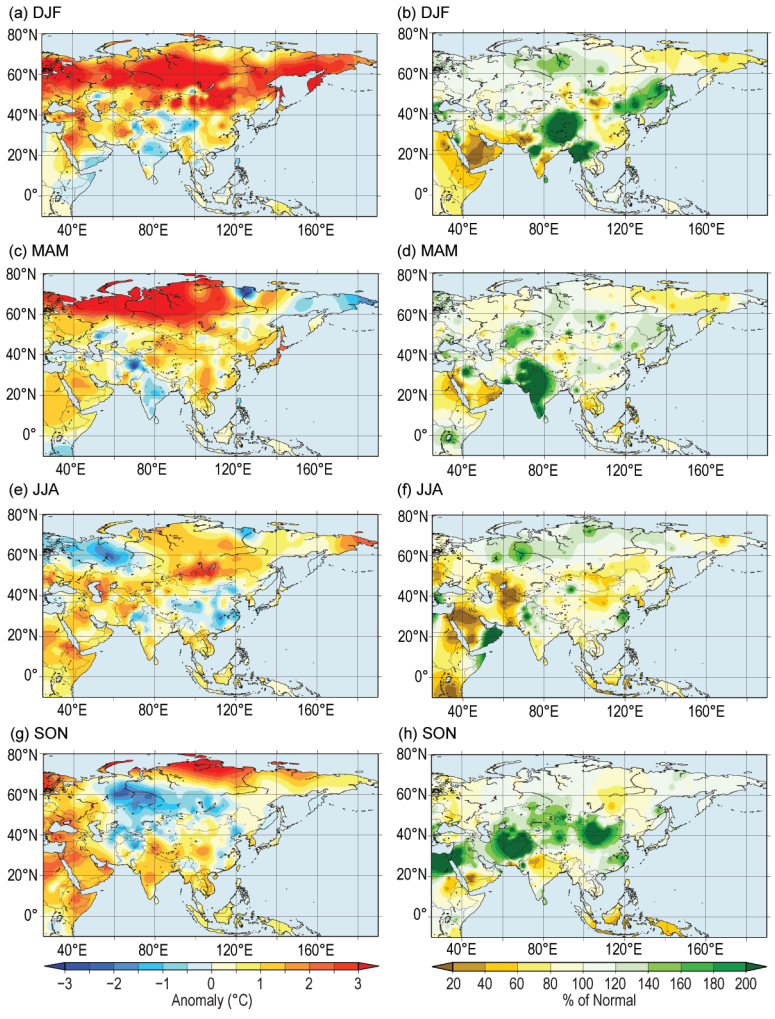

Fig. 7.40. Seasonal temperature anomalies (°C, left column) and precipitation ratios (%, right column) over Asia in 2015 for (a), (b) winter (Dec–Feb 2014/2015); (c), (d) spring (Mar–May); (e), (f) summer (Jun–Aug); and (g), (h) autumn (Sep–Nov), with respect to the 1981–2010 base period. (Source: Japan Meteorological Agency.)

tion Network. Datasets are officially registered and available at meteo.ru/english/climate/cl_data.php. The national average temperature and precipitation records began in 1935, while seasonal averages are considered reliable only since 1939.

(i) Temperature

The mean annual Russia-averaged air temperature was 2.2°C above the 1961–90 normal (Fig. 7.43), making 2015 the warmest year since records began in 1935. Positive mean annual air temperature anomalies were observed across all regions of Russia, with the largest anomalies in northern European Russia and western Siberia (Fig. 7.38).

For Russia as a whole, winter was record warm, with the mean temperature 3.6°C above normal (Fig. 7.43). Central European Russia experienced mean temperature anomalies of +4°–6°C, and +6°–8°C anomalies were observed across the Far East. Daily temperature records were exceeded many times across European Russia. Daily and monthly record-breaking air temperatures were repeatedly registered in many cities, including Moscow, St. Petersburg, Tambov, Voronezh, Tomsk, and Kemerovo.

Spring 2015 was also very warm, with a Russia-averaged mean seasonal air temperature anomaly of +2.3°C (Fig. 7.43), the fourth highest in the 77-year period of record. In northern European Russia and western Siberia, the spring mean air temperature anomaly reached a record-breaking value of +5.2°C.

Summer 2015 continued to be warmer-than-average across Russia, with a national seasonal air temperature anomaly of +1.2°C, the seventh warmest on record (Fig. 7.43).

Autumn was mild over most of Russia with a seasonal mean temperature anomaly of +0.9°C (Fig. 7.43). Positive anomalies were recorded in all regions, except southern West Siberia. From 11 to 30 September, all regions of European Russia experienced abnormally warm weather, and many meteorological stations, from Novaya Zemlya to northern Caucasia, registered several daily record-breaking maximum temperatures.

In December (Fig. 7.44), positive anomalies of mean monthly air temperature were recorded over a vast area, from the western boundaries to the Sea of Okhotsk coast. For the whole of Russia, the anomaly was +4.1°C, the second highest on record. The largest anomalies occurred in northwestern European Russia and in the central Krasnoyarsk Territory and southern West Siberia. In St. Petersburg, with nearly 200 years of meteorological observations, the December 2015 mean monthly air temperature of +2.1°C was the second highest for December on record (see inset in Fig. 7.44).

(ii) Precipitation

In 2015, Russia as a whole received slightly above-normal precipitation, 106% of the 1961–90 normal (Fig. 7.45).

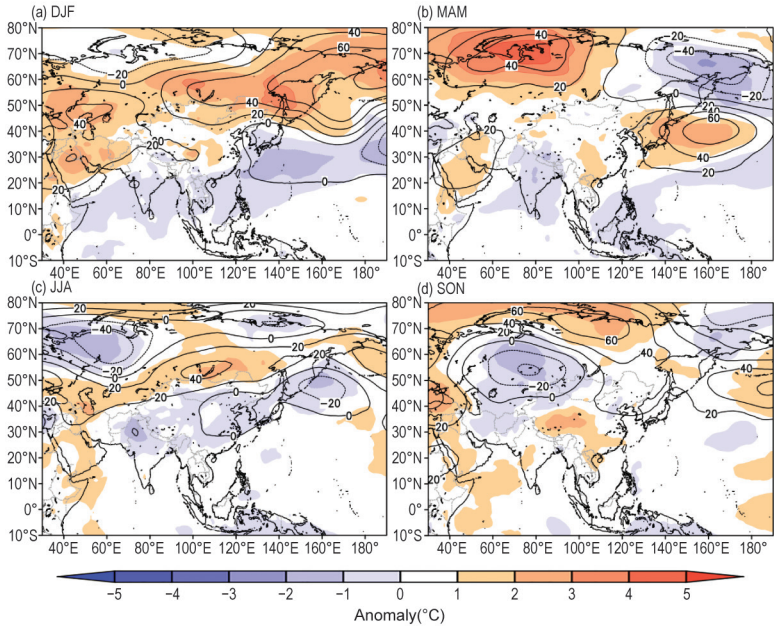

Fig. 7.41. Seasonal mean anomalies of 850-hPa stream function (contour, 1 × 10^6 m^2 s^{-1}) using data from the JRA-55 reanalysis and outgoing longwave radiation (OLR, shading, W m^{-2}) using data originally provided by NOAA for (a) winter (Dec–Feb 2014/15), (b) spring (Mar–May), (c) summer (Jun–Aug), and (d) autumn (Sep–Nov), with respect to the 1981–2010 base period. (Source: Japan Meteorological Agency.)

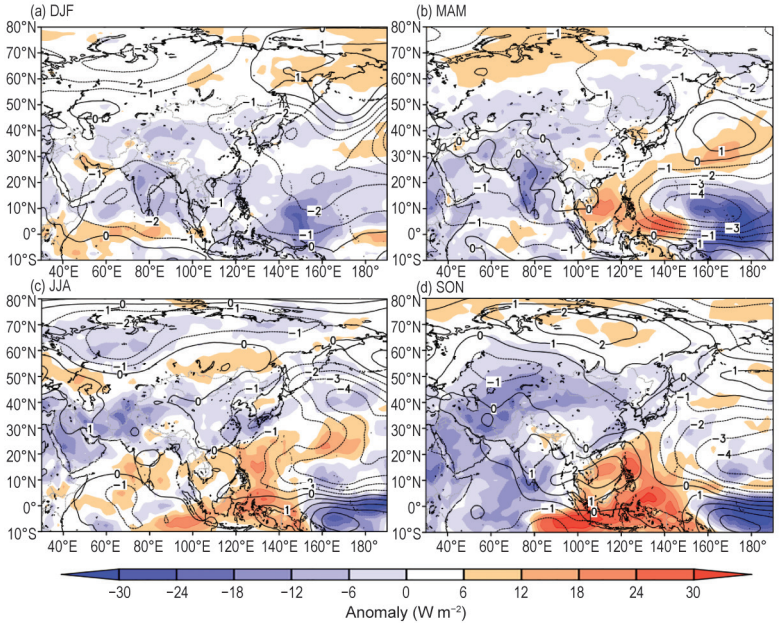

Fig. 7.42. Seasonal mean anomalies of 500-hPa geopotential height (contour, gpm) and 850-hPa temperature (shading, °C) for (a) winter (Dec–Feb 2014/15), (b) spring (Mar–May), (c) summer (Jun–Aug), and (d) autumn (Sep–Nov), with respect to the 1981–2010 base period. Data from the JRA-55 reanalysis. (Source: Japan Meteorological Agency.)

Winter precipitation was 119% of normal, tying (with 2007/08) as the second wettest since 1935 (the wettest winter was 1965/66, 136% of normal). In spring, Russia on average received 115% of normal precipitation. Over European Russia, a significant precipitation deficit was recorded in March.

The summer precipitation total averaged over Russia was normal (99%). Near-normal precipitation was also recorded in autumn, 101% of normal. In December, Atlantic cyclones brought heavy precipitation to northwestern European Russia, the Urals, southern western Siberia, and the central Krasnoyarsk Territory.

(iii) Notable events

On 14 January, Kazan reached +2.3°C, the warmest for this date since records began in 1880.

During the last five days of January, the city of Magadan received nearly five times its normal monthly precipitation.

On 12 April, strong winds (25–31 m s^{-1}) in Khakassia caused a rapid propagation of natural fires that killed five people and injured 121. The fire destroyed 1205 homes.

On 24–25 June, heavy rain fell in Sochi, with 122 mm of precipitation observed in less than 11 hours. As a result, roads, 2000 houses, and the railroad station were inundated. Damage was estimated to be 760 million rubles (~10 million U.S. dollars). In the city of Adler, 211 mm of precipitation fell in 18 hours; 200 houses, the local airport, and the railroad station were inundated. Damage was estimated to be 10–13 billion rubles (150–195 million U.S. dollars), mostly associated with the temporary closure of the airport.

On 11 July, heavy rain and hail fell in the Ulyanovsk Region, with 31 mm of precipitation falling in 48 minutes. Hail with diameters reaching 5.6 cm damaged roofs, glass panes, and 150 cars.

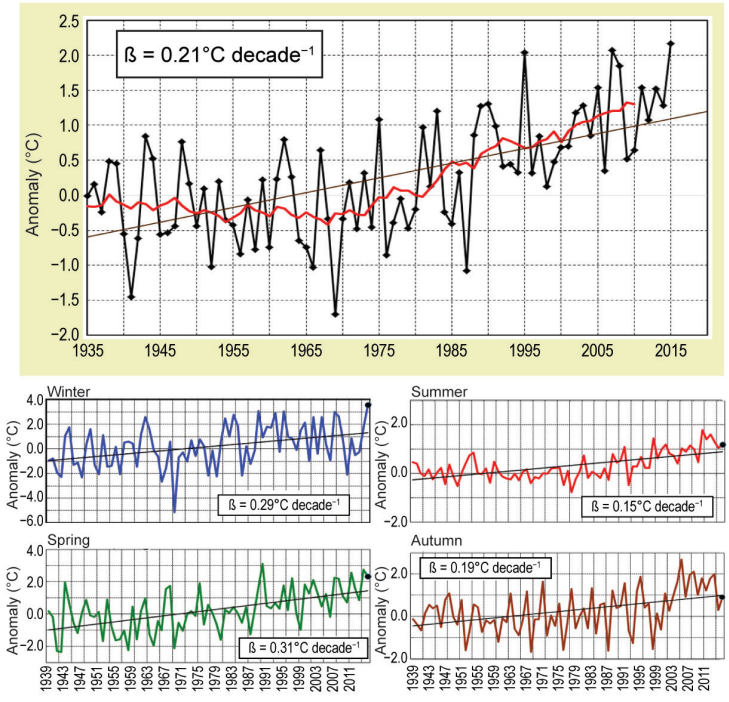

Fig. 7.43. Mean annual (1935–2015) and seasonal (1939–2015) air temperature anomalies (°C) averaged over the Russian territory for 1939–2015 (base period: 1961–90). Seasons are Dec–Feb (winter) 2014/15 and Mar–May (spring), Jun–Aug (summer), and Sep–Nov (autumn) 2015. The smoothed annual mean time series (11-point binomial filter) is shown in red in the top panel.

On 7–8 September, as a result of heavy rain (20 mm in 4 hours), large hail (2.0 cm in diameter), and strong winds (up to 24 m s^{-1}) in Tatarstan, 19 people were injured, 31 cars were damaged, trees were toppled, and roofs were damaged.

3) East Asia—P. Zhang, A. Goto, S.-Y. Yim, and L. Oyunjargal

Countries considered in this section include: China, Japan, Korea, and Mongolia. Unless otherwise noted, anomalies refer to a normal period of 1981–2010.

(i) Temperature

The annual mean temperature over China was 10.5°C, 0.9°C above normal, the highest since records began in 1961. The seasonal mean surface temperature anomalies were +1.1°C, +1.0°C, +0.3°C, and +0.8°C for winter, spring, summer, and autumn, respectively. Annual mean temperatures were above normal across Japan, especially in northern Japan and Okinawa/Amami. In western Japan, temperatures were below normal in summer and autumn but above normal for the year as a whole.

The annual mean surface air temperature over the Republic of Korea was 13.4°C, 0.9°C above normal, the second warmest since national records began in 1973. In 2015, temperatures for most months except summer were higher than normal. May was the warmest on record, at 1.4°C above normal. The annual mean temperature over Mongolia for 2015 was 1.8°C, 1.3°C above normal, the second warmest since national records began in 1961 and 0.8°C warmer than 2014. Most monthly mean temperature anomalies for Mongolia were above normal, ranging from +0.2° to +4.4°C. January was the warmest month in 2015 with respect to departures from average, 4.4°C above normal and marking the warmest January for Mongolia in the 55-year record. Positive anomalies were as high as 5°–7°C in some areas.

(ii) Precipitation

The mean annual total precipitation in China was 648.8 mm, 103% of normal and 2% higher than 2014. The total seasonal precipitation was below normal in winter (94% of normal) and summer (91% of normal), and near-normal in spring but above normal in autumn (126% of normal). In 2015, the major rain belt of China lay south of its normal position, over areas from the middle and lower reaches of the Yangtze River to South China, especially during summer and autumn, associated with a weak East Asian monsoon. Regionally, total annual precipitation was significantly above normal in the Yangtze River basin (112% of normal, the wettest in 17 years) and in the Zhujiang River basin (111% of normal), and below normal in Northeast China (94% of normal), in the Liaohe River basin (86% of normal), and in the Yellow River basin (73% of normal, the driest in 13 years). The rainy season in the Meiyu region started approximately 16 days early on 26 May and ended around 17 days late on 27 July with about 169% of normal precipitation. The rainy season in North China started on 23 July (5 days later than normal) and ended on 17 August (slightly earlier than normal), and was the second driest season in the past 13 years.

In western Japan, annual precipitation amounts were above normal, especially on the Pacific side, since the seasonal northward expansion of the North Pacific subtropical high was weak and convection was often active in summer. On the Pacific side of eastern Japan, annual precipitation amounts were also above normal, including record-breaking rain in September.

SIDEBAR 7.2: EXTREMELY WET CONDITIONS IN JAPAN IN LATE SUMMER 2015

From mid-August to early September 2015, most of western to northern Japan experienced unseasonably wet conditions. Regional average precipitation totals in the 32 days starting on 11 August were 245% and 209% of normal for the Pacific side of western Japan and eastern Japan, respectively. Sunshine duration averaged over the Sea of Japan side of eastern Japan was nearly half the normal amount. Toward the end of the period, record-breaking torrential rainfalls led to large river overflows and flooding in parts of eastern Japan.

The lasting, extremely wet weather conditions were associated with low pressure systems repeatedly forming and migrating eastward along a frontal zone that persisted over the Japanese Archipelago. The persistence of the frontal zone in turn appears related to warm air and vorticity advection in the middle troposphere induced by nearly stationary cyclonic circulation anomalies to the west of Japan (Fif. SB7.4). Meanwhile the northwestern Pacific subtropical high, which would bring hot and sunny days during a normal summer, shifted far southward of its normal position and became a factor in enhancing southwesterly moist air inflow toward Japan in the lower troposphere. These anomalous atmospheric circulation patterns were sustained in connection with suppressed convective activity across the Asian summer monsoon area (Fig. SB7.5), which is consistent with that observed in past El Niño events. Upper tropospheric wave trains propagating from the west across the Eurasian continent may also have played a part in sustaining the cyclonic anomalies to the west of Japan.

A further contribution to the above-normal precipitation amount came from two tropical cyclones during the second week of September. Typhoon Etau made landfall on mainland Japan and Typhoon Kilo passed northward over the Pacific off the coast of Japan, both of which induced moist air inflow and set the environment conducive to torrential rainfalls observed in parts of eastern to northern Japan.

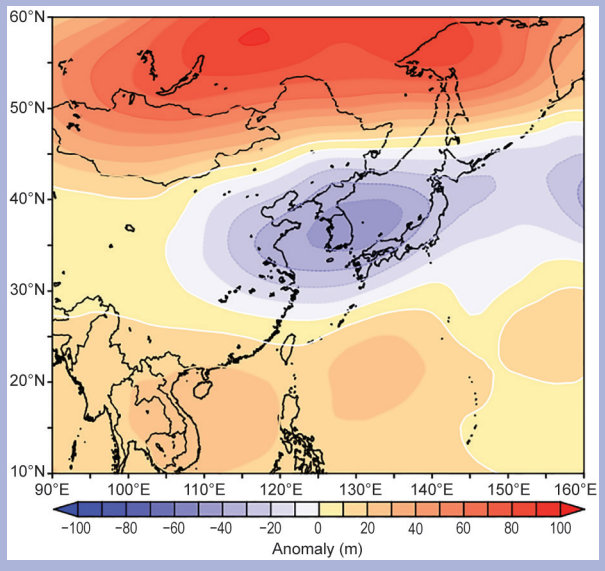

FIG. SB7.4. Geopotential height anomalies (m) at 500 hPa averaged over 11 Aug to 11 Sep, 2015 (base period: 1981–2010). (Source: Japanese 55-year reanalysis.)

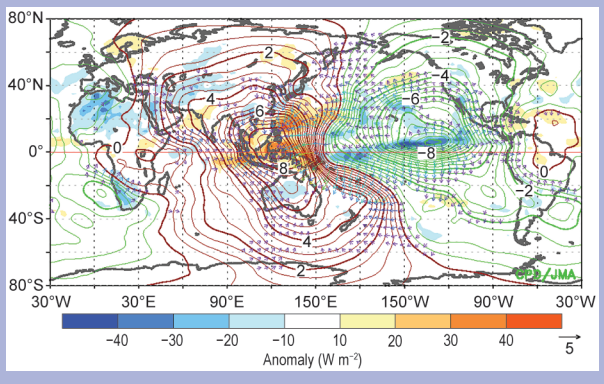

FIG. SB7.5. Velocity potential anomalies at 200 hPa (thick and thin contours at intervals of 2.0 × 10⁶ and 0.5 × 10⁶ m² s⁻¹, respectively) and outgoing longwave radiation (OLR; shading) anomalies averaged over the same period as Fig. SB7.4 (base period: 1981–2010). Arrows indicate associated divergent flow, where it is significantly different from climatology. [Source: Japanese 55-year reanalysis (velocity potential) and NOAA/CPC (OLR).]

In the Republic of Korea, the annual total precipitation was 948.2 mm, 72% of normal, the third lowest since national records began in 1973. In Mongolia, the annual average precipitation in 2015 was 202 mm, near normal. However, the temporal and spatial distribution of precipitation was unfavorable for agriculture. At the beginning of the growing season, late June was warmer and drier than normal in Mongolia, resulting in drought and economic losses in the agriculture sector. November was the wettest month of the year and wettest November on record (181% of normal) while July was the driest month of the year (80% of normal). The high November precipitation total included a lot of snowfall, with snow covering at least 80% of Mongolia during the month, making livestock husbandry difficult. Warm conditions in December helped alleviate this somewhat.

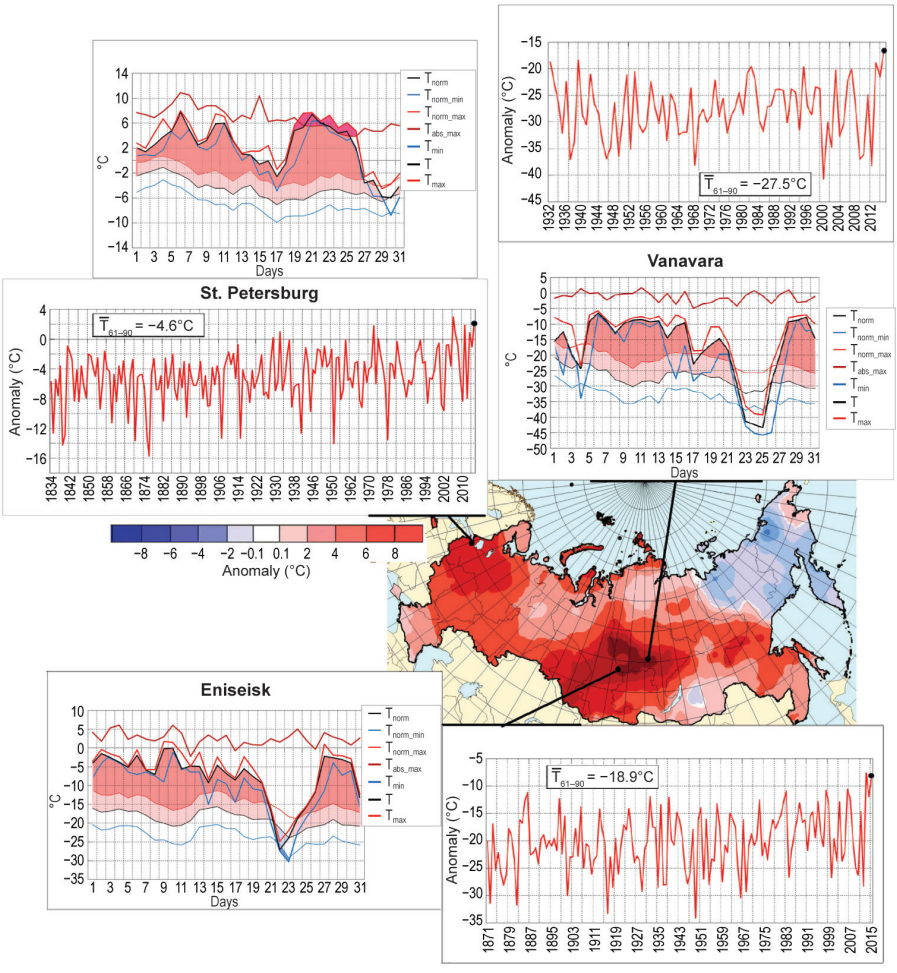

Fig. 7.44. Air temperature anomalies (°C) in Dec 2015. Insets show the time series of mean monthly and mean daily air temperatures (°C) for the month at meteorological stations St. Petersburg, Eniseisk, and Vanavara.

(iii) Notable events

Liaoning province in North China had its driest summer since records began in 1961, which contributed to severe drought in the area. Xinjiang had 25 days of daily maximum temperature exceeding 35°C (normal is 10 days).

In early September, the Kanto and Tohoku regions of Japan experienced record-breaking rainfall, due to warm, moist airflow associated with approaching typhoons Kilo and Etau. Total precipitation during 7–11 September was 647.5 mm at Imaichi in Tochigi Prefecture and 556.0 mm at Hippo in Miyagi Prefecture. Heavy rain caused large river overflows and serious damage.

Typhoon Mujigae in October was the strongest typhoon to make landfall in Guangdong province, China, since records began in 1949. The storm caused a major disaster, with 24 deaths and direct economic losses estimated at over 4.5 billion U.S. dollars (see section 4e4 for more details).

The worst large-scale and persistent haze event over China in 2015 occurred in Huanghuai and North China from late November to early December. It had a maximum extent of 41.7 km^2, with particulate matter smaller than 2.5 μm in diameter (PM2.5) exceeding 150 μg m^{-3} and visibility below 3 km.

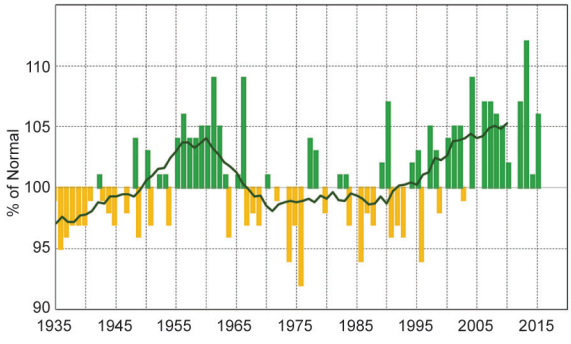

Fig. 7.45. Annual precipitation anomaly (% of normal) averaged over the Russian territory for the period 1935–2015. The smoothed time series (11-point binomial filter) is shown as a continuous line (base period: 1961–90).

4) South Asia—A. K. Srivastava, J. V. Revadekar, and M. Rajeevan

Countries in this section include: Bangaladesh, India, Pakistan, and Sri Lanka. Climate anomalies are relative to the 1961–90 normal. Monsoon precipitation is defined relative to a 50-year base period (1951–2000) because there is strong interdecadal variability in Indian monsoon precipitation (Guhathakurta et al. 2015). In the text below, this is referred to as the long-term average (LTA).

(i) Temperature

South Asia generally experienced well-above-normal temperatures in 2015. The annual mean land surface air temperature averaged over India was 0.7°C above the 1961–90 average, making 2015 the third warmest year since records commenced in 1901 (Fig. 7.46; 2009 and 2010 are warmest and second warmest, respectively). Record warmth was observed during July–September (+0.9°C) and October–December (+1.1°C).

(ii) Precipitation

The summer monsoon set in over Kerala (southern peninsular India) on 5 June, 4 days later than normal, but covered the entire country on 26 June, 20 days ahead of its normal date of 15 July. The pace of advance of the monsoon over different parts of the country was the third fastest in the 1950–2015 period.

Indian summer monsoon rainfall (ISMR) during 2015 was significantly below normal, 86% of its LTA of 890 mm. ISMR during 2015 was characterized by marked spatial and temporal variability. The eastern/northeastern region of the country received normal rainfall overall, with regional variability, while the central, peninsular, and northwestern regions of the country received below-normal rainfall (Fig. 7.47). Rainfall over many parts of northern, western, and central India was less than 70% of the LTA. Rainfall activity was also variable in time. During the first half of the season (1 June–31 July), the country received 95% of the LTA, falling to 77% of the LTA in the second half of the season (1 August–30 September).

During the monsoon season, only 1 meteorological subdivision (West Rajasthan) of 36 received excess rainfall. Eighteen subdivisions received normal rainfall, and the remaining 17 received below-normal rainfall. Except for June, rainfall averaged over the country was below normal on most days during the season (Fig. 7.48).

During winter (January–February), rainfall over the country was 92% of its LTA, while it was above normal (138% of the LTA) during the premonsoon season (March–May). During the post-monsoon season (October–December), it was 77% of the LTA.

The northeast monsoon (NEM) typically sets in over southern peninsular India during October and over Sri Lanka in late November. The NEM generally contributes 30%–50% of the annual rainfall over southern peninsular India and Sri Lanka as a whole. The 2015 NEM seasonal rainfall over southern pen-

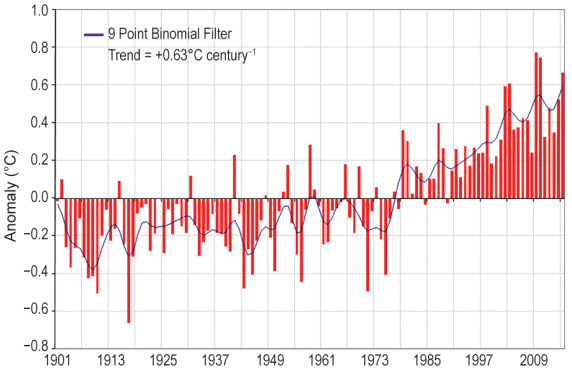

Fig. 7.46. Annual mean temperature anomalies (base period: 1961–90) averaged over India for the period 1901–2015. The smoothed time series (9-point binomial filter) is shown as a continuous line.

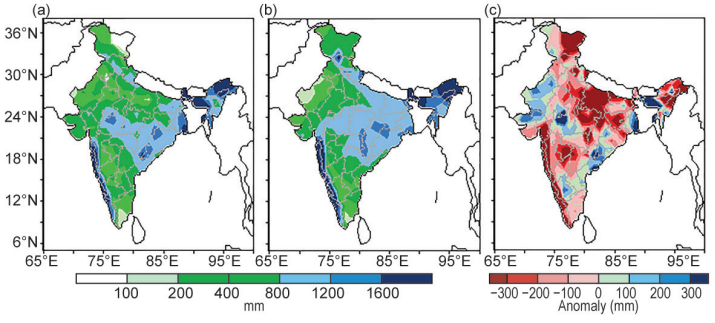

Fig. 7.47. Spatial distribution of monsoon seasonal (Jun–Sep) rainfall (mm) over India in 2015 for (a) observed rainfall, (b) normal rainfall, and (c) the difference between (a) and (b).

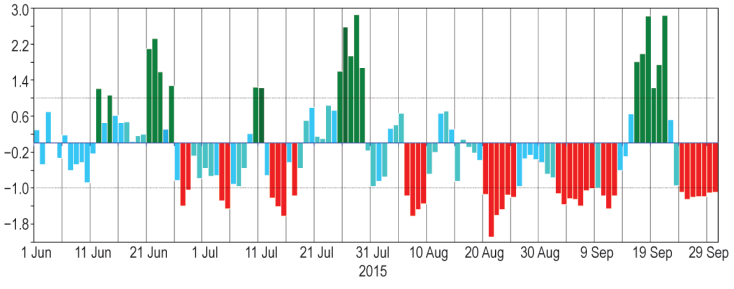

Fig. 7.48. Daily standardized rainfall time series averaged over the monsoon core zone over India (1 Jun–30 Sep).

insular India and Sri Lanka was above normal (132% of the LTA). Sri Lanka received below-normal rainfall during its summer monsoon season (May–September). However, northeast monsoon rainfall activity over the island nation during October–December was enhanced.

Pakistan, at the western edge of the pluvial region of the South Asian monsoon, generally receives 60%–70% of its annual rainfall during its summer monsoon season (July–September). In 2015, summer monsoon rainfall over Pakistan was 117% of the LTA and was marked by spatial and temporal variability. Southwestern/southern Pakistan received below-normal rainfall, while other regions received normal or above-normal rainfall during the season. Bangladesh also received above-normal rainfall overall during its summer monsoon season.

(iii) Notable events

A severe Nor'wester (a line of strong thunderstorms) affected 12 districts of Bihar (eastern India) during the nighttime/early morning hours of 22–23 April. Over 50 lives were lost.

Heat wave conditions prevailed over central, peninsular, and northern parts of India during the second half of May. Maximum temperatures were more than 5°C above normal at many eastern and central stations for several days. Some stations in Odissa and coastal Andhra Pradesh reported temperatures of near 47°C during 23–26 May. Overall, the intense heat over central and peninsular parts of the country during May took a toll of around 2500 lives, and more than 2000 deaths were reported in the south Indian states of Telangana and Andhra Pradesh.

One of the most severe heat waves since 1980 affected Karachi, Pakistan, during the second half of June and took a toll of more than 1000 lives. Temperatures reached 44°C for two days during the period. The heat wave coincided with the beginning of the holy month of Ramadan, when many Muslims do not eat or drink during daylight hours, increasing susceptibility to heat stroke.

During 25–26 June, heavy rain and floods associated with a deep depression over the Arabian Sea took a toll of more than 80 lives in Gujarat in western India.

Floods caused about 70 deaths in West Bengal (eastern India) during 30 July–5 August.

Many parts of Bangladesh experienced severe floods from late June through the first week of August. An estimated 30 people were killed and around one million were affected.

Very heavy rainfall during an active period of the NEM during 9–17 November and 2–5 December led to more than 350 fatalities in Tamil Nadu (southernmost India) and more than 50 deaths in the adjoining state of Andhra Pradesh. Heavy rainfall and flooding affected around 1.8 million people in Tamil Nadu. Tambaram (near Chennai) reported an all-time 24-h record rainfall of 490 mm on 2 December, while Chennai reported 345 mm of rain on the same day. Economic loss due to these events was estimated to be around 2 billion rupees (~29 million U.S. dollars).

Northeast monsoon activity during the first week of December also led to floods in Sri Lanka, which caused 40 deaths and displaced more than 1.2 million residents.

5) Southwest Asia—F. Rahimzadeh, M. Khoshkam, S. Fateh, and A. Kazemi

This subsection currently covers only Iran. Turkey is incorporated in the Europe subsection. Climate anomalies are relative to the 1981–2010 normal.

(i) Temperature

Winter 2014/15 and spring 2015 were considerably warmer than normal, with anomalies up to +6.4°C during winter. Most of the country was also warmer than normal in summer and near-normal overall in autumn (Fig. 7.49).

(ii) Precipitation

Generally, in 2015, Iran experienced drier-than-normal conditions in winter and spring, while summer and autumn were wetter than normal (Fig. 7.50).

During winter 2014/15, 30%–90% of normal precipitation fell across most parts of the country. Areas with average or above-average rainfall (up to 170% of normal) were confined to a small part in the northwest of the country adjacent to the Turkish border and a small part in the southeast. During spring, precipitation amounts were 30%–90% of normal across most of the country. The middle of the country received more than 90% of normal precipitation.

In summer, most of the country experienced normal or above-normal precipitation (90%–170% of normal). During autumn, precipitation was more than 90% of normal in much of the northern and southern regions, while the rest of country received 30%–90% of normal.

(iii) Notable events

Significant dust storms during spring and summer spread over many parts of the country, especially southern and southwestern Iran.

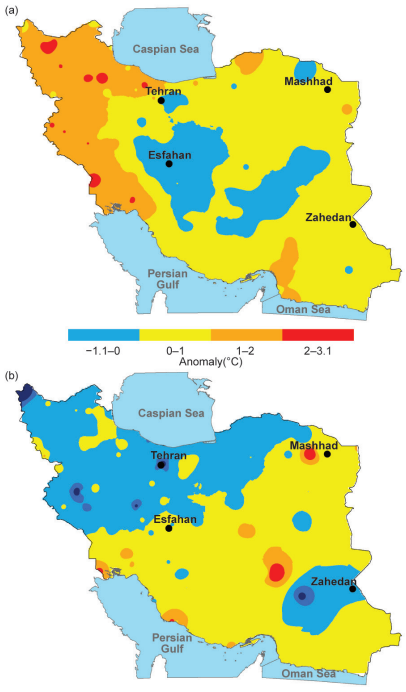

Fig. 7.49. Seasonal mean surface temperature anomalies (°C) in (a) summer (Jun–Aug) and (b) autumn (Sep–Nov). (Source: I.R. of Iran Meteorological Organization & National Center for Drought and Disaster Risk Management.)

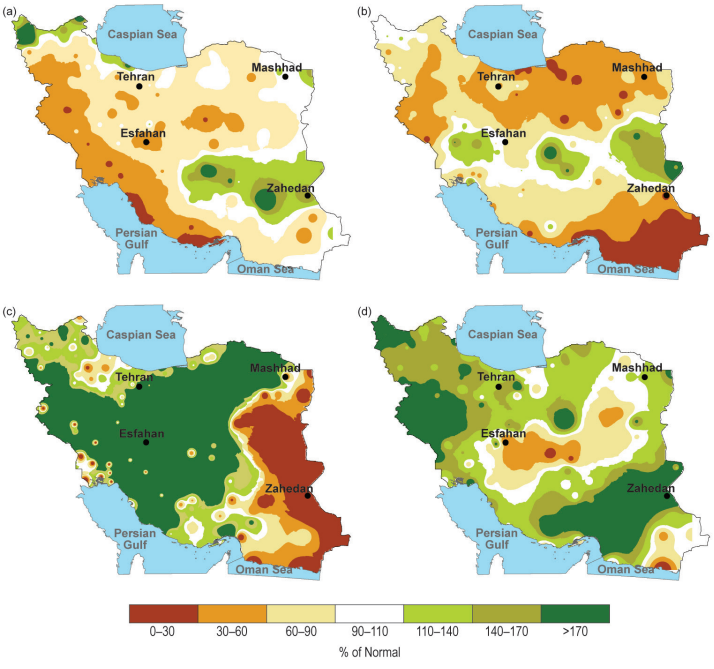

Fig. 7.50. Observed precipitation over Iran (% of normal) for (a) winter (Dec–Feb 2014/15), (b) spring (Mar–May), (c) summer (Jun–Aug), and (d) autumn (Sep–Nov). (Source: I.R. of Iran Meteorological Organization.)

h. Oceania

1) Overview—J. A. Renwick

During the first half of 2015, substantial warming of the equatorial Pacific sea surface and subsurface waters clearly signaled the arrival of El Niño. Extremes typical of El Niño onset were observed across the region, including rainfall extremes and an abundance of early-season tropical cyclones.

Following warm SSTs in the central and eastern equatorial Pacific in 2014 that almost reached El Niño thresholds (defined by NOAA as +0.5°C SST anomaly in the Niño-3.4 region for three consecutive months), El Niño became established in spring (March–May) 2015 and evolved into one of the strongest such events on record (alongside 1972/73, 1982/83, and 1997/98; see section 4b). El Niño–associated air temperature and rainfall patterns were observed across most of the South Pacific in 2015. A number of South Pacific countries experienced agricultural and/or hydrological drought.

Temperatures were generally above normal in Australasia, with Australia having another warm year, especially in the spring (Sidebar 7.3). Precipitation totals for 2015 were generally near-normal for both Australia and New Zealand. The southern annular mode (SAM) was generally positive through much of 2015, becoming strongly positive at the end of the year (www.cpc.ncep.noaa.gov/products/precip/CWlink/daily_ao_index/aao/month_aao_index.shtml). The base period used throughout this section is 1981–2010, unless otherwise indicated.

2) Northwest Pacific and Micronesia—M. A. Lander and C. P. Guard

This assessment covers the area from the international date line west to 130°E, between the equator and 20°N. It includes the U.S.-affiliated islands of Micronesia, but excludes the western islands of Kiribati and nearby northeastern islands of Indonesia.

(i) Temperature

Temperatures across Micronesia in 2015 were mostly above average. The warmth was persistent, with above-average temperatures occurring during most or all of the year. Only Yap Island had a substantial negative departure for any of the time periods summarized in Table 7.5. At islands located in the west of the region (e.g., Palau, Yap, Guam, and Saipan) there was a tendency for daytime maximum temperature anomalies to be greater than those of nighttime minima. In the east (Chuuk to Kosrae and Majuro), the reverse pattern was observed, as also seen in 2014. Average monthly maximum and minimum temperatures across most of Micronesia

have gradually increased for several decades, with a total rise in average temperature on par with the global average increase of +0.74°C in the last century (Guard and Lander 2012).

(ii) Precipitation

Dryness was observed across the Republic of the Marshall Islands (RMI) during early 2015, with very low rainfall totals reported at Utirik and Wotje in the northern RMI during January and February. However, rainfall throughout the RMI had a dramatic rebound to very wet conditions during March and April, even at the normally driest of the atolls in the north (e.g., Kwajalein, Utirik, and Wotje). Very wet conditions in the Marshall Islands typically occur in late winter and spring during years of El Niño onset. Dryness associated with El Niño typically begins earlier in the western bounds of Micronesia (e.g., Palau) and spreads eastward later in the year to the RMI. Meanwhile, locations in the far west of Micronesia experienced an early onset of dry conditions that became extreme late in the year.

Annual totals during 2015 were mostly higher than average, with early wetness outweighing dryness later in the year. The 2015 fourth quarter rainfall totals at Yap Island and at Palau were the lowest and second lowest in their ~65-year post-World War II historical record, respectively. By late December 2015, persistent dry conditions were becoming established at most of the islands of Micronesia. The 6-month and annual rainfall values for selected locations across Micronesia are summarized in Table 7.5.

(iii) Notable events

Micronesia was the overwhelming focus of the 2015 western North Pacific typhoon track distribution, with Guam at the primary nexus, by virtue of the passage of 12 named tropical cyclones within 550 km (see section 4e8 for more detail).

After nearly a decade of high values, sea level across Micronesia began to fall in 2014 and continued to fall dramatically in 2015 (Fig. 7.51). The maximum drop in monthly mean sea level (since 2013) at both Guam and at Kwajalein was approximately 40 cm (the drop in 12-month means was around 25 cm). A sharp drop in mean sea level typically occurs during El Niño, with the lowest sea level occurring in December of the year of the El Niño peak.

Table 7.5. Temperature and rainfall anomalies for selected Micronesia locations during 2015, (base period: 1981–2010). Latitudes and longitudes are approximate. "Kapinga" stands for Kapingamarangi Atoll in Pohnpei State, Federated States of Micronesia.

Location	Max/Min Temp Anomaly		Precipitation					
	Jan–Jun °C	Jul–Dec °C	Jan–Jun mm	Jan–Jun % of avg.	Jul–Dec mm	Jul–Dec %	Year mm	Year %
Saipan 15°N,146°E	+1.92 +1.04	+1.83 +1.46	570.0	126.9	**939.3**	71.0	**1509.3**	85.2
Guam 13°N,145°E	+0.40 −0.06	+0.58 +0.37	881.6	127.5	**2058.4**	115.1	**2940.1**	118.5
Yap 9°N,138°E	−1.44 −0.29	−0.30 +0.25	**1319.5**	112.8	**1818.9**	95.6	**3138.4**	102.2
Palau 7°N,134°E	+0.96 +0.03	+1.00 +0.31	**1185.2**	69.0	**1265.9**	62.3	**2451.1**	65.4
Chuuk 7°N,152°E	+0.31 +0.48	+0.28 +0.97	**2147.8**	135.6	**1823.0**	99.4	**3970.8**	116.2
Pohnpei 7°N,158°E	+0.18 +0.10	−0.10 +0.78	**3039.4**	134.1	**2470.9**	105.8	**5510.3**	119.7
Kapinga 1°N,155°E	N/A	N/A	**2411.7**	137.7	**1486.9**	98.4	**3261.4**	119.5
Kosrae 5°N,163°E	+0.38 +1.29	−0.21 +1.34	**2552.5**	99.4	**2007.6**	85.7	**4560.1**	92.9
Majuro 7°N,171°E	+0.01 +0.91	−0.03 +1.17	**1854.7**	135.5	**1713.5**	91.7	**3568.2**	110.2
Kwajalein 9°N,168°E	+0.37 +0.09	+0.22 +0.32	**1737.1**	216.8	**1593.6**	100.9	**3330.7**	139.9

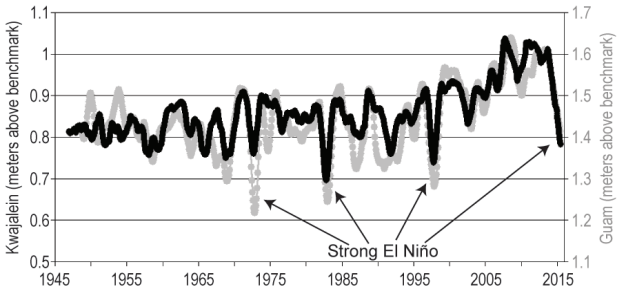

Fig. 7.51. Observed sea level rise/fall (12-month moving average) over the period 1945–2015 at Kwajalein (black, left vertical axis) and Guam (gray, right vertical axis).

3) Southwest Pacific—E. Chandler and S. McGree

Countries considered in this section include: American Samoa, Cook Islands, Fiji, French Polynesia, Kiribati, New Caledonia, Niue, Papua New Guinea (PNG), Samoa, Solomon Islands, Tokelau, Tonga, Tuvalu, and Vanuatu. Air temperature and rainfall anomalies are relative to the 1981–2010 period.

(i) Temperature

Mean air temperatures in 2015 (derived from NCEP–NCAR reanalysis) were strongly influenced by El Niño, which dominated the climate of the South Pacific during the year. Temperatures were near normal or above normal between January and March (Fig. 7.52a) across much of the southwest Pacific. Positive anomalies peaked at around +1.3°C near the equatorial date line. Below-average temperatures occurred near PNG, with anomalies up to –1.5°C over a small region covering the PNG Islands.

Positive temperature anomalies centered on the equator expanded westward towards the Solomon Islands and strengthened during the second quarter (Fig. 7.52b). The largest positive anomalies over central Kiribati exceeded +1.2°C. Negative anomalies persisted over the PNG Islands, while a large area of negative anomalies covered Vanuatu, Fiji, Tonga, and Niue during April–June, associated with cool surrounding ocean. Temperatures were within 0.3°C of average around the Solomon Islands, New Caledonia, Samoa, Tuvalu, and parts of French Polynesia.

The temperature anomaly pattern from April to June persisted into the third quarter with negative anomalies strengthening in the south (Fig. 7.52c). By the end of September, the characteristic El Niño signal was established: positive anomalies dominated the equatorial region, southwest of which was a band of negative anomalies aligned northwest–southeast. A narrow strip of near-average temperatures was sandwiched between the two major anomaly features.

Below-normal air temperatures near the PNG Islands persisted into the last three months of the year, although the band of negative anomalies stretching southeast from PNG through Fiji to the southern Cook Islands weakened considerably in the last quarter (Fig. 7.52d). In contrast, positive anomalies intensified along the equator and expanded southward to encompass northern French Polynesia.

(ii) Precipitation

In addition to ENSO, key climate features in the southwest Pacific are the west Pacific Monsoon (WPM), which lies over the west Pacific warm pool, the South Pacific convergence zone (SPCZ) aligned northwest–southeast in the southwest Pacific, and the subtropical high pressure belt which is part of the Hadley Circulation.

Due mainly to enhanced activity in the WPM and SPCZ, the year began with above-normal rainfall recorded during January–March in many western places and the Cook Islands (Table 7.6). High rainfall in central Vanuatu was associated with Tropical

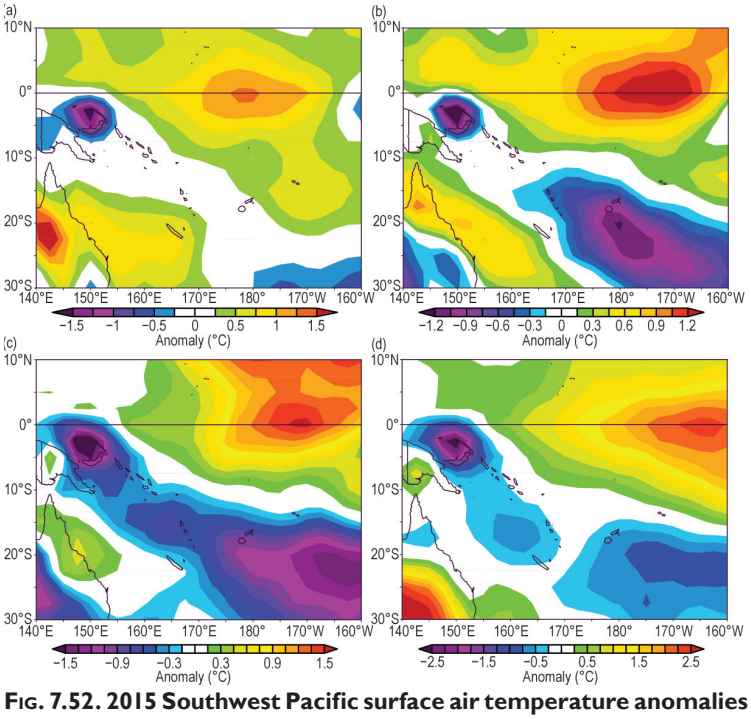

Fig. 7.52. 2015 Southwest Pacific surface air temperature anomalies from NCEP–NCAR reanalysis (°C; 1981–2010 base period); for (a) Jan–Mar, (b) Apr–Jun, (c) Jul–Sep, and (d) Oct–Dec.

Table 7.6. Observed 2015 rainfall relative to base period at capital towns/cities in the South Pacific.

	Jan	Feb	Mar	Apr	May	Jun	Jul	Aug	Sep	Oct	Nov	Dec
Port Moresby, PNG												
Honiara, Solomon Is												
Noumea, N. Caledonia												
Port Vila, Vanuatu												
Suva, Fiji												
Nuku'alofa, Tonga												
Alofi, Niue												
Apia, Samoa												
Pago Pago, A. Samoa												
Rarotonga, Cook Is												
Funafuti, Tuvalu												
Tarawa, Kiribati												

< 40%	≥ 80% to < 120%	≥ 120% to < 160%
≥ 40 to < 80%		> 160%

Cyclone Pam (see Notable events and section 4e8 for more details). Below-normal rainfall was recorded in the New Guinea Islands, northern and southern Vanuatu, southern Tuvalu, Fiji, northern Tonga, Niue, northern French Polynesia, and parts of Samoa. At Pekoa and Lamap in northern Vanuatu, January–March was second (out of 45 years of record) and fourth (out of 54 years of record) driest, respectively.

In the second quarter the SPCZ was displaced to the northeast. Rainfall was below normal in parts of PNG, Vanuatu, Fiji, Tonga, Niue, the Cook Islands, and French Polynesia. In contrast to typical El Niño conditions, the northern Cook Islands were drier than normal. At Suva (Fiji), April–June was the driest since 1942. Kiritimati (eastern) and Tarawa (western) Kiribati recorded their wettest and third wettest April–June respectively, with rainfall in excess of 1100 mm received across the country.

The extent of suppressed rainfall in the southwest Pacific expanded over the third quarter (July–September) to include most of PNG and most of the islands southwest of the SPCZ. Above-normal rainfall continued in the Kiribati, Tuvalu, and Tokelau region. Rainfall was strongly suppressed in the far western Pacific, with enhanced convection in the equatorial Pacific east of the Solomon Islands, a pattern typical of El Niño.

In the fourth quarter, the SPCZ continued to be displaced to the northeast. The central Pacific remained wetter or much wetter than average, with the region of enhanced rainfall extending to the northern Cook Islands and northern French Polynesia in November. Most islands between PNG and southern French Polynesia, with the exception of the Solomon Islands and Samoa, received below-normal rainfall. Rainfall for October–December at Garoka in the PNG highlands was the lowest in 45 years and second and third lowest at Momote and Wewak, respectively. Very low rainfall was also observed in western and southeastern Fiji, southern Cook Islands, and central Tonga.

(iii) Notable events

On 6 March, Tropical Disturbance 11F developed about 1140 km to the northwest of Nadi, Fiji. The disturbance was upgraded to a tropical depression two days later, then named Pam on 9 March. Located in an area of favorable conditions, Pam gradually intensified and became a Category 5 severe tropical cyclone on 12 March. Pam's 10-min maximum sustained winds peaked at 135 kt (69 m s^{-1}), along with a minimum pressure of 896 hPa, making Pam the most intense TC of the southwest Pacific basin since Zoe in 2002 (and third most intense storm in the Southern Hemisphere, after Zoe in 2002 and Gafilo in 2004). In addition, Pam had the highest 10-minute sustained wind speed recorded of any South Pacific TC. The center of Pam passed just east of Efate where the capital Port Vila is located (Fig. 7.53), and Erromango and Tanna suffered a direct hit, making Pam the single worst natural di-

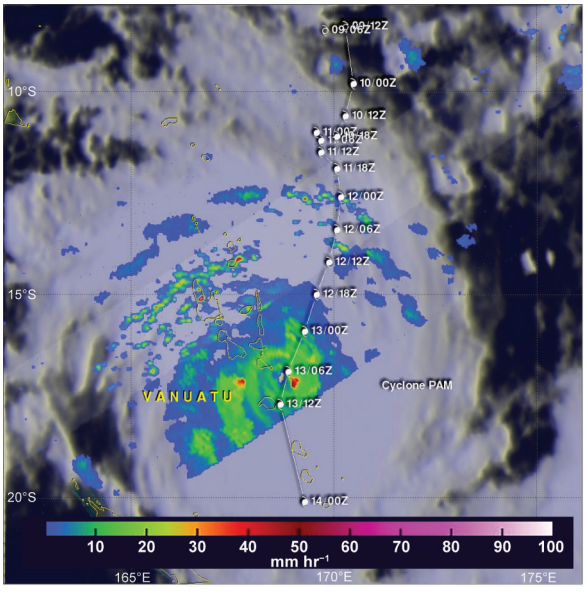

Fig. 7.53. Tropical Rainfall Measuring Mission (TRMM) satellite over Cyclone Pam on 13 March 2015 UTC. The image shows the cyclone track and a rainfall analysis from TRMM's Microwave Imager (TMI) and Precipitation Radar (PR) instruments. Rainfall in part of the cyclone was measured by TRMM PR at more than 119mmh^{-1}.(Source:trmm.gsfc.nasa.gov/trmm_rain/Events/pam_trmm_tmi_pr_13_march_2015_0923_utc.jpg.)

saster in the history of Vanuatu. The cyclone crippled infrastructure, with an estimated 90% of Vanuatu's buildings impacted by the storm. Communications were devastated and there was a shortage of water for several days following the storm. At least 132000 people were affected by Pam, including 54000 children. There were at least 15 fatalities.

4) Australia—C. Ganter and S. Tobin

The information presented here has been prepared using the homogenized Australian temperature dataset (ACORN-SAT) for area-averaged temperature values and the observational dataset (AWAP) for area-averaged rainfall values and mapped analyses for both temperature and rainfall. See www.bom.gov.au/climate/change/acorn-sat/ and www.bom.gov.au/climate/maps/#tabs=About-maps-and-data for more information.

(i) Temperature

Australia's annual mean temperature for 2015 was 0.83°C above the 1961–90 average, making it the fifth warmest year since national observations commenced in 1910. Eight of Australia's ten warmest years have occurred since 2002, with the most recent three years among the five warmest. In 2015, Western Australia, Queensland, Victoria, South Australia, and New South Wales all observed one of their ten warmest years on record.

The Australian annual mean maximum temperature (Fig. 7.54) was 0.96°C above average, and annual mean minimum temperature (Fig. 7.55) was 0.69°C above average; both sixth highest on record. Several exceptional warm spells occurred during 2015, with an especially warm October–December (see Notable events and Sidebar 7.3 for more details). April and May were the only months in which national mean temperatures were below average.

Annual maxima were in the highest decile (top 10%) of the historical distribution (since 1900) for the north of the Northern Territory, most of Queensland and Victoria, southeast and western South Australia, and large areas of Western Australia (highest on record for part of southwest Western Australia). Annual anomalies of +1.5°C to +2.0°C were observed in the southwest and southern interior of Western Australia and over a large area of southwestern to central Queensland.

Annual minima were also in the highest 10% of historical observations for most of Western Australia, large parts of Queensland, western South Australia, areas of New South Wales, and far eastern Victoria. Annual minima were near-average for most of the Northern Territory, northeastern Western Australia, other smaller areas in western Tasmania, the northern Cape York Peninsula and near Rockhampton in Queensland, and pockets of the southern half of

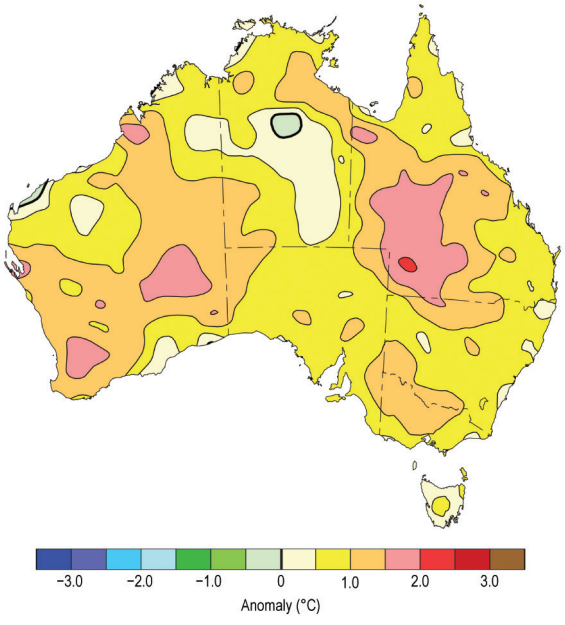

Fig. 7.54. Maximum temperature anomalies (°C) for Australia, averaged over 2015, relative to a 1961–90 base period. (Source: Australia Bureau of Meteorology.)

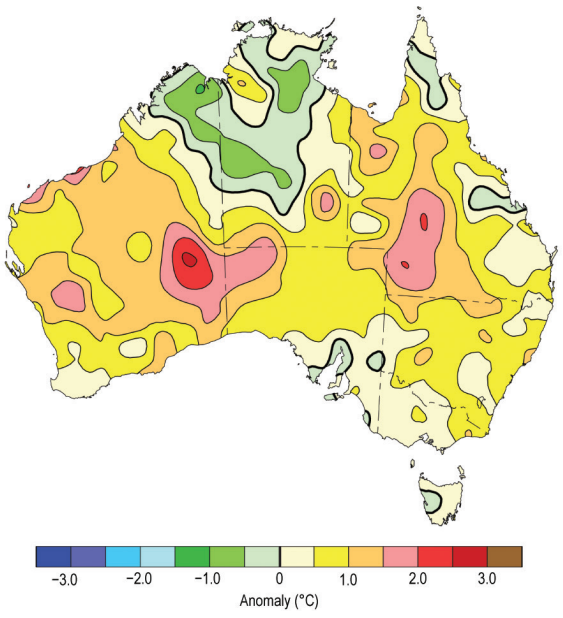

Fig. 7.55. Minimum temperature anomalies (°C) for Australia, averaged over 2015, relative to a 1961–90 base period. (Source: Australia Bureau of Meteorology.)

South Australia. They were cooler than average for some areas of the Northern Territory and northern Western Australia. Large areas of Western Australia and the western half of Queensland observed anomalies in excess of +1.0°C, rising to more than +2.0°C in the southeastern interior of Western Australia. Cool anomalies within 1°C of average were observed over the northern Kimberley and large parts of the Northern Territory.

(ii) Precipitation

Rainfall averaged across Australia for 2015 was 445.8 mm, or 96% of the 1961–90 average, the 59th driest year since records commenced in 1900 and close to the median. The near-average national total masks some regional differences. Notable areas of below-average rainfall were recorded in the southwest of Western Australia, large areas of southwest to central Queensland, and large areas of the southeast, extending from Tasmania through Victoria and into South Australia. Above-average precipitation was recorded in the Pilbara and Gascoyne regions of Western Australia, and across most of the Northern Territory extending into northern South Australia. Scattered parts of the eastern seaboard, extending from Victoria to southern Queensland, also had above-average precipitation for the year (Fig. 7.56).

State-wise, only Western Australia and the Northern Territory had above-average precipitation for the year, but within 20% of their annual total. All other states had below-average rainfall, with Victoria 14th driest and Tasmania 8th driest; both experiencing their driest year since the 2006 El Niño year. For Victoria, 16 of the last 19 years (1997–2015) have brought below-average rainfall with similar, though not quite as persistent, runs in other parts of southern Australia (e.g., southeastern Australia, 13 of the last 19 years).

Large parts of eastern Australia commenced the year with continuing long-term rainfall deficiencies (on the two- to three-year scale). These deficiencies persisted across much of inland Queensland in 2015, while drought increased through Victoria and southeast South Australia, and also emerged in Tasmania and southwest Western Australia. The deficiencies echo long-term declines in cool-season rainfall across southern Australia and poor wet-season rainfall in Queensland over three successive years.

After a wet January, much of northern and central Australia was very dry from February onwards, marking a dry end to the northern Australian wet season (October–April).

The combination of a strong El Niño and a record warm Indian Ocean (see section 4b) is an unusual set of climate drivers, and for Australia the presence of a very warm Indian Ocean appears to have limited the broad-scale rainfall anomalies in the cooler part of the year in inland southern and eastern Australia. However, southwest Western Australia recorded its second driest May–July while Victoria and southern South Australia were also dry, but to a lesser extent.

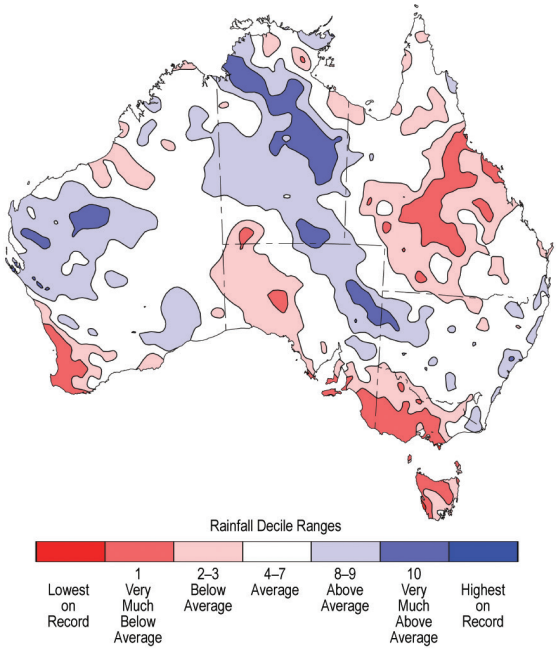

Fig. 7.56. Rainfall deciles for Australia for 2015, based on the 1900–2015 distribution. (Source: Australia Bureau of Meteorology.)

A late-developing positive Indian Ocean dipole was associated with a very dry September–October, which had significant impacts on agricultural production in southern areas. December closed the year with heavy rainfall over large parts of the north.

(iii) Notable events

An exceptional heat wave affected large parts of northern and central Australia during March, with prolonged heat peaking on the 19th and 20th. The other most notable heat waves occurred during the last three months of the year—record early-season heat across southern Australia in early October, contributing to Australia's warmest October on record and extreme heat in much of southeastern Australia in the third week of December (see Sidebar 7.3 for more detail).

Many significant bushfires occurred during the year. The most destructive, in terms of property loss or total area burned, are described below:

- Early January, South Australia's Mount Lofty Ranges, 27 houses destroyed and 20 000 hectares burned;
- Late January and early February, southwest Western Australia, 150 000 hectares burned—the most significant fires for the region in many decades;
- 15–21 November, around Esperance in Western Australia, 145 000 hectares burned;
- 25–27 November, South Australia's Mid North, at least 87 houses at Pinery (north of Adelaide) severely damaged or destroyed and 90 000 hectares burned;
- 25 December, near Lorne on Victoria's southwest coast, 116 homes and holiday houses destroyed at Wye River and Separation Creek.

Two east coast lows brought significant damage. The first caused severe weather and flooding in coastal New South Wales between 20 and 23 April, with 12 regions declared natural disaster areas and several deaths reported due to flash flooding at Dungog. The second low produced heavy rain and damaging winds over southeast Queensland and parts of New South Wales between 1 and 4 May.

A significant, but far from record-breaking, cold outbreak over southeastern Australia during 11–17 July brought widespread snow along the Great Dividing Range, extending from the hills east of Melbourne into southern Queensland. This was the most significant snow event in Queensland since 1984.

Four tropical cyclones made landfall in Australia during 2015: Lam, Marcia, Nathan, and Olwyn with a fifth, Quang, weakening below cyclone intensity just prior to landfall. Marcia was the strongest at landfall (Category 5) and the most intense known tropical cyclone so far south on the east coast [maximum 10-minute sustained winds of 110 kt (57 m s^{-1}), crossing near Yeppoon, and causing damage as far south as Bundaberg]. Lam made landfall in the eastern Top End on the same day, 20 February—the first time in recorded history that two severe tropical cyclones made landfall in Australia on the same day (see also section 4e7).

For further detail on these and other significant events please see the Monthly Weather Reviews, Annual Climate Statement, and Annual Climate Report available from www.bom.gov.au/climate/current/.

5) New Zealand—N. Fedaeff

In the following discussion, the base period is 1981–2010 for all variables, unless otherwise noted. The nation wide average temperature is based upon the National Institute of Water and Atmospheric Research (NIWA) seven-station temperature series that begins in 1909 (www.niwa.co.nz/our-science/climate/information-and-resources/nz-temp-record/seven-station-series-temperature-data). All statistics are based on data available as of 8 January 2016.

(i) Temperature

New Zealand had a relatively mild 2015, with annual mean temperatures within 0.5°C of the annual average across much of the country (Fig. 7.57).

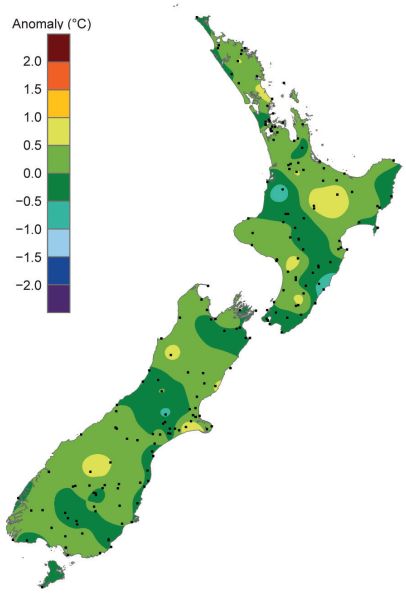

Fig. 7.57. 2015 annual mean temperature anomalies (°C) relative to 1981–2010 normal. Dots show observing station locations. (Source: NIWA.)

SIDEBAR 7.3: AUSTRALIA'S WARM RIDE TO END 2015

The last three months of 2015 saw a very warm end to the year for Australia. It was the warmest October on record with respect to both maximum and minimum temperatures, with the October mean temperature anomaly of +2.89°C the largest anomaly on record for Australia for any month in 106 years of records. Maximum temperatures for October in Victoria, South Australia, and New South Wales were close to values typical of an average December, with monthly anomalies of more than +5°C for the three states (Fig. SB7.6).

October's most significant daily extremes occurred in the first half of the month. Significantly high daytime temperatures occurred in southwest Western Australia beginning 1 October, spreading eastwards and peaking in extent during 4–6 October in the southeast; each day, some part of southern Australia had daily anomalies in excess of +12°C. Another bout of extreme heat occurred over southern Western Australia from 8 to 13 October. Later in the month, there were several other periods which had temperatures well above average, but no individual event in the latter part of October surpassed the extremes of the first 10 days (www.bom.gov.au/climate/current/statements/scs52.pdf).

November mean temperatures were the third warmest on record and, overall, spring 2015 was second warmest on record. The most recent three springs were the three warmest, with 2014 remaining the warmest on record.

The last notable warm period for the year occurred in December. Following a consistently warm first half of December for the southeast interior of Australia, a burst of more extreme warmth occurred in mid-December over South Australia. Adelaide reached 40°C each day during 16–19 December—the first time this has occurred in Adelaide in December (previous earliest run of four or more days of at least 40°C was 3–6 January in 1906). Heat peaked for this event on 19 December in South Australia and western Victoria ahead of a front, with the cool change passing through southeast Australia on 20 December. Individual daytime and nighttime December records were set on the 19th and 20th across South Australia, Victoria, New South Wales, and Tasmania (Fig. SB7.7). Mildura measured a minimum of 31.9°C on 20 December. This was a new record high minimum temperature for a Victorian site for any month, surpassing 30.9°C also at Mildura on 24 January 2001. A number of other locations in northern Victoria experienced their hottest night on record for any month (www.bom.gov.au/climate/current/statements/scs53.pdf).

Overall, October–December was the warmest such period on record, with a mean temperature anomaly of +1.93°C. It also tied with July–September 2013 for highest positive anomaly for any three month period.

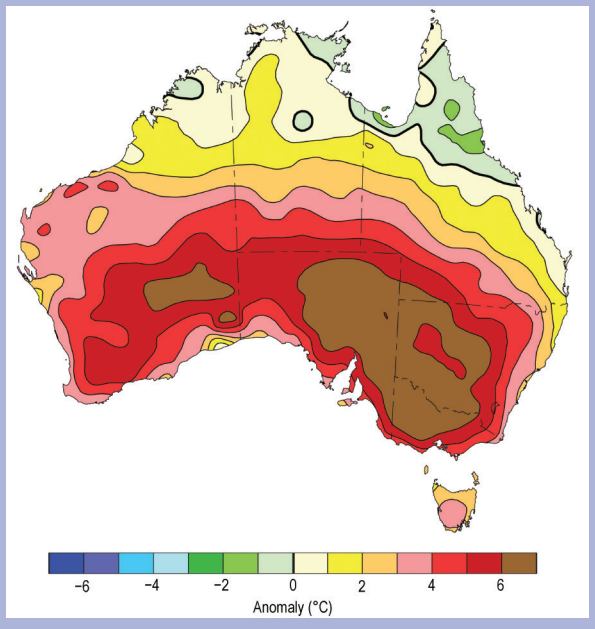

Fig. SB7.6. Maximum temperature anomalies for Oct 2015 for Australia (1961–90 base period). (Source: Australia Bureau of Meteorology.)

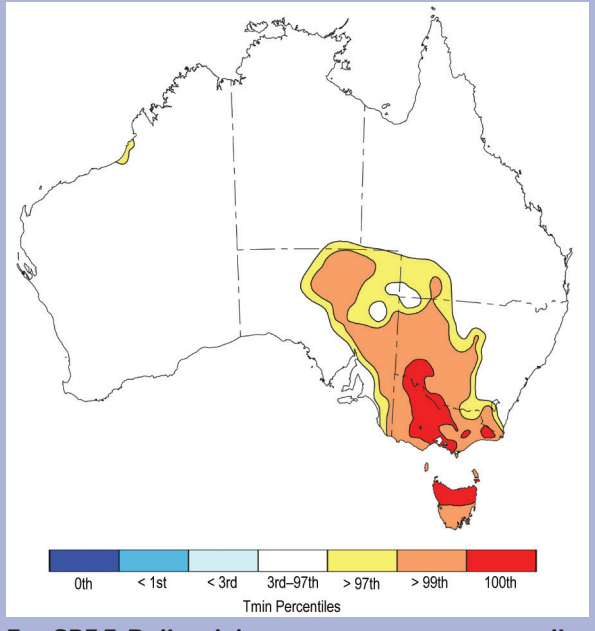

Fig. SB7.7. Daily minimum temperature percentiles for 20 Dec 2015 (1961–90 base period). (Source: Australia Bureau of Meteorology.)

The nation wide average temperature for 2015 was 12.7°C (0.1°C above average). According to NIWA's seven-station temperature series, 2015 was the 27th warmest year for New Zealand in the 107-year period of record. Above-average temperature anomalies were observed throughout many regions of the country in January and March, while below-average temperature anomalies were prominent in September.

(ii) Precipitation

Annual rainfall totals for 2015 were below normal (50%–79% of the annual normal) in the north and east of the country: Northland, Tasman, Nelson, and Canterbury as well as parts of eastern Waikato, Bay of Plenty, Gisborne, and Wellington—a pattern typically observed during El Niño. Rainfall was within 20% of the annual normal for the remainder of New Zealand (Fig. 7.58). It was the driest year on record for Kaitaia and Kerikeri (both located in Northland), which recorded 75% and 63% of their normal annual rainfall, respectively. There were no high total rainfall records or near-records set in 2015. January was a particularly dry month for New Zealand with rainfall totals well below normal (less than 50% of the January normal) or below normal (50%–79% of the January normal) for most parts of the country. Parts of Northland, Auckland, Taranaki, Manawatu-Whanganui, Kapiti Coast, Wellington, Marlborough, north Canterbury, and Central Otago each received less than 10% of their respective January normal rainfall. Conversely, rainfall during April and June was well above normal (greater than 149% of normal) in Taranaki and large parts of Manawatu-Whanganui.

Of all of the regularly reporting gauges, the wettest location in 2015 was Cropp River, in the Hokitika River Catchment (West Coast, South Island, 975 m a.s.l.) with an annual rainfall total of 11 632 mm. The driest of the regularly reporting rainfall sites in 2015 was Clyde (Central Otago), which recorded 267 mm of rainfall for the year. North Egmont (Taranaki) experienced the highest 1-day rainfall total in 2015 of 466 mm on 19 June.

(iii) Notable events

See Fig. 7.59 for a schematic of notable events. On 16 and 17 March, ex-Tropical Cyclone Pam passed east of New Zealand and was associated with strong winds and heavy rain in northern and eastern parts of the North Island. About 2200 Auckland and Northland properties lost power as strong winds brought down trees onto power lines. Over 100 people in the East Cape area were evacuated from their homes as a precaution, particularly in low lying coastal townships as high seas were expected to cause flooding and damage.

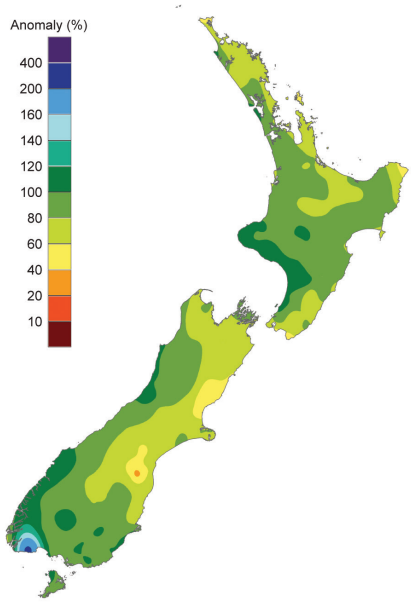

Fig. 7.58. 2015 annual total rainfall (%) relative to 1981–2010 normal. Distribution of observing station locations is as in Fig. 7.57. (Source: NIWA.)

On 3 June, Dunedin (Otago) was inundated by heavy and prolonged rainfall, which resulted in significant flooding, loss of electricity, evacuations, and road closures throughout the city and nearby areas. Dunedin (Musselburgh) received 113 mm of rainfall in the 24 hours to 9 a.m. on 4 June—its second-highest 1-day rainfall total on record for all months (records began in 1918).

Another sigificant flooding event occurred during 20–21 June in Whanganui. Heavy and prolonged rainfall caused evacuation of more than 100 households and the Whanganui River breached its banks, spilling floodwaters into Whanganui's central business district. This event was the worst flood on record for the area and led to the declaration of a state of emergency.

From 23 to 26 June, record-low temperatures were observed in many regions of the country. A high pressure system over and west of New Zealand combined clear skies with a southerly flow, resulting in very cold temperatures for many parts of the country. In particular, sites in the Mackenzie Country and Central Otago dropped to well below 0°C. The lowest recorded air temperature for 2015 (excluding high elevation alpine sites) was –21.0°C, observed at Tara Hills (Mackenzie Country) on 24 June. This was the fourth coldest temperature ever recorded in New Zealand.

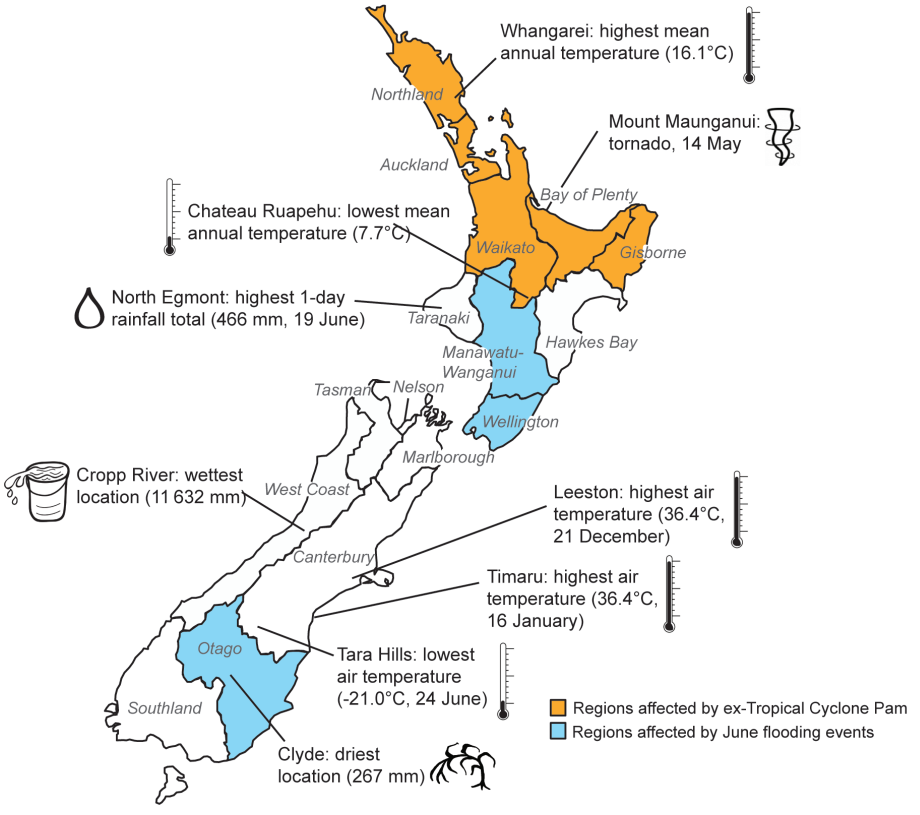

Fig. 7.59. Notable weather events and climate extremes for New Zealand in 2015. (Source: NIWA.)